THE EFFECT OF PRESSURES BELOW ONE ATMOSPHERE ON THE PERFORMANCE OF A WETTED WALL DISTILLATION COLUMN

A THESIS

Presented to

the Faculty of the Graduate Division

By

Sydney Vaughn Stern

In Partial Fulfillment

of the Requirements for the Degree

Doctor of Philosophy in the School

of Chemical Engineering

Georgia Institute of Technology

September 1962

cem
H.S.
12R

THE EFFECT OF PRESSURES BELOW ONE ATMOSPHERE ON THE PERFORMANCE OF A WETTED WALL DISTILLATION COLUMN

Approved:

W. M. Newton, Chairman

H. V. Grubb

Clyde Orr, Jr.

Date Approved by the Chairman: Aug. 20, 1962

"In presenting the dissertation as a partial fulfillment of the requirements for an advanced degree from the Georgia Institute of Technology, I agree that the Library of the Institution shall make it available for inspection and circulation in accordance with its regulations governing materials of this type. I agree that permission to copy from, or to publish from, this dissertation may be granted by the professor under whose direction it was written, or, in his absence, by the dean of the Graduate Division when such copying or publication is solely for scholarly purposes and does not involve potential financial gain. It is understood that any copying from, or publication of, this dissertation which involves potential financial gain will not be allowed without written permission.

_____

_____"

DEDICATION

To my wife, Marion, for faith, patience and devotion during a trying time.

ACKNOWLEDGMENTS

I am deeply indebted to my advisor, Dr. W. M. Newton, not only for assistance and guidance during this work, but also for inspiration and encouragement throughout the course of my graduate studies.

I am grateful to the Phillips Petroleum Company and the Ethyl Corporation for fellowships which supported a major portion of this work.

My special thanks are due Mr. Don Lillie for his skill and ingenuity in constructing and assembling special parts of the apparatus.

TABLE OF CONTENTS

LIST OF TABLES

LIST OF FIGURES

Figure Page

NOMENCLATURE

A	cross-sectional area of column; $cm.^2$
B	effective gas film thickness; cm.
B_f	thickness of laminar vapor layer; cm.
C	molar vapor concentration of more volatile component; $gm.-moles/cm.^3$
C_A	molar vapor concentration of component A; $gm.-moles/cm.^3$
C_V	molar density of vapor mixture; $gm.-moles/cm.^3$
d	column diameter; cm.
D_f	rotometer float diameter; inches
D_L	liquid diffusion coefficient; gm.-moles/sec.-cm.
D_m	vapor diffusion coefficient in molal units; gm.-moles/sec.-cm.
D_V	vapor diffusion coefficient in volume units; $cm.^2/sec.$
F	liquid film Froude number; dimensionless
G	mass vapor velocity; $gm./sec.-cm.^2$
g_c	acceleration due to gravity; $cm./sec.^2$
HETP	height equivalent to a theoretical plate; cm.
h_f	rotometer float height; cm.
H_G	height of a gas film transfer unit; cm.
k_G	gas film mass transfer coefficient for mole fraction driving force; $gm.-moles/sec.-cm.^2$
k'_G	gas film mass transfer coefficient for partial pressure driving force; $gm.-moles/sec.-cm.^2-atm.$

k_{Gf}	laminar vapor layer mass transfer coefficient for mole fraction driving force; gm.-moles/sec.-cm.^{2}
k'_{Gf}	laminar vapor layer mass transfer coefficient for partial pressure driving force; gm.-moles/sec.-cm.^{2}-atm.
k_L	liquid film mass transfer coefficient for mole fraction driving force; gm.-moles/sec.-cm.^{2}
K_G	overall mass transfer coefficient based on gas driving force; gm.-moles/sec.-cm.^{2}
K_L	overall mass transfer coefficient based on liquid driving force; gm.-moles/sec.-cm.^{2}
L	molal liquid flow rate; gm.-moles/sec.
m	liquid reflux film thickness; cm.
M_m	average vapor molecular weight; gm./gm.-mole
n	number of theoretical plates, counting from the bottom of the column; dimensionless
N_A	molar flux of component A; gm.-moles/sec.-cm.^{2}
N_{tG}	number of gas film transfer units; dimensionless
p	partial pressure; atm.
p*	equilibrium partial pressure corresponding to main body of liquid; atm.
P	total pressure; atm. of mm. of Hg
q	slope of equilibrium curve; dimensionless
Q	volumetric flow rate; cm.^{3}/min.
r_c	mass transfer resistance of turbulent core; sec.-cm.^{2}-atm./gm.-mole

r_f	mass transfer resistance of laminar layer; sec.-cm.^{2}-atm./gm.-mole
r_O	column radius; cm.
R	universal gas constant; cm.^{3}-atm./gm.-mole-$^\circ$K.
Re	Reynolds number relative to column wall; dimensionless
$\overline{Re}_V$	vapor Reynolds number relative to liquid film surface; dimensionless
R_T	total resistance to mass transfer; various units
S	surface area normal to direction of mass transfer; cm.^{2}
Sc_V	vapor Schmidt number; dimensionless
T	temperature, $^\circ$K. or $^\circ$C.
U	local velocity; cm./sec.
$\overline{U}$	average velocity relative to column wall; cm./sec.
U_S	liquid film surface velocity; cm./sec.
U_V	local vapor velocity; cm./sec.
$\overline{U}_V$	average vapor velocity relative to column wall; cm./sec.
$\overline{U}'_V$	average vapor velocity relative to liquid film surface; cm./sec.
W	mass transfer rate; gm.-moles/sec.
$\overline{W}$	mass flow rate; gm./min.
W_f	rotometer float weight; gm.
X	liquid mole fraction; dimensionless
X*	equilibrium liquid mole fraction corresponding to main body of vapor; dimensionless
Y	vapor mole fraction; dimensionless

Y^*	equilibrium vapor mole fraction corresponding to main body of liquid; dimensionless
Z	test section length; cm.
α_R	relative volatility; dimensionless
β	proportionality constant; various units
β'	proportionality constant; various units
Γ	liquid mass flow rate per unit wall width; gm./sec.-cm.
μ	viscosity; poise
ρ	density; gm./cm.^{3}
ρ_f	rotometer float density; gm./cm.^{3}

SUBSCRIPTS, UNLESS DEFINED ABOVE

A	value for component A
B	conditions at bottom of test section
f	conditions at edge of laminar layer
i	conditions at vapor liquid interface
L	value for liquid
S	conditions in still
T	conditions at top of test section
V	value for vapor

SUMMARY

The effect of reduced pressure on distillation efficiency in packed columns has been the subject of numerous investigations. Although these investigations have contributed a wealth of experimental data covering many kinds of packing and many different test mixtures no theory has been advanced which will satisfactorily explain the pressure effects which have been observed.

The purpose of this investigation was to study the effect of reduced pressure on the performance of a wetted wall distillation column operating under conditions of total reflux. A wetted wall column was chosen rather than a packed column in the expectation that the elimination of the column packing as a variable would permit a more fundamental view of the effect of reduced pressure on the distillation process to be taken.

Up to the present time no investigation of the effect of reduced pressure on distillation in a wetted wall column has been reported. Therefore, a secondary purpose of this investigation was to test the existing distillation theories and correlations under somewhat different experimental conditions than have hitherto been examined.

The vapor stream in a wetted wall column is bounded by a liquid film on the interior column wall. Hence, the condition of the liquid surface can be expected to influence the vapor stream in much the same way that wall roughness influences flow in pipes.

The point of view taken in this investigation was that an understanding of the hydrodynamic conditions existing in wetted wall columns and the influence of these conditions on the distillation process is essential to the proper interpretation and explanation of the data obtained.

The apparatus used consisted of a wetted wall distillation column having an internal diameter of 1.9 centimeters and a mass transfer length of 125.1 centimeters. Provisions for the maintenance of adiabatic operating conditions, the withdrawal of samples, and the measurement and control of temperature, pressure, and boil-up rate were included in the column design.

The performance of the column was studied by distilling a chlorobenzene-ethylbenzene test mixture under conditions of total reflux. Various runs were conducted at each of the following four pressures: 736, 300, 100, and 20 millimeters of mercury.

The flow rates studies covered a vapor Reynolds number range of from 520 to 18,600 and thus provided data in the laminar, transition, and turbulent regions of vapor flow. This range of flow rates is greater than that obtained in any previous investigation which included all three regions of vapor flow. At 20 millimeters of mercury pressure the column flooded before the turbulent region of vapor flow could be entered, and consequently, at this pressure the data cover only the laminar and transitional regions. In this investigation the transition region is taken to be that region between laminar and fully developed turbulent flow.

The results of this investigation showed that in the region of laminar vapor flow a decrease in pressure at constant vapor velocity caused an increase in column efficiency. This result is in agreement with a theoretical relation presented by Westhaver (Industrial and Engineering Chemistry, 34, 126 (1942)).

In the region of transitional vapor flow a decrease in operating pressure at constant vapor Reynolds number caused a decrease in column efficiency. This was found to be due to the influence of liquid film rippling on the vapor turbulence conditions.

In the region of turbulent vapor flow a decrease in operating pressure at constant vapor Reynolds number caused an increase in column efficiency. This result is in agreement with a mass transfer theory, previously applied to vaporization data by Gilliland (Industrial and Engineering Chemistry, 30, 506 (1938)), which assumes that the resistance to mass transfer is the sum of the resistance of the turbulent core and the resistance of the true laminar layer.

The results of this investigation were compared with a number of empirical relations, such as those of Gilliland and Sherwood (Industrial and Engineering Chemistry, 26, 516 (1934)) and Johnstone and Pigford (Transactions of the American Institute of Chemical Engineers, 38, 25 (1942)), which included the Schmidt number to a fractional power. Although the data which were obtained at atmospheric pressure were in excellent agreement with the correlations developed by previous investigators of distillation and vaporization at atmospheric pressure, it was found that the observed effect of reduced pressure could not be correlated

by these relations. This was shown to be due to a fundamental fault in the form of the correlations.

The influence of the liquid film surface on the vapor stream was greatest in the region of transitional vapor flow. The vapor Reynolds number at which turbulent flow began in the vapor was a function of the degree of rippling of the liquid reflux film and varied with the operating pressure.

The most important conclusion drawn from the results of this investigation is that in all regions of vapor flow, laminar, transitional, and turbulent, a decrease in operating pressure at constant vapor turbulence conditions causes an increase in column efficiency.

CHAPTER I

INTRODUCTION

General

The reduction in operating temperatures which accompanies distillation under reduced pressure accounts for the extensive application of vacuum distillation in industry. Thermally unstable substances which would be subject to decomposition or polymerization at the temperatures of atmospheric distillation may be safely separated by vacuum distillation. Vacuum distillation is also widely used for the separation of heat-stable compounds which boil at inconveniently high temperatures and for the separation of mixtures which form azeotopes at atmospheric pressure.

The effect of reduced pressure on the efficiency of packed columns has been studied by many investigators. A review of the literature on this subject shows wide disagreement among the results which have been obtained.

The first published report of an investigation of the effect of reduced pressure on distillation appeared some 27 years ago. Docksey and May (1) obtained a limited amount of data on the distillation of nitrobenzene-aniline mixtures at pressures of 10 and 253 millimeters of mercury in a two-inch diameter column packed for a height of thirty-six inches with one-fourth inch Lessing rings. The data were in agreement with a theory developed by the authors on the assumption that the

interchange of material from one phase to the other depends only on the rate of diffusion through that portion of the vapor in which the flow is streamline. It is remarkable that no further confirmation or study of this theory has been reported.

Subsequent investigators have contributed a wealth of data covering many kinds of packing and many different test mixtures but have been unable to present any theory which will satisfactorily explain all of the observed data. Most (4)(5)(6)(7)(11)(12)(16) have found the effect of reduced pressure to be slight although some (2)(8)(10)(14)(17) have found the efficiency to be definitely improved by a reduction in operating pressure. Others (3)(13)(15) have noted a decrease in efficiency with decreased pressure and one investigator (9) has even observed that as the pressure was reduced the efficiency reached a maximum and then decreased again.

The purpose of this investigation was to study the effect of reduced pressure on the performance of a wetted wall distillation column operating under conditions of total reflux. A wetted wall column was chosen rather than a packed column in the expectation that the elimination of the column packing as a variable would permit a more fundamental view of the effect of reduced pressure on the distillation process to be taken. Up to the present time no investigation of the effect of reduced pressure on distillation in a wetted wall column has been reported and hence a secondary purpose of this investigation was to test the existing distillation theories and correlations under somewhat different experimental conditions than have hitherto been investigated.

The scope of this investigation includes not only the laminar and turbulent regions of vapor flow but also the region of transitional flow, i.e., that region between laminar and fully developed turbulent flow. The region of transitional vapor flow has been almost entirely ignored by previous investigators of distillation in wetted wall columns.

The advantages of wetted wall columns as devices for the study of mass transfer have long been recognized. Their simplicity permits a precise evaluation of the interfacial area available for mass transfer and their resemblence to simple pipes permits estimates of both vapor and liquid phase turbulence conditions to be made. To exploit fully these advantages, it is necessary to take into account the influence of the hydrodynamic condition of the liquid and vapor phases on the mass transfer process.

The vapor stream in a wetted wall column is bounded by a liquid film on the interior column wall. Consequently, the condition of the liquid surface can be expected to influence the vapor stream in much the same way that wall roughness influences flow in pipes. Of course the hydrodynamic condition of the liquid film can be expected to be of primary importance in determining mass transfer within the liquid.

These general considerations form the basis for the point of view taken in this investigation, i.e., that an understanding of the hydrodynamic conditions existing in wetted wall columns and the influence of these conditions on the distillation process is essential to the proper interpretation and explanation of the data obtained.

The purpose of this chapter is to review the literature necessary to establish a basis for the application of this point of view to the data of this investigation.

Distillation and Vaporization in Wetted Wall Columns

Gilliland and Sherwood (18) studied the evaporation of eight organic liquids and water into both cocurrent and countercurrent turbulent air streams flowing in a wetted wall column 2.67 centimeters in diameter and 117 centimeters long. The vapor phase Reynolds number was varied from 2,000 to 36,000 and the total pressure was varied from 110 to 2,330 millimeters of mercury. The liquid rate in all runs was approximately 790 cubic centimeters per minute. The liquid temperature varied between 30 and 100 degrees centigrade depending on the liquid being used. The entering air was heated to within three degrees centigrade of the liquid temperature. When the data were corrected for variations in Reynolds number no trend with pressure was noted.

Early investigations (19)(20)(21)(22)(23)(24) of the performance of wetted wall distillation columns were undertaken to compare empirically the relative efficiencies of empty and packed columns rather than to make any fundamental study of the apparatus. The columns used were of small diameter, generally less than 1.0 centimeter, and the liquid rates were such that laminar vapor flow prevailed. In general, the data showed that the efficiency decreased with increasing liquid rate.

Rose (25) made one of the earliest fundamental studies of distillation in a wetted wall column. Benzene-carbon tetrachloride

mixtures were distilled in wetted wall columns three and six millimeters in diameter and 30.3 centimeters long. At very low rates of boiling the columns had high efficiencies but the efficiency decreased rapidly as the rate of boiling was increased. At the same rate of boiling the 3 millimeter and 6 millimeter columns had approximately the same efficiency. Rose also investigated the effect of column insulation and concluded that: "For successful operation at very low rates of boiling the columns should be insulated almost as well as a calorimeter."

Surowiec and Furnas (26) obtained data on the distillation of ethyl alcohol-water mixtures in a wetted wall column twelve inches in diameter and eleven feet long. The flow rates studied were sufficiently high to insure turbulent vapor flow. The data obtained were compared with that previously observed (27) when the same column had been operated as a packed column with the same binary mixture. At low rates of flow the wetted wall column was at least as efficient as the packed column. The investigation of the packed column had indicated that the principal resistance to mass transfer was in the liquid film, whereas the data obtained in the wetted wall column showed that the principal resistance was in the gas film. This was tentatively explained by the assertion that the packing decreased the gas film resistance by decreasing the average diameter of the vapor path but had essentially no effect on the liquid film.

Johnstone and Pigford (28) studied both distillation and absorption in a wetted wall column 1.17 inches in diameter and six feet long.

Five systems were investigated, including ethanol-water, acetone-chloroform, benzene-toluene, ethylene dichloride-toluene, and benzene-ethylene dichloride. The apparatus was operated at total reflux on the first four systems and as an absorption column on the last two. The vapor rates investigated were all in the turbulent region. The results indicated that not more than ten per cent of the total resistance to mass transfer was in the liquid phase. The observed resistance in the liquid phase was considerably smaller than was predicted by a theoretical equation derived by Johnstone and Pigford on the assumption of diffusion into a laminar liquid layer. This discrepancy was attributed to the effect of wave motion on the liquid surface. The experimental data for the four systems studied at total reflux and the absorption of ethylene dichloride vapors by benzene were correlated by an empirical equation utilizing the vapor Reynolds number and the Schmidt number. The authors point out that the range of Schmidt numbers investigated was too narrow to establish the dependency of the data on the Schmidt group with any certainty. The influence of the liquid surface on the vapor phase turbulence was recognized and allowed for by basing the vapor Reynolds number on the average vapor velocity relative to the liquid surface velocity.

Kuhn and Ryffel (29) investigated the distillation of carbon tetrachloride-benzene mixtures at very low flow rates in wetted wall columns eleven and one hundred centimeters long and 1.0 centimeter in diameter. Data for two runs in the eleven centimeter column and three runs in the one hundred centimeter column under a total pressure

of 60 millimeters of mercury are reported. In addition a single point is reported for the distillation of the carbon tetrachloride-benzene mixture at 80 millimeters of mercury in a column 150 centimeters long and 0.4 centimeters in diameter and two points are reported for the distillation of a m-xylene-p-xylene mixture in the same column at a pressure of 95 millimeters of mercury. The data were obtained to test a distillation theory developed by one of the authors (71) for the case of laminar vapor flow. The investigation was carried out under reduced pressure merely to alleviate the strict insulation requirements necessary (25) for satisfactory operation at low flow rates.

Peck and Wagner (30) determined the relative film resistance in both a wetted wall and a plate distillation column. The wetted wall column consisted of a 57.25 inch length of 2.07 inch I. D. tubing. The systems studied were methanol-water, acetone-water, and isopropanol-water. All runs were conducted under conditions of turbulent vapor flow. The results showed that in the wetted wall column all of the resistance to mass transfer resided in the gas film, whereas in the plate column the gas film comprised only about fifty per cent of the total resistance.

Chari and Storrow (31)(32) developed a unique approach to the study of distillation in wetted wall columns. By using thermocouples to measure the condensation temperature of the vapor it was possible to derive curves of vapor composition along the contact path of the two phases. The test column was a glass tube 137 centimeters long and 2.55 centimeters in diameter. The systems studied were ethanol-water

and methanol-water. All tests were carried out under conditions of turbulent vapor flow. The data obtained indicated a hitherto unobserved dependency of column efficiency on vapor composition. This composition dependency was attributed to the influence of liquid film resistance although previous investigators of relative resistance (28) (30) had found the resistance of the liquid film to be negligible.

Jackson and Ceaglski (33) studied composition effects on distillation and vaporization in a wetted wall column by sampling the liquid reflux at various points along the column length. The column used was constructed of six one-foot sections of hard copper tubing 1.505 inches in diameter so that samples could be withdrawn at the junction of each section. Data were obtained for the distillation of the 2-propanol-water system at total and partial reflux, and for the vaporization into air of water, 2-propanol, toluene, and water from glycerol solutions. The distillation data showed that in most instances the efficiency at the individual sections reached a minimum value at some point in the column. This was considered to indicate an unexpected effect of composition on the mass transfer process. However, the efficiency based on data at the top and bottom of the column showed no dependency on composition. Unlike previous investigators (31)(32) of composition effects, the liquid film resistance was considered to be negligible and the composition dependence to be due to association in the vapor phase. All of the data were taken under conditions of turbulent vapor flow and were found to be amenable to correlation by a procedure based on the measured friction factor in the column. A direct comparison

of the distillation and vaporization data showed these processes to be analogous when considered from the point of view of simple film theory. It was also suggested that the quantitative disagreement among the various investigators of distillation in wetted wall columns could be attributed to the influence of end effects.

Yoshida (34) investigated distillation in the region of turbulent vapor flow in a wetted wall column 101 centimeters long and 2.2 centimeters in diameter under conditions of both total and partial reflux. The systems studied were methanol-water, ethanol-water, benzene-toluene, and carbon tetrachloride-toluene. The data obtained for each system were in substantial agreement with that of previous investigators but the effect of the variation of physical properties from one system to another was not well correlated by conventional empirical relations such as those of Gilliland (18) and Johnstone and Pigford (28).

Nikolaev (36) studied the effect of length to diameter ratio on distillation in wetted wall columns. The columns used were brass tubes of 8, 12, 16, and 20 millimeters internal diameter, with length-to-diameter ratios of 278, 185, 132, and 111.3, respectively. Ethanol-water was used for the test mixture. The study included flow rates in the laminar, transition, and turbulent regions of vapor flow. Correlations were obtained which showed that the influence of the length-to-diameter ratio depended on the character of the vapor flow and was greatest in the regions of laminar and transitional flow. The data are presented in the form of two small graphs and no explanation of the effects observed is given.

Zuiderweg and Harmons (55) investigated surface tension effects in wetted wall distillation columns and found that the surface tension characteristics of the liquid film could significantly influence the efficiency. It was observed that the liquid reflux film was stable when the surface tension of the reflux increased down the column, whereas with decreasing surface tension the reflux film tended to break up into narrow rivulets or droplets. The magnitude of the effect depended on the relative volatility of the components as well as their surface tensions as appreciable concentration gradients were required for destabilization of the film to occur.

Quershi and Smith (56) have recently obtained data for the distillation of both binary and ternary mixtures in a wetted wall column 134 centimeters long and 2.5 centimeters in diameter. Six binary mixtures, acetone-benzene, chloroform-benzene, acetone-chloroform, heptane-methyl cyclohexane, heptane-toluene, methyl cyclohexane-toluene, and two ternary mixtures were investigated. All of the data were obtained at atmospheric pressure at total reflux and at the same flow rate ($2750 < Re_V < 3800$). The binary data showed a composition dependency similar to that noted in previous studies (31)(32)(33) of distillation using alcohol-water systems. No explanation of the composition effect was given but an empirical expression was developed which compensated for the effect in both the binary and the ternary systems.

Transition from Laminar to Turbulent Flow

The actual mechanism of the transition from laminar to turbulent flow is not well understood and even the mechanism of fully developed

turbulent flow is itself but partially understood. Nevertheless, certain experimental facts seem clearly established.

Reynolds (37) conducted the first detailed experimental investigation of the phenomena of the transition from laminar to turbulent flow in pipes. In his classic experiments, Reynolds observed the behavior of a dye filament injected into a tube with a trumpet shaped entry fed from a tank of still water. For smooth conditions of entry the dye filament was observed to break down at a Reynolds number of 13,000.

Knudsen (38) and Goldstein (39) have reviewed the results of subsequent investigators. When care is taken to eliminate disturbances at the entry laminar flow can be observed at Reynolds numbers as high as 50,000. The experimental evidence indicates that there is no upper limit of Reynolds numbers for laminar flow. It would appear that if disturbances could be reduced to zero laminar flow could be maintained at any Reynolds number.

In fact, this assumption is implicit in the theory of stability enunciated by Schlichting (40). This theory assumes that laminar flow is always a possible mode of flow and that the type of flow ultimately assumed in a pipe depends on the type and magnitude of the disturbances to which the flowing fluid is subjected. Schlichting also states that it has been established that the Reynolds number at which transition takes place "...depends very strongly on the conditions which prevail in the initial pipe length as well as in the approach to it."

Goldstein (39) points out that although the experimental data on flow in pipes indicates that the effect of roughness on transition

is slight, roughness can influence the transition from laminar to turbulent flow when the disturbances due to roughness are larger than those due to the entry.

The experimental evidence regarding the lowest value of the Reynolds number for which turbulent flow has been observed seems conclusive. Goldstein (39) states that turbulent flow in pipes cannot occur at Reynolds numbers below about 2100 regardless of the degree of disturbance introduced by the entry. However, this value of the lower critical Reynolds number applies only to the disappearance of turbulence as determined by friction factor measurements in pipes. Prengle and Rothfus (41)(42) have observed other departures from true laminar flow in pipes at Reynolds numbers as low as 850.

Flow of Liquid Films

The influence of the liquid film on the hydrodynamic condition of the vapor stream in wetted wall columns has not been fully appreciated by previous investigators. Some (18)(26)(30)(31)(32)(34) have ignored this influence. Others (28)(33) have attempted to make some allowances for this effect by basing the vapor Reynolds number on the velocity relative to the liquid surface. In addition, those investigators of distillation in wetted wall columns who have found the resistance of the liquid film to be negligible (28)(30)(33)(34) have attributed this observation to the rippling phenomena associated with the flow of falling liquid films.

The equations pertinent to the flow of a viscous isothermal liquid film are easily derived from a force balance on a fluid element

and are available in standard texts (43). The average film thickness, m, is given by

$$m = \left[\frac{3\mu_L \Gamma}{g_c \rho_L^2}\right]^{1/3} \quad (1)$$

and the ratio of surface velocity to average velocity is

$$U_S / \bar{U}_L = 1.5 \quad (2)$$

Early experimental data on the thickness of liquid films flowing on slightly inclined surfaces have been compared with equation (1) by Cooper, Drew, and McAdams (44) who concluded that the theoretical relation was valid up to liquid Reynolds numbers of about 2100.

Kirkbride (45) measured the maximum film thickness on the outside of a vertical tube and found that equation (1) was valid for liquid Reynolds numbers up to about 8.0 but that above this value the maximum film thickness was considerably greater than the average due to the formation of ripples on the liquid surface. The liquids studied covered a viscosity range of from 0.45 to 75.0 centipoises.

Average film thicknesses for flow inside vertical tubes were measured by Fallah, Hunter, and Nash (46) and were found to be in good agreement with equation (1) up to liquid Reynolds numbers of about 1000 even when the surface of the liquid film was in rippling motion. The average film thickness was determined by suddenly stopping the flow of liquid into the tube and then measuring the drainage from the tube.

This drainage technique was also used by Friedman and Miller (47) in an investigation of the flow of water, kerosene, toluene, and a light oil on the inside surface of vertical tubes. Their data also showed good agreement with equation (1) up to a liquid Reynolds number of 500, the limit of the investigation. Their study was the first to include measurements of the velocity of the liquid surface. This was accomplished by measuring the time required for a drop of dye injected at the liquid surface to traverse a known distance. The ratio of the surface velocity to the average velocity, $U_S / \bar{U}_L$, departed from the theoretical value of 1.5 at a liquid Reynolds number of about 25. For liquid Reynolds numbers from 25 to 150, $U_S / \bar{U}_L$ increased smoothly up to a maximum of about 2.5. The dye injection technique failed at Reynolds numbers above 150. The first departure of the $U_S / \bar{U}_L$ ratio from the theoretical value was observed to be coincident with the first appearance of waves on the liquid surface. It was postulated that the increase in surface velocity was due to the formation of waves and that the surface velocity measured in the experiments was the velocity of the wave crests.

Grimley (48) made a detailed study of the flow of liquid films on vertical surfaces which includes photographs of the liquid surface during rippling. He gives an excellent description of the phenomena:

> At high flow rates the layer is thick, the flow turbulent, and the exposed surface shows the agitation associated with turbulent flow. As the rate of flow is reduced the film becomes thinner and the agitation so reduced as to be hardly visible. At still lower flow rates a new surface disturbance appears, this time in the form of a regular wave motion consisting of groups of waves which pass down the liquid surface

in the direction of flow. As the flow is further reduced this wave motion disappears and the liquid surface is once more undisturbed. Finally as a further reduction is made the film becomes so thin that it breaks into a series of disconnected streams.

Grimley's measurements of surface velocity confirmed the previous observation (47) that departure from the theoretical $U_S / \bar{U}_L$ ratio is coincident with the formation of waves. Grimley also observed that the ripple range varied with the properties of the liquid studied. For water at room temperature, ripples persisted over a range of Reynolds numbers of from 25 to about 1000. It was also noted that ripples could be suppressed by the addition of surface-active agents.

Jackson, Johnson, and Ceaglski (49) investigated the countercurrent flow of air and water-glycerol solutions in a wetted wall column. The study covered a liquid viscosity range of 0.55 to 2.8 centipoises. The liquid surface velocity was calculated from measurements of the pressure drop of the air stream and was in good agreement with the data of previous investigators (47)(48). The $U_S / \bar{U}_L$ ratio began to increase above the theoretical value of 1.5 at a liquid Reynolds number of about 25, but the increase continued only up to a liquid Reynolds number of about 80 at which point the ratio had attained a value of 2.0. The $U_S / \bar{U}_L$ ratio remained constant at 2.0 as the liquid rate was further increased up to a Reynolds number of 2000 which was the upper limit of the investigation. In agreement with the previous investigators (47)(48), wave formation was observed to be coincident with the departure of the $U_S / \bar{U}_L$ ratio from the theoretical value. It was concluded that the drag effect of the air stream was negligible for the range of air velocities employed ($8000 < \overline{Re}_V < 13{,}000$).

Dukler and Bergelin (50) obtained quantitative data on the wave profile for the flow of water down a vertical plate by measuring the electrical capacitance of the air gap between the liquid film and a capacitometer mounted at a known distance from the flow plate. At low rates the waves were widely spaced and appeared to be quite regular in nature. As the flow rate was increased a greater frequency of large waves was observed with the individual waves no longer being simple in form. Measurements of the average film thickness were in good agreement with equation (1) up to liquid Reynolds numbers of about 1000.

A method of film thickness measurement employing radioactive tracers has recently been reported by Jackson (51). A Geiger-Mueller instrument positioned in the center of a wetted wall column was used to register the radioactivity of an isotope dissolved in the film liquid. Since the observed activity depended on the film thickness an appropriate calibration served to relate the two quantities. This technique was used to determine film thicknesses for a series of liquids covering a viscosity range of 0.5 to 20 centipoises. For liquids of viscosity equal to or less than that of water the observed film thicknesses were in good agreement with equation (1) regardless of whether or not ripples were present. For liquids of viscosity greater than that of water the observed film thickness departed from the value for true viscous flow at the point of wave inception and was less than equation (1) would predict.

Jackson used flow rates covering a range of liquid Reynolds numbers of from 4000 to 5000 although this range was not obtained with

each liquid. The initial formation of waves was sharply defined as the appearance or disappearance of the waves could be effected by only a small change in the flow rate. At inception the waves appeared over the entire column except for a very short distance at the top. The spacing between the waves at inception was estimated to be 1.25 to 1.50 inches and was observed to decrease rapidly as the flow rate was increased until a condition was reached where individual waves could no longer be followed visually.

In contrast to the observations of Grimley (48), Jackson found that the surface tension was not a significant factor in either wave inception or flow pattern when waves were present. However, it should be mentioned that studies have been made (52) which indicate that an optimum concentration of surface-active agent exists for the suppression of rippling.

In accordance with the classical treatment (53) of flows involving free surfaces where only gravity effects are important, Jackson found that a Froude number of unity represented the critical point for the appearance of waves in film flow. For this application the Froude number was expressed as

$$F = \left[\frac{Re_L}{12}\right]^{1/2} \qquad (3)$$

which gave a wave point Reynolds number of 12 corresponding to a Froude number of unity. However, Jackson points out that taking the first departure of the $U_S / \bar{U}_L$ ratio from the theoretical as corresponding to the inception of waves gave a critical Froude number of 1.3 and that

this would correspond to a critical Reynolds number of about 20. The observed behavior of the $U_S / \bar{U}_L$ ratio was in substantial agreement with previous investigators (47)(48)(49) except that instead of remaining constant for liquid Reynolds numbers greater than 80 as had been previously noted (49), the ratio decreased slightly as the Reynolds number increased from 80 to 2000.

Thomas and Portalski (54) have recently investigated the countercurrent flow of water and air in a wetted wall column. Air rates covering a range of vapor Reynolds numbers of from 933 to 2000 and water rates corresponding to liquid Reynolds numbers of from 350 to 1800 were studied. The data indicated that for the range of air velocities employed the effect of the air stream on the liquid flow was negligible. On the other hand, the pressure drop in the gas phase was found to be higher for flow past the countercurrent liquid film than for flow past the just wetted column wall. This was attributed to the influence of form drag at the rippling liquid surface; however, the transition from laminar to turbulent flow in the gas phase was defined by the same values of the gas velocity regardless of the liquid rate.

Summary of the Literature

Despite numerous investigations of the effect of reduced pressure on distillation in packed columns there exists no theory, qualitative or quantitative, which will satisfactorily explain all of the observed data. Although several fundamental studies of distillation in wetted wall columns have been made at atmospheric pressure, the effect of reduced

pressure on distillation in wetted wall columns has not been investigated. In addition, there is only one report in the literature of a distillation study which includes data in all three regions of vapor flow, laminar, transitional, and turbulent.

The experimental evidence available in the literature regarding the transition from laminar to turbulent flow in pipes may be summarized as follows:

(1) In the absence of turbulence at the entrance, there appears to be neither experimental evidence of, nor theoretical reason for, an upper limiting Reynolds number for laminar flow.

(2) The Reynolds number at which transition takes place is strongly influenced by the entry conditions.

(3) Roughnesses of the order of magnitude of those encountered in ordinary piping arrangements have little influence on the transition point although such an influence is possible for relatively undisturbed entries.

(4) Departures from true laminar motion occur at Reynolds numbers as low as 850.

Those aspects of the available studies of the hydrodynamics of wetted wall columns which are essential to the proper interpretation and explanation of the data obtained in this investigation may be summarized as follows:

(1) For liquids having viscosities less than that of water rippling can be expected to begin at a Reynolds number between 8 and 25.

(2) The effect of surface tension on rippling is unresolved although as regards surface-active agents there is avidence that an optimum concentration exists for the suppression of rippling.

(3) For Reynolds numbers up to about 2000 the theoretical equation for the liquid film thickness can be expected to hold even when rippling is present.

(4) The effect of air velocities corresponding to vapor Reynolds numbers of up to 13,000 on the liquid film is negligible.

(5) As the liquid Reynolds number is increased past the point of ripple inception the ripples become more closely spaced and eventually disappear although the liquid film remains in a highly turbulent state.

(6) The ratio $U_S / \bar{U}_L$ deviates from the theoretical value of 1.5 at the inception of rippling and as the liquid Reynolds number is increased up to about 80 the ratio increases to a value of 2.0. That the $U_S / \bar{U}_L$ ratio remains essentially constant for $80 < Re_L < 2000$ has not been explained but it is likely that this indicates the attainment of a stable surface configuration which remains largely unchanged over this range of Reynolds numbers.

(7) Rippling enhances the drag experienced by the countercurrent vapor stream.

(8) For liquid Reynolds numbers greater than 350 increased liquid rate has no effect on the transition range of a countercurrent vapor stream.

(9) No satisfactory explanation of the rippling phenomena has been presented in the literature.

Scope

This investigation covers a study of the effect of reduced pressure on distillation efficiency in a wetted wall column operating at total reflux. The study includes efficiency determinations at four pressures using a chlorobenzene-ethylbenzene test mixture and at boil-up rates providing laminar, transitional, and turbulent vapor flow.

CHAPTER II

DISTILLATION THEORY

Introduction

In broadest terms distillation is a process of separation based on the experimental fact that the composition of the vapor produced by partially vaporizing a mixture of two miscible liquids is in general different from that of the original liquid. When such a mixture is partially vaporized the resulting vapor is richer in the more volatile component and the remaining liquid is proportionately poorer in the more volatile component.

Distillation columns may employ either stagewise or continuous contacting of the vapor and liquid phases. In plate-type columns contacting is stagewise while in packed and wetted wall columns contacting is continuous.

The theory of plate-type columns utilizes the concept of the theoretical plate. A theoretical plate is defined as a contacting device on which equilibrium between the vapor and liquid phases is achieved. Liquid and vapor enter the plate and exchange mass and energy to attain physical and thermal equilibrium, resulting in enrichment of the vapor leaving and depletion of the liquid leaving. For a column operating at total reflux the application of the theory is particularly simple since the compositions of the vapor and liquid streams passing each other between plates are equal; i.e., $Y_{n-1} = X_n$.

Consider a theoretical plate in a column operating at total reflux. If the vapor-liquid equilibrium of the mixture being distilled follows the relative volatility relation

$$\frac{Y^*}{1 - Y^*} = \alpha_R \frac{X}{1 - X} \tag{4}$$

then the relation between the composition of the vapor leaving the still and the liquid in the still is

$$\frac{Y_S^*}{1 - Y_S^*} = \alpha_R \frac{X_S}{1 - X_S} \tag{5}$$

The relation between the compositions of the vapor and liquid leaving the first theoretical plate is

$$\frac{Y_1^*}{1 - Y_1^*} = \alpha_R \frac{X_1}{1 - X_1} = \alpha_R \frac{Y_S^*}{1 - Y_S^*} = \alpha_R^2 \frac{X_S}{1 - X_S} \tag{6}$$

Similarly, the composition of the vapor leaving the n^{th} theoretical plate is related to the composition of the liquid in the still by

$$\frac{Y_n^*}{1 - Y_n^*} = \alpha_R \frac{Y_{n-1}^*}{1 - Y_{n-1}^*} = \ldots = \alpha_R^{n+1} \frac{X_S}{1 - X_S} \tag{7}$$

Equation (7) is the Fenske (57) equation. When written in the form

$$n = \frac{\text{Ln} \dfrac{Y_n^*}{1 - Y_n^*} - \text{Ln} \dfrac{X_S}{1 - X_S}}{\text{Ln } \alpha_R} - 1 \tag{8}$$

the equation gives the number of theoretical plates required to achieve a vapor from the n^{th} theoretical plate having a composition Y_n from a still composition X_S.

A complete discussion of the theory of plate type columns is not pertinent to this investigation. General treatments of the theory of plate columns are available in standard texts on distillation (58)(59).

Molecular Diffusion

General

The theory of molecular diffusion in gases and liquids is essential to the development of the theory of distillation in wetted wall columns. Mechanistically, molecular diffusion is the transfer of a substance resulting from random molecular motion. When a concentration difference exists this random motion of the molecules results in a net transfer of the diffusing substance from the region of high concentration to the region of low concentration.

The fundamental differential equations for diffusion of gases were first derived by Maxwell (60). They were later reexamined along somewhat different lines by Stefan (61) who also applied the diffusion laws to liquid mixtures. The following exposition of the theory follows the simplified derivation given by Lewis and Chang (61).

Consider a single molecule of one component, A, diffusing unidirectionally through a binary gas mixture of A and B. Experimental evidence indicates that the resistance to transfer by diffusion is proportional to the relative velocity of the diffusing component relative to the interfering one and to the length of the diffusion path.

In addition, the resistance should be proportional to the number of molecules of B which block the path, a number which in turn is proportional to the concentration of B. The total resistance to diffusion of component A will equal the resistance encountered by a single molecule of A times the total number of molecules of A. But the total number of molecules of A is proportional to the concentration of A. Hence, the total resistance to diffusion of A is given by the expression

$$R_T = \beta' C_A C_B (U_A - U_B) dx \tag{9}$$

If it is assumed that the influence of any external force acting upon A is negligible and that the acceleration of A is small, the resistance given by equation (9) must be overcome by an equivalent change in the concentration of A if diffusion is to occur. Thus

$$- dC_A = \beta C_A C_B (U_A - U_B) dx \tag{10}$$

This is the fundamental equation for the diffusion of gases.

Equation (10) is more conveniently expressed in terms of the molar fluxes of A and B. Making use of the fact that $C_A = Y_A C_V$ and $C_B = Y_B C_V$ equation (10) may be expressed as

$$- dY_A = \beta (C_A U_A Y_B - C_B U_B Y_A) dx \tag{11}$$

By definition, $N_A = C_A U_A$ and $N_B = C_B U_B$. Therefore,

$$- dY_A = \beta (N_A Y_B - N_B Y_A) dx \tag{12}$$

But in a binary solution $Y_B = 1 - Y_A$; consequently

$$- dY_A = \beta[N_A - (N_A + N_B)\ Y_B]\ dx \tag{13}$$

If the diffusion coefficient is defined as $D_V = 1/\beta\ C_V$, then

$$- dY_A = \frac{1}{C_V\ D_V}[N_A - (N_A + N_B)\ Y_A]\ dx \tag{14}$$

and solving for N_A yields

$$N_A = - C_V\ D_V \frac{dY_A}{dx} + (N_A + N_B)\ Y_A \tag{15}$$

Equation (15) is one of the many forms of Fick's First Law of Diffusion and may be taken as the definition of the diffusion coefficient in a binary system. The first term of equation (15) is the flux of A due to molecular diffusion and the second term is the flux of A due to the bulk motion of the fluid in the x-direction.

The derivation of expressions for the molar fluxes in three-dimensional systems is accomplished by arguments analogous to those utilized in the development of equation (15) and leads to the following expressions for the fluxes in rectangular coordinates:

$$N_{Ax} = - C_V\ D_V \frac{\partial Y_A}{\partial x} + (N_{Ax} + N_{Bx})\ Y_A \tag{16}$$

$$N_{Ay} = - C_V\ D_V \frac{\partial Y_A}{\partial y} + (N_{Ay} + N_{By})\ Y_A \tag{17}$$

$$N_{Az} = - C_V D_V \frac{\partial Y_A}{\partial z} + (N_{Az} + N_{Bz}) Y_A \qquad (18)$$

Equations (16) through (18) when combined with a material balance on the diffusing substance form the basis for the exact solution to diffusion problems in stagnant systems and systems in laminar flow.

A material balance on component A is derived by an application of the law of conservation of matter to a differential element of volume in (x,y,z) space. At steady state the accumulation of component A is zero. Hence the sum of the fluxes entering the element must equal the sum of the fluxes leaving the element. Equating the entering and leaving fluxes leads to

$$\frac{\partial N_{Ax}}{\partial x} + \frac{\partial N_{Ay}}{\partial y} + \frac{\partial N_{Az}}{\partial z} = 0 \qquad (19)$$

which is the continuity equation for component A in a binary mixture.

Substitution of the flux expressions, equation (16) through (18), into the continuity equation assuming constant fluid properties and noting that $(N_{Ax} + N_{Bx}) = C_V U_x$, $(N_{Ay} + N_{By}) = C_V U_y$, and $(N_{Az} + N_{Bz}) = C_V U_z$ yields

$$U_x \frac{\partial Y_A}{\partial x} + U_y \frac{\partial Y_A}{\partial y} + U_z \frac{\partial Y_A}{\partial z} = D_V \left[\frac{\partial^2 Y_A}{\partial x^2} + \frac{\partial^2 Y_A}{\partial y^2} + \frac{\partial^2 Y_A}{\partial z^2} \right] \qquad (20)$$

The equivalent of equation (20) in right circular cylindrical coordinates is

$$U_r \frac{\partial Y_A}{\partial r} + U_\theta \frac{1}{r} \frac{\partial Y_A}{\partial \theta} + U_z \frac{\partial Y_A}{\partial z} = D_V \left[\frac{1}{r} \frac{\partial}{\partial r} \left(r \frac{\partial Y_A}{\partial r} \right) + \frac{1}{r^2} \frac{\partial^2 Y_A}{\partial \theta^2} + \frac{\partial^2 Y_A}{\partial z^2} \right] \qquad (21)$$

Equations (20) and (21) are valid for steady state diffusion in stagnant binary systems or binary systems in laminar motion when the fluid properties of the mixture are assumed constant.

Solutions of equations (20) and (21) have been obtained for the case of the evaporation of a pure liquid into a laminar vapor stream and the absorption of a solute gas by a laminar liquid film. Sherwood and Pigford (62) review these solutions and compare them with experimental data. These authors point out that in the case of the evaporation of a pure liquid into a laminar air stream the theoretical and experimental data are brought into agreement by allowing for the effect of density gradients on the velocity profile of the air stream.

Pigford (28) has obtained a solution to equation (21) for the absorption of a solute gas by a laminar liquid film. Discrepancies between theory and experiment were appreciable and were attributed to the influence of rippling at the liquid surface. The effect of rippling was presumed to enhance radial mixing in the laminar film and hence reduce its resistance to mass transfer.

Westhaver's Equation

By making an ingenious set of simplifying assumptions, Westhaver (63) solved equation (21) for the case of the distillation of a binary mixture in a wetted wall column where the vapor phase is in laminar flow. Allowing for symmetry about the axis of the column, equation (21), written in terms of the mole fraction of the more volatile component, becomes

$$U_V \frac{\partial Y}{\partial z} = \frac{D_V}{r} \frac{\partial}{\partial r} \left(r \frac{\partial Y}{\partial r} \right) + D_V \frac{\partial^2 Y}{\partial z^2} \qquad (22)$$

The coordinates r and z are measured from the axis and base of the column, respectively.

At total reflux and steady state there is no net accumulation of the more volatile component at any point in the column. Therefore a material balance on the more volatile component passing through a plane at height z extending across the entire column yields

$$\int^{A} C\, U_V\, dA - \int^{A} D_V \frac{\partial C}{\partial z}\, dA - X\, L = 0 \qquad (23)$$

Assuming equal molal overflow and total reflux, the molal liquid rate down the column is equal to the molal vapor rate up the column. Expressed mathematically

$$L = C_V \bar{U}_V A = \int_0^{r_0} C_V U_V (2\pi r\, dr) \qquad (24)$$

Substituting into equation (23) and integrating across the vapor space gives

$$\int_0^{r_0} [(C - XC_V) U_V - D_V \frac{\partial C}{\partial z}] 2\pi r\, dr = 0 \qquad (25)$$

By noting that $C = C_V Y$, equation (25) may be written in terms of the mole fraction of the more volatile component.

$$\int_0^{r_0} [(Y - X) U_V - D_V \frac{\partial Y}{\partial z}] r\, dr = 0 \qquad (26)$$

Neglecting diffusion in the z-direction in comparison with bulk transport in the z-direction, equation (22) becomes

$$U_V \frac{\partial Y}{\partial z} - \frac{D_V}{r} \frac{\partial}{\partial r} \left(r \frac{\partial Y}{\partial r}\right) = 0 \qquad (27)$$

The velocity distribution in the vapor phase is given by the familiar Hagen-Poissuille law (64).

$$U_V = 2\bar{U}_V \left[1 - \frac{r^2}{r_O^2}\right] \tag{28}$$

Substitution of equation (28) into equation (27) and integration under the assumption that $\frac{\partial Y}{\partial z}$ is independent of r using the boundary condition that $r \frac{\partial Y}{\partial r} = 0$ at $r = 0$; i.e., there is no transfer across the center line of the column, gives

$$dY = \frac{\bar{U}_V}{D_V} \frac{\partial Y}{\partial z} \left(r - \frac{r^3}{2r_O^2}\right) dr \tag{29}$$

By assuming $\frac{\partial Y}{\partial z}$ is independent of r and substituting for U_V from equation (28), equation (26) can be integrated by parts to give

$$(Y^* - X)\ \bar{U}_V \frac{r_O^2}{2} - D_V \frac{\partial Y}{\partial z} \frac{r_O^2}{2} - \int_0^{r_O} \bar{U}_V \left(r^2 - \frac{r^4}{2r_O^2}\right) dY \tag{30}$$

The boundary condition used in obtaining equation (30) is $(Y - X) = (Y^* - X)$ at $r = r_O$; i.e., equilibrium obtains at the vapor-liquid interface. Furthermore, it is necessary to assume that the liquid composition is invariant in the r-direction.

Substituting for dY in equation (30) by using equation (29) and completing the integration, again assuming that $\frac{\partial Y}{\partial z}$ is independent of r, yields

$$\frac{dY}{y^* - X} = \frac{dz}{\frac{11}{48}\frac{\bar{U}_V r_O^2}{D_V} + \frac{D_V}{\bar{U}_V}} \tag{31}$$

If $1 < \alpha_R < 1.1$, than as Westhaver (63) points out, $(Y^* - X)$ is closely approximated by $(\text{Ln } \alpha_R)[Y^*(1 - X)]$ and, since $Y = X$ at total reflux, equation (31) may be integrated to give

$$\text{Ln} \frac{\left(\frac{Y^*}{1 - Y^*}\right)_T}{\left(\frac{Y^*}{1 - Y^*}\right)_B} = \frac{(\text{Ln } \alpha_R)\ Z}{\frac{11}{48}\frac{\bar{U}_V r_O^2}{D_V} + \frac{D_V}{\bar{U}_V}} \tag{32}$$

Rearranging,

$$\frac{Z}{\frac{\text{Ln}\left(\frac{Y^*}{1 - Y^*}\right)_T - \text{Ln}\left(\frac{Y^*}{1 - Y^*}\right)_B}{\text{Ln } \alpha_R}} = \frac{11}{48}\frac{\bar{U}_V r_O^2}{D_V} + \frac{D_V}{\bar{U}_V} \tag{33}$$

Now recall that equation (8) gives the number of theoretical plates required to effect a given separation,

$$n = \frac{\text{Ln}\left(\frac{Y^*}{1 - Y^*}\right)_T - \text{Ln}\left(\frac{Y^*}{1 - Y^*}\right)_B}{\text{Ln } \alpha_R} \tag{8}$$

Thus equation (33) may be written as

$$\frac{Z}{n} = \frac{11}{48}\frac{\bar{U}_V r_O^2}{D_V} + \frac{D_V}{\bar{U}_V} \tag{34}$$

The quantity on the left was defined by Peters (65) to be the "height equivalent to a theoretical plate." Thus,

$$\text{HETP} = \frac{11}{48}\frac{\bar{U}_V\, r_o^2}{D_V} + \frac{D_V}{\bar{U}_V} \tag{35}$$

Equation (35) is the final result obtained by Westhaver (63).

A similar result has been independently obtained by Kuhn (66) and Cohen (28). More recently Aris (67) has shown that Westhaver's equation is a special case of a general analysis of the apparent dispersion of the mean concentration in fluids in laminar flow.

Before comparing the theory with experiment it will be useful to list the assumptions both implicit and explicit in Westhaver's derivation. These assumptions are:

(1) The mixture under consideration is close boiling; i.e., $1 < \alpha_R < 1.1$.

(2) The column is operating under steady state conditions at total reflux.

(3) The flow of the vapor is laminar.

(4) The velocity of the vapor is constant and independent of the height.

(5) The average vapor velocity is large compared with the average liquid velocity.

(6) The liquid film flows evenly over the entire inner surface of the column.

(7) The vapor and the liquid are in equilibrium at the vapor-liquid interface.

(8) The liquid film is uniform in composition in the radial direction.

(9) The vertical concentration gradient in the vapor is essentially independent of the radial gradient.

(10) Diffusion in the z-direction is negligibly small compared to the bulk transport in that direction.

The restriction that the mixture be close boiling can be removed by direct integration of equation (31). Thus, at total reflux $Y = X$ and therefore integration of equation (31) yields

$$\int_{Y_B}^{Y_T} \frac{dY}{y^* - Y} = \frac{Z}{\frac{11}{48}\frac{\bar{U}_V r_O^2}{D_V} + \frac{D_V}{\bar{U}_V}} \tag{36}$$

Rearranging gives,

$$H_G = \frac{Z}{\int_{Y_B}^{Y_T} \frac{dY}{Y^* - Y}} = \frac{11}{48}\frac{\bar{U}_V r_O^2}{D_V} + \frac{D_V}{\bar{U}_V} \tag{37}$$

The quantity H_G is called the "height of a transfer unit" and is discussed in detail later in this chapter. It is entirely analogous in meaning to the HETP in Westhaver's original result, equation (35).

Glasebrook (68) and Westhaver (63) compared equation (35) with the available experimental data and found qualitatively good agreement between the theory and experiment. Exact quantitative agreement was

generally not obtained due to the difficulty of providing adequate column insulation (25) at low flow rates and uncertainties regarding the correct value of the diffusion coefficient.

Mass Transfer in Turbulent Flow

General

In turbulent flow in conduits, particles of fluid no longer flow in the orderly manner characteristic of laminar flow. Instead, the character of the flow at a point exhibits a marked dependency on the distance from the conduit wall. In the region near the center of the conduit the fluid motion is highly random with large discrete eddies of fluid moving rapidly from one position to another. As the conduit wall is approached the fluid motion becomes more regular until finally in a region close to the wall the fluid motion becomes essentially laminar.

In laminar flow the radial transfer of mass depends only on molecular motion of the diffusing substance. In turbulent flow a second mechanism is involved: that of mixing and interchange between macroscopic fluid entities. In the vicinity of the conduit wall the motion of the eddies is damped, since they cannot move radially, and mass transfer depends primarily on molecular motion. In the main fluid stream transfer by eddy mixing and interchange is much more rapid than transfer by molecular motion. Near the wall transfer by molecular diffusion is slow, but the distances involved are small; in the turbulent core transfer by eddy diffusion is rapid, but the distances involved

are relatively large. Hence, both molecular diffusion and the turbulence conditions influence the overall rate of mass transfer in the fluid. Because of the lack of a fundamental understanding of the process of eddy motion and its interrelation with molecular motion the treatment of the problem of mass transfer in turbulent flow has been essentially empirical.

Film Theory

Measurements of concentration gradients in turbulent flow (69) have shown that the major resistance to the overall transfer process lies in the region near the wall of the conduit. This fact led to the "film" concept proposed by Whitman and Keats (70) which assumed that the entire resistance to mass transfer was confined to a thin film of stagnant fluid next to the conduit wall. Under this assumption, at steady state, the rate of mass transfer through the film can be obtained by integration of equation (15).

$$N_A = - C_V D_V \frac{dY_A}{dx} + (N_A + N_B) Y_A \qquad (15)$$

One of the basic assumptions of conventional distillation theory under conditions of total reflux is that of equi-molal overflow; that is, the molal liquid and vapor rates at any point in a column are equal. This assumption is generally valid for distillation involving close boiling mixtures and, for the use intended here, takes the form

$$N_A = - N_B \qquad (38)$$

Making this substitution and integrating across the film thickness B, assuming $C_V D_V$ is constant gives

$$N_A = -\frac{C_V D_V}{B}(Y - Y_i) = \frac{C_V D_V}{B}(Y_i - Y) \qquad (39)$$

In terms of the molar diffusion coefficient, D_m, equation (39) may be expressed as

$$N_A = \frac{D_m}{B}(Y_i - Y) \qquad (40)$$

Since for a given set of circumstances D_m/B is constant, these terms serve to define the gas film mass-transfer coefficient, k_G.

$$k_G = \frac{D_m}{B} = \frac{C_V D_V}{B} \qquad (41)$$

The quantity B is the thickness of a fictitious or effective film which has a resistance to mass transfer by molecular diffusion equal to that offered by the real laminar film and the turbulent core.

The mass transfer rate in terms of k_G is then

$$N_A = k_G (Y_i - Y) \qquad (42)$$

Analogous derivations have been carried out for diffusion in liquids (71) and lead to the equation

$$N_A = \frac{D_L}{B}(X - X_i) = k_L (X - X_i) \qquad (43)$$

In equation (43), the quantity B refers to the thickness of an effective liquid film.

The more general problem of distillation in a wetted wall column in which the vapor is in turbulent flow involves mass transfer between

two phases. Hence the resistance to mass transfer of both phases must be considered.

The first systematic treatment of mass transfer between phases is due to Lewis and Whitman (72) who proposed that the entire resistance to mass transfer could be assumed to reside in two thin films on either side of the gas-liquid interface. It was also assumed that the gas and liquid were in equilibrium at the interface and that outside the films the compositions of the two phases were uniform.

If these films are thin the actual amount of material contained in them is negligible compared to the amount of material diffusing through them. Therefore, transport due to the bulk motion of the films is negligible and the rates of mass transfer through the films may be equated. Thus,

$$N_A = k_G (Y_i - Y) = k_L (X - X_i) \tag{44}$$

In practice the local coefficients k_G and k_L are difficult to determine and the interfacial compositions X_i and Y_i are unknown. If the relation between the interfacial compositions is linear, equation (44) may be expressed in terms of overall coefficients (73). Therefore,

$$N_A = K_G (Y^* - Y) = K_L (X - X^*) \tag{45}$$

The overall and individual coefficients are related (73) by

$$\frac{1}{K_G} = \frac{1}{k_G} + \frac{q}{k_L} \tag{46}$$

The quantity K_G is an overall mass transfer coefficient accounting for the entire diffusional resistance present in both phases in terms of a vapor mole fraction driving force. The terms $1/k_G$ and a/k_L represent the relative resistances to mass transfer within the individual phases.

In general, both the gas film and the liquid film may be expected to offer appreciable resistance to mass transfer in distillation columns. However, the majority of investigators (28)(30)(33)(34) of distillation in wetted wall columns have found the resistance of the liquid film to be negligible and have attributed this to the agitation of the liquid surface caused by rippling.

Assuming the liquid film resistance to be negligible, equation (46) becomes

$$\frac{1}{K_G} = \frac{1}{k_G} \tag{47}$$

and equations (40) and (45) may be written as

$$N_A = \frac{D_m}{B} (Y^* - Y) = k_G (Y^* - Y) \tag{48}$$

The mass transfer coefficient is related to the column height by a material balance over a differential element of the column of height dz. Thus,

$$dW = \frac{G A \, dY}{M_m} = k_G (Y^* - Y) \, dS \tag{49}$$

In a wetted wall column the surface area normal to mass transfer is $(\pi d)\, dz$ and the cross sectional area is $\pi d^2/4$. Thus,

$$\frac{(\pi d^2/4)\,G\,dY}{M_m} = k_G\,(Y^* - Y)(\pi d)\,dz \tag{50}$$

Rearranging and integrating,

$$\int_{Y_B}^{Y_T} \frac{dY}{Y^* - Y} = \frac{4\,k_G\,M_m\,Z}{Gd} \tag{51}$$

This equation serves as the basis for the computation of mass transfer coefficients from experimental data.

The integral on the left of equation (51) was defined by Chilton and Colburn (74) as the number of transfer units. That is,

$$N_{tG} = \int_{Y_B}^{Y_T} \frac{dY}{Y^* - Y} \tag{52}$$

The height of a transfer unit is defined in the same way that Peters (65) defined the HETP. Thus,

$$H_G = Z/N_{tG} \tag{53}$$

The quantity H_G is related to k_G and B by equations (48) and (51). Therefore,

$$H_G = \frac{Z}{N_{tG}} = \frac{Gd}{4\,k_G\,M_m} = \frac{BG\,d}{4\,D_m\,M_m} \tag{54}$$

Since the effective film thickness, mass transfer coefficient, and height of a transfer unit are quantitatively related, none of these quantities has any more theoretical significance than any of the others. The method of data presentation is purely a matter of convenience.

However, presentation in terms of H_G and B has some advantage over the use of k_G since the former quantities are expressible in terms of a single dimension, length, while k_G has the dimensions of moles transferred/ unit area - unit time. To facilitate the comparison of the data of this investigation with that of previous investigators both H_G and B have been used.

The evaluation of N_{tG} from equation (52) requires a relation between Y* and Y. In general this relation is provided by the vapor-liquid equilibrium data and the operating line. If the distillation is carried out under total reflux the operating line is Y = X. Then if the vapor-liquid equilibrium data can be expressed as

$$\frac{Y^*}{1 - Y^*} = \alpha_R \frac{X}{1 - X} \tag{4}$$

equation (52) may be integrated in closed form (74) to obtain

$$N_{tG} = \frac{2.303}{\alpha_R - 1} \left[\text{Log} \frac{Y_T}{Y_B} - \alpha_R \text{ Log} \frac{1 - Y_T}{1 - Y_B} \right] \tag{55}$$

Equation (54) may then be used to calculate values of H_G, k_G, and B. Thus,

$$H_G = Z / N_{tG} \tag{53}$$

$$k_G = \frac{G N_{tG} d}{4 M_m Z} \tag{56}$$

$$B = \frac{4 D_m M_m Z}{G N_{tG} d} \tag{57}$$

The film concept has been of great value in furnishing a simple picture of a complicated process and in providing a common basis for the presentation and comparison of mass transfer data; however, as a theoretical basis for the correlation and interpretation of data it leaves much to be desired. Consequently, studies of mass transfer in turbulent flow have primarily been directed toward the discovery of the variables which influence the rate of mass transfer and the incorporation of these variables into useful empirical correlations.

As has been previously stated, the development of the film concept was motivated by a recognition of the fact that measured concentration gradients in turbulent flow show that the majority of the resistance to mass transfer lies in a thin layer next to the conduit wall and that there is a thin layer of fluid next to the conduit wall whose motion is essentially laminar. The thickness of the laminar film is a function of the degree of turbulence of the fluid and can be described by the vapor Reynolds number (41)(42). The resistance of the turbulent region should also be a function of the Reynolds number. The molecular diffusivity should be important in determining the rate of transfer through the laminar film. Therefore, the rate of mass transfer should depend on the vapor diffusivity and the quantities making up the vapor Reynolds number. Dimensional analysis (75) of these variables leads to the conclusion that

$$\frac{d}{B} = f(Re_V, Sc_V) \tag{58}$$

Most investigations of distillation in wetted wall columns have been concerned with empirically defining the form of the functional relationship indicated by equation (58).

Johnstone and Pigford (28) correlated distillation data on four systems covering a Schmidt number range of 0.54 to 0.72 and a Reynolds number range of 4000 to 26,000 by the empirical equation

$$\frac{H_G}{d} = 7.63\ \overline{Re}_V^{0.23}\ Sc_V^{0.67} \tag{59}$$

which may be equivalently expressed as

$$\frac{d}{B} = 0.033\ \overline{Re}_V^{0.77}\ Sc_V^{0.33} \tag{60}$$

Jackson and Ceaglski's data (33) for the distillation of 2-propanol-water over a Reynolds number range of 1800 to 72,000 at both total and partial reflux were in good agreement with equation (59).

Gilliland and Sherwood's data (18) for the vaporization of eight organic liquids and water covered a Schmidt number range of 0.60 to 2.26 and a Reynolds number range of 2000 to 36,000. In addition, the pressure was varied from 110 to 2330 millimeters of mercury. All of the data were correlated by the empirical equation

$$\frac{d}{B} = 0.023\ Re_V^{0.83}\ Sc_V^{0.44} \tag{61}$$

which in terms of H_G / d is

$$\frac{H_G}{d} = 10.9\ Re_V^{0.17}\ Sc_V^{0.56} \tag{62}$$

It is interesting to note that Gilliland and Sherwood found that a Reynolds number relative to the tube wall correlated their data for both cocurrent and countercurrent vapor flow better than a Reynolds number relative to the liquid surface velocity. The authors explained this paradox by postulating that the apparatus which they used was too short for the velocity gradient of the air stream to be appreciably affected by the liquid surface.

The data of Yoshida (34) for the distillation of four binary systems covering a Schmidt number range of 0.41 to 0.72 and a Reynolds number range of 2200 to 22,000 showed the same Reynolds number dependence as equation (61) but the data for the individual systems were neither correlated by the factor $Sc_v^{0.44}$ nor the factor $Sc_V^{0.33}$; however, the data were well correlated by a different concept which will be discussed later.

As regards the effect of the vapor Reynolds number, the agreement among the various investigators is very good. It seems reasonably certain that the effects of vapor turbulence on the effective film thickness can be expressed by the relation

$$\frac{d}{B} \alpha \ Re_V^{0.80} \tag{63}$$

over the Reynolds number range of 2000 to 70,000 provided that the vapor stream is truly in turbulent flow.

The effect of the molecular properties of the fluid, as they are incorporated in the Schmidt number, is still open to question. The empirical relations which have been presented would indicate that

$$\frac{d}{B} \alpha \, Sc_V^{0.33} = \left(\frac{\mu_V}{\rho_V D_V}\right)^{0.33} \tag{64}$$

or that

$$\frac{d}{B} \alpha \, Sc_V^{0.44} = \left(\frac{\mu_V}{\rho_V D_V}\right)^{0.44} \tag{65}$$

As Sherwood (76) points out, this discrepancy cannot be settled on the basis of data covering a Schmidt number range of only 0.41 to 2.26. In fact, the problem would seem to be much more than simply deciding whether d/B is proportional to $Sc_V^{0.33}$ or $Sc_V^{0.44}$.

The successful application of the principles of dimensional analysis depends on the inclusion of all the pertinent variables affecting the situation for which the analysis is to be made. There is ample evidence that the effective film thickness depends on more than just the vapor velocity, density, viscosity, and diffusivity, and on the tube diameter.

A recent investigation (36) of the effect of the length-to-diameter ratio on distillation in wetted wall columns has shown that for laminar flow

$$\frac{d}{B} \alpha \left(\frac{d}{Z}\right)^{0.324} \tag{66}$$

while for flow in the transition region

$$\frac{d}{B} \alpha \left(\frac{d}{Z}\right)^{0.722} \tag{67}$$

and for turbulent flow

$$\frac{d}{B} \alpha \left(\frac{d}{Z}\right)^{0.10} \tag{68}$$

However, the apparatus used in the investigation provided a minimum of calming ahead of the test section and, hence, probably magnified the effect of the length-to-diameter ratio above what would be observed in a column which provided a calming section of normal length.

Some investigators (31)(32)(33)(56) have found an influence of composition on d/B which could not be correlated by a simple power law relationship with the Schmidt number. Storrow (31), in discussing this composition effect, concluded that "... a correlation equation containing simple powers of dimensionless groups, such as Reynolds number and Schmidt number, can only be expected to be of general use for data obtained over a limited range of vapor composition with a specific binary system."

There is evidence (55) that the surface tension characteristics of the liquid reflux film can significantly influence the mass transfer rate in wetted wall columns. However, this effect should be limited to systems of high relative volatility and then only at the lower flow rates.

The phenomena of liquid film rippling (45)(48)(50)(51) and its effect on distillation in wetted wall columns has not been extensively studied. Since the vapor stream is bounded by the liquid film, rippling would be expected to influence the vapor stream turbulence, and hence the mass transfer rate, as a form of "wall" roughness. Although there is experimental evidence (48)(51) that the character of the rippling varies with the physical properties of the liquid film, the general agreement of the distillation data of the various investigators would indicate that the effect of rippling is slight in the region of turbulent vapor flow.

It has often been suggested that there is a theoretical basis for expecting that the exponent on the Schmidt group in equation (61) should be between zero and unity since mass transfer in the turbulent core should be essentially independent of the molecular diffusivity while mass transfer in the laminar film should be proportional to the first power of the molecular diffusivity. An exponent between zero and unity is then supposed to indicate the duality of the mass transfer mechanism. As Gilliland (35) points out, this is an erroneous conclusion since for the mechanism described above the actual effect of diffusivity should be represented by a sum of terms and not a power function.

Turbulent Core - Laminar Layer Concept

A modification of the original film concept which conforms more closely to the actual situation existing in turbulent flow has been successfully applied to vaporization (35) and distillation (34) in wetted wall columns. This modification, just as the simple film concept, assumes that mass transfer in turbulent flow takes place ty two different mechanisms. In the laminar layer, where turbulence is at a minimum, the transfer is assumed to be largely by molecular diffusion; in the turbulent core the transfer is assumed to be mainly by convection due to rapid eddy motion. However, instead of assuming that the entire resistance to mass transfer resides in a fictitious laminar film, it is assumed that the total resistance is the sum of the resistance of the turbulent core and the resistance of the true laminar layer.

The turbulent core-laminar layer concept has the advantage of presenting a simple picture of the mass transfer mechanism from which

calculations can be made while at the same time conforming closely to the actual physical situation. It is distinguished from the simple film concept in two fundamental ways: first, it recognizes that the turbulent core does offer resistance to mass transfer, and second, it recognizes that a laminar layer of definite thickness (41)(42) actually does exist where molecular diffusion controls.

Equation (48) was derived for equimolal counter diffusion through a stagnant film under conditions of negligible liquid film resistance. As has been previously discussed, the equations for molecular diffusion through stagnant films are equally applicable to transfer in laminar films in a direction normal to the streamlines. Hence, for a thin laminar layer of thickness B_f equation (48) takes the form

$$N_A = \frac{D_m}{B_f} (Y^* - Y_f) = k_{Gf} (Y^* - Y_f) \tag{69}$$

In terms of partial pressure driving forces equation (69) becomes

$$N_A = \frac{D_m}{P\ B_f} (p^* - p_f) = k'_{Gf} (p^* - p_f) \tag{70}$$

Thus,

$$k'_{Gf} = \frac{D_m}{P\ B_f} = \frac{D_V}{R\ T\ B_f} \tag{71}$$

The resistance of the laminar layer is then

$$r_f = \frac{1}{k'_{Gf}} = \frac{R\ T\ B_f}{D_V} = \frac{P\ B_f}{D_m} \tag{72}$$

Assuming that the total resistance to mass transfer between the interface and the main body of the gas can be taken as two resistances in series, that of the turbulent core and that of the laminar layer,

$$N_A = \frac{p_f - p}{r_c} = \frac{p^* - p_f}{r_f} = \frac{p^* - p}{R_T} = k'_G (p^* - p) \qquad (73)$$

The overall gas phase resistance is then

$$R_T = \frac{1}{k'_G} = r_c + \frac{R\ T\ B_f}{D_V} \qquad (74)$$

As has been previously stated the mechanism of mass transfer in the turbulent core is not well understood; however, there is experimental evidence (34)(35) that for distillation and vaporization in wetted wall columns the resistance of the turbulent core and the thickness of the laminar layer are power functions of the vapor Reynolds number; i.e.,

$$r_c = c\ Re_V^{\ a} \quad \text{and} \quad B_f = f\ Re_V^{\ a} \qquad (75)$$

where c and f are proportional constants referring to the turbulent core and the laminar layer, respectively.

Applying these relations to equation (74) yields

$$\frac{1}{k'_G} = \left[c + \frac{R\ T\ f}{D_V}\right] Re_V^{\ a} \qquad (76)$$

The coefficient k'_G is related to the customary quantities used for the evaluation of mass transfer data as follows:

$$k_G = k'_G P \tag{77}$$

$$H_G = \frac{G d}{4 M_m k'_G P} \tag{78}$$

$$B = \frac{D_m}{k'_G P} \tag{79}$$

Gilliland (35) has applied the turbulent core-laminar layer concept to data (18) obtained for the vaporization of liquids into a turbulent air stream. The application of the simple film concept to these data has already been discussed and it was pointed out that the data were well correlated by the empirical relation given by equation (61).

Gilliland obtained an equally good correlation by applying equation (76) to the data. This correlation may be expressed as

$$\frac{1}{k'_G} = \left[903 + \frac{135}{D_V}\right] Re_V^{-0.80} \tag{80}$$

Gilliland points out that although equation (61) is convenient and gives good results for the data it is incompatible with the turbulent core-laminar layer concept. Gilliland also suggests that the variations in D_V are not large enough to test adequately the two methods of correlation.

Yoshida (34) applied the turbulent core-laminar layer concept to distillation data obtained in a wetted wall column and developed the correlation

$$\frac{d}{B} = 0.022 \left[\frac{1.0/D_m}{130 + 1.0/D_m}\right] Re_V^{0.80} \tag{81}$$

Yoshida's data could not be correlated by either of the simple power law expressions given by equations (60) and (61).

To use equations (80) and (81) the diffusivity must be expressed in the units for which the equations were derived. Taking D_V in (cm.^{2}/sec.) in equation (80) gives k'_G in (lb.-moles/ft.^{2}-hr.-atm.). Taking D_m in (kg.-moles/hr.-meter) makes d/B dimensionless in equation (81). Equations (80) and (81) cannot be quantitatively compared because the empirical constants contained in the equations cannot be related.

Even though the turbulent core-laminar layer concept is in much closer accord with known mass transfer behavior in turbulent flow than the simple film theory it is still an oversimplification of the true situation. Its primary fault is that is makes no allowance for the length of the diffusion path in its treatment of the resistance of the turbulent core. The correlations developed by Gilliland and Yoshida ignore this factor and hence should be applicable only to data obtained in tubes of the same diameter as those for which the correlations were originally developed. In addition, Treybal (77) points out that despite theoretical indications that physical properties should be unimportant in determining mass transfer in the turbulent core there is experimental evidence (69) to the contrary. Gilliland and Yoshida also neglected the possible influence of physical properties in the turbulent core.

Analogies

Another approach to mass transfer in turbulent flow is based on the similarity of the processes of mass transfer, heat transfer, and

momentum transfer. Since each of these processes depends on molecular properties and on the motion of eddies in the turbulent stream, it is reasonable to assume that they are closely related. In fact, it can be demonstrated (78) that under certain idealized conditions the three transport processes are mathematically analogous in the sense that an equation derived for one of the processes can be transformed into a valid representation of either of the other two by an appropriate change of variables.

The analogies among the transport processes have received considerable attention and the literature on the subject is quite extensive; however, Sherwood (79) has recently provided an excellent critical review of this general topic. Sherwood points out that basically most of the analogies differ only in their treatment of the variation of the degree of turbulence with radial position and that for Schmidt or Prandtl numbers close to unity they are all in close agreement. Hence the purpose of this investigation can be served by considering only one of these analogies.

Perhaps the best known and most widely used analogy is that of Chilton and Colburn (80)(81). These authors modified the analogy between heat transfer and fluid friction, as conceived by Reynolds, by introducing an empirical correction for the effect of molecular properties and later extending the analogy to include mass transfer. The analogy is conveniently summarized in terms of the "j-factors":

$$j_H = \frac{h}{Cp\ G}\left(\frac{Cp\ \mu_V}{k}\right)^{2/3} = j_D = \frac{k'_G\ P\ M_m}{G}\left(\frac{\mu_V}{\rho_V\ D_V}\right)^{2/3} = f/2 \qquad (82)$$

The friction factor for flow in smooth pipes can be expressed empirically (82) as

$$f/2 = 0.023\ Re_V^{-0.20} \tag{83}$$

Combining equations (82) and (83), the Chilton-Colburn analogy may then be expressed as

$$\frac{H_G}{d} = 10.9\ Re_V^{0.20}\ Sc_V^{0.67} \tag{84}$$

or alternatively as

$$\frac{d}{B} = 0.023\ Re_V^{0.80}\ Sc_V^{0.33} \tag{85}$$

There is considerable experimental evidence confirming the qualitative validity of the general analogy among the transport processes. For example, heat transfer data for turbulent flow in pipes (82) has been correlated by

$$\frac{hd}{k} = 0.023\ Re_V^{0.8}\ Sc_V^{0.3} \tag{86}$$

which may be compared with

$$\frac{d}{B} = 0.023\ Re_V^{0.83}\ Sc_V^{0.44} \tag{61}$$

for mass transfer in turbulent flow. Jackson (33) compared j_D factors derived from distillation data with friction factors and found j_D and $f/2$ to be in good agreement.

Johnstone and Pigford (28) found that the Chilton-Colburn analogy predicted values of H_G / d about 30 per cent higher than were actually

observed although a 2/3 power on the Schmidt group correlated the data over a Schmidt number range of 0.54 to 0.72. Gilliland and Sherwood's data (18) cover the widest range of Schmidt numbers (0.60 to 2.26) that have been investigated in vapor phase mass transfer and therefore offer the best test of the analogy. As equation (61) shows, the data are correlated by a Schmidt number exponent of 0.44 instead of the exponent 0.33 predicted by the analogy. Yoshida's data (34), which covered a Schmidt number range of 0.41 to 0.74, could not be correlated by any of the relations which included the Schmidt number raised to a fractional power.

Treybal (82) suggests that the discrepancy in the Schmidt group exponent is probably due to experimental error and thus does not really exist. However, if the experimental errors are large enough to account for the discrepancy it seems much more logical to conclude that the analogy has not really been experimentally verified for vapor phase mass transfer. As Sherwood (76) has pointed out, the range of Schmidt numbers which has been investigated is simply too narrow to settle this discrepancy on the basis of the available data.

The fact that a discrepancy exists and that it can be reconciled only by experiment emphasizes the fundamental limitation of the general analogy concept. All of the analogies depend on experimental data not only for their verification but also for their derivation. For example, the 2/3 power on the Schmidt group in the Chilton-Colburn analogy was taken by analogy with the empirically determined 2/3 power on the Prandtl group. In more sophisticated analogies (79) the empiricism enters as an

experimentally determined velocity profile or in the form of "universal" empirically determined constants. Therefore, any mass transfer equation derived by analogy with heat transfer or momentum transfer is really nothing more than a transposed representation of heat or momentum transfer data, and consequently, its applicability under conditions in any way different from those existing during the acquisition of the original data is questionable.

From the point of view of this investigation, the most serious limitation of the analogy concept is that it offers no theoretical basis for predicting the effect of reduced pressure on distillation. However, the data of this investigation will provide a test of the analogy concept under conditions somewhat different than have hitherto been examined.

Prediction of the Effect of Reduced Pressure

Laminar Flow

In the region of laminar vapor flow the theoretical equation originally derived by Westhaver (63) and modified by the present author is available:

$$H_G = \frac{11}{48} \frac{\bar{U}_V \, r_O^2}{D_V} + \frac{D_V}{\bar{U}_V} \qquad (37)$$

The term $D_V / \bar{U}_V$ is due to back diffusion and is negligible for the range of velocities normally attainable (63) in laminar flow. Hence, equation (37) may be written as

$$H_G = \frac{11}{48} \frac{\bar{U}_V \, r_O^2}{D_V} \qquad (87)$$

Therefore, at constant vapor velocity the efficiency should be inversely proportional to the volumetric diffusion coefficient. Experimentally (83), D_V is found to be inversely proportional to the pressure and approximately proportional to the 3/2 power of the absolute temperature. Therefore

$$H_G \alpha \frac{P}{T^{3/2}} ; \quad (\bar{U}_V = \text{constant}) \tag{88}$$

In distillation columns the operating temperature and operating pressure are related by the requirements of phase equilibrium. Consequently, a reduction in pressure is accompanied by a reduction in operating temperature. Since the pressure-temperature relation is logarithmic (84), the pressure decreases faster than the temperature. Therefore, according to equation (88), the net effect of a decrease in pressure at constant vapor velocity would be a decrease in H_G; i.e., an increase in efficiency.

The magnitude of the pressure effect depends on the mixture being distilled but an estimate of the order of magnitude to be expected can be made by calculating the expected change in H_G for the chlorobenzene-ethylbenzene mixture used in this investigation. At a pressure of 736 millimeters of mercury the operating temperature would be approximately 133 degrees centigrade and at 20 millimeters of mercury the temperature would be about 38 degrees centigrade. Then,

$$\frac{(H_G)_{20}}{(H_G)_{736}} = \frac{20/(311)^{3/2}}{736/(406)^{3/2}} = 0.0406 \tag{89}$$

At constant vapor velocity a 40-fold reduction in pressure would therefore be expected to cause a 25-fold increase in efficiency.

A prediction of the effect of pressure at constant vapor Reynolds number may be made by putting equation (87) in the form

$$\frac{H_G}{d} = \frac{11}{192} \frac{\bar{U}_V \, d}{D_V} \frac{\rho_V / \mu_V}{\rho_V / \mu_V} = \frac{11}{192} \left(\frac{\bar{U}_V \, \rho_V \, d}{\mu_V} \right) \left(\frac{\mu_V}{\rho_V \, D_V} \right) \qquad (90)$$

Then at constant vapor Reynolds number the efficiency should be directly proportional to the Schmidt number.

Simple kinetic theory (85) predicts that the Schmidt number of a gas should be a constant independent of temperature and pressure; however, when the influence of intermolecular forces on the viscosity is included, the Schmidt number is found to be a function of the temperature.

Assuming the density to be given by the ideal gas law, the Schmidt number may be expressed as

$$Sc_V = \frac{\mu_V}{\rho_V \, D_V} \alpha \frac{\mu_V}{\frac{P \, M_m}{RT} \frac{T^{3/2}}{P}} = \frac{\mu_V}{\frac{M_m}{R} \, T^{1/2}} \qquad (91)$$

At low pressures the viscosity of a gas is independent of the pressure, and the temperature dependency can be approximated empirically (86) by a relation of the form

$$\mu_V \alpha \frac{T^{3/2}}{T + \beta} \qquad (92)$$

Substituting this relation into equation (91) yields

$$Sc_V \propto \frac{R/M_m}{1 + \beta/T} \tag{93}$$

from which it can be seen that the decrease in temperature accompanying a decrease in operating pressure causes a decrease in the Schmidt number.

A calculation based on the chlorobenzene-ethylbenzene mixture shows that at 736 millimeters of mercury the Schmidt number is 0.679 while at 20 millimeters of mercury the Schmidt number is 0.632. These figures may be taken as indicative of the general magnitude of the effect.

Applying these values to equation (90) yields

$$\frac{(H_G/d)_{20}}{(H_G/d)_{736}} = \frac{(Sc_V)_{20}}{(Sc_V)_{736}} = \frac{0.632}{0.679} = 0.931 \tag{94}$$

Thus, at constant vapor Reynolds number a 40-fold reduction in operating pressure would be expected to cause about a 7 per cent increase in efficiency.

Turbulent Flow

In the region of turbulent vapor flow a number of empirical correlations are available. That of Gilliland and Sherwood (18) may be taken as typical of those derived from dimensional analysis:

$$\frac{d}{B} = 0.023\ Re_V^{0.83}\ Sc_V^{0.44} \tag{61}$$

$$\frac{H_G}{d} = 10.9\ Re_V^{0.17}\ Sc_V^{0.56} \tag{62}$$

The remarks previously made concerning the variation of the Schmidt number with pressure in laminar flow are applicable in turbulent flow; i.e., a decrease in pressure causes a slight decrease in the Schmidt number.

According to equation (61) a decrease in the Schmidt number at constant vapor Reynolds number would cause a decrease in d/B, that is, an increase in the effective film thickness. In view of the definition of the effective film thickness this must be interpreted as an increase in the overall resistance to mass transfer and, consequently, a decrease in efficiency. But according to equation (62), a decrease in the Schmidt number at constant vapor Reynolds number would cause a decrease in H_G/d and this must be interpreted as an increase in efficiency. Therefore, equations (61) and (62) predict opposite effects for a reduction in pressure at constant vapor Reynolds number.

As has been previously pointed out, equations (61) and (62) are entirely equivalent in both a numerical and conceptual sense. Therefore, the fact that they predict precisely opposite effects for a decrease in pressure at constant vapor Reynolds number must mean that the effect of the Schmidt number cannot be expressed by a power law representation, and hence, neither equation (61) nor equation (62) nor any other equation which includes the Schmidt number raised to a fractional power can be expected to predict the effect of reduced pressure on distillation efficiency.

It is of interest that although equation (62) cannot predict the effect of reduced pressure in distillation it successfully correlates

vaporization data (18) over a range of total pressures from 110 to 2330 millimeters of mercury. An examination of the effect of pressure in vaporization as compared to distillation will resolve this apparent conflict.

As has been previously stated, in distillation the operating temperature and pressure are related by the requirements of phase equilibrium. In vaporization into an inert atmosphere the temperature and pressure may be varied independently over a wide range. This is the reason why Gilliland and Sherwood's data were observed to be independent of the total pressure.

It has been demonstrated that the Schmidt number is independent of the pressure per se and depends approximately on the temperature as shown by the following relation:

$$Sc_V \alpha \frac{R/M_m}{1 + \beta/T} \tag{93}$$

Therefore, in vaporization the Schmidt number would be independent of the total pressure and would depend only on the temperature.

Although Gilliland and Sherwood varied the pressure over a wide range they maintained the temperature essentially constant for each series of runs with a given liquid. Thus, the Schmidt number was necessarily independent of the pressure for each such series of runs and consequently the vaporization data showed no trend with pressure within a series of runs with a given liquid.

The effect of reduced pressure as predicted by any equation which includes the Schmidt number raised to a fractional power will depend on

whether the equation is written in terms of H_G/d or d/B. Therefore, the Johnstone and Pigford (28) correlations for distillation

$$\frac{d}{B} = 0.033\ \overline{Re}_V^{0.77}\ Sc_V^{0.33} \tag{60}$$

$$\frac{H_G}{d} = 7.63\ \overline{Re}_V^{0.23}\ Sc_V^{0.67} \tag{59}$$

and the Chilton-Colburn (80)(81) equations

$$\frac{d}{B} = 0.023\ Re_V^{0.80}\ Sc_V^{0.33} \tag{85}$$

$$\frac{H_G}{d} = 10.9\ Re_V^{0.20}\ Sc_V^{0.67} \tag{84}$$

are also entirely inadequate for the prediction of the effect of reduced pressure on distillation efficiency in the region of turbulent vapor flow.

There remains the results of the turbulent core-laminar layer concept applied by Gilliland (35) and Yoshida (34). Gilliland correlated the previously discussed vaporization data (18) by this concept and found that the empirical equation

$$R_T = \frac{1}{k'_G} = \left[903 + \frac{135}{D_V}\right] Re_V^{-0.80} \tag{80}$$

represented the vaporization data equally as well as equation (61).

According to equation (80) a decrease in pressure would cause a decrease in the overall resistance to mass transfer at constant

vapor Reynolds number because of the rapid increase of the volumetric diffusion coefficient, D_V, with decreasing pressure ($D_V \alpha T^{3/2}/P$ and p increases faster than $T^{3/2}$). Consequently, this equation predicts an increase in efficiency for a decrease in pressure at constant vapor Reynolds number.

The correlation developed by Yoshida from distillation data (34) is given by

$$\frac{d}{B} = 0.022 \left[\frac{1.0}{1.0 + 130\ D_m}\right] Re_V^{0.80} \tag{81}$$

The molar diffusion coefficient, D_m, is related to the volumetric diffusion coefficient, D_V, by

$$D_m = \frac{P\ D_V}{RT} \tag{95}$$

Then, since $D_V \alpha T^{3/2}/P$, it follows that

$$D_m \alpha T^{1/2} \tag{96}$$

Since a decrease in pressure is accompanied by a decrease in temperature and hence a decrease in D_m, equation (81) predicts that a decrease in pressure at constant vapor Reynolds number would cause a decrease in the effective film thickness and therefore an increase in the efficiency.

Equation (81) may be rearranged by the use of equation (54) to give

$$\frac{H_G}{d} = 11.4\ (1.0 + 130\ D_m)\ Re_V^{0.20}\ Sc_V \tag{97}$$

Both D_m and Sc_V decrease with decreasing pressure. Therefore, equation (97) predicts that a decrease in pressure at constant vapor Reynolds number would cause a decrease in H_G / d and consequently an increase in the efficiency, a result in agreement with the prediction of equation (81) in terms of d/B.

Since there is no conflict in interpretation inherent in the application of the turbulent core-laminar layer concept, it is concluded that equations (80), (81), and (97) form a reasonable basis for a qualitative prediction of the effect of reduced pressure on distillation efficiency in the region of turbulent vapor flow.

Transitional Flow

No mass transfer theory applicable to the region of transitional vapor flow is available and there is only one set of experimental data (36) in the literature that covers this region. Therefore, there is nothing in the work of previous investigators that could serve as a basis for the prediction of the effect of reduced pressure in the transition region.

Summary

In the region of laminar vapor flow Westhaver's equation, equation (84), predicts that a decrease in pressure at constant vapor velocity would cause an increase in distillation efficiency.

In the region of turbulent vapor flow the conventional correlations cannot predict the effect of reduced pressure; however, the turbulent core-laminar layer concept predicts that a decrease in

pressure at constant vapor Reynolds number would cause an increase in distillation efficiency.

No distillation theory applicable to the region of transitional vapor flow was found in the literature.

A comparison of the experimental results obtained in this investigation with the predictions from the theory presented, based on equations (81), (87), and (97), is given in Chapter VI, RESULTS AND DISCUSSION.

CHAPTER III

APPARATUS

General

The apparatus used in this investigation consisted of a wetted wall distillation column and auxiliary equipment required for operation under vacuum. Provisions for the maintenance of adiabatic operating conditions, the withdrawal of samples, and the measurement and control of temperature, pressure, and boil-up rate were included in the design.

The entire column, exclusive of control elements, was mounted on a frame ten feet tall, constructed from one-half inch aluminum rod. Elements of the column were attached to the frame by standard apparatus clamps. All parts of the apparatus in contact with the test mixture were constructed of glass.

A photograph and a schematic drawing of the apparatus showing the relationship among the various parts are given in Figures 1 and 2, respectively. The details of the design and construction of the apparatus are discussed in succeeding sections of this chapter.

Still, Test Section, and Condenser

The still consisted of a standard two-liter, heavy wall, glass filtering flask modified to include a thermocouple well and a charging line. The flat bottom afforded by this design made it possible to stir magnetically the test mixture in the still and thus eliminate bumping

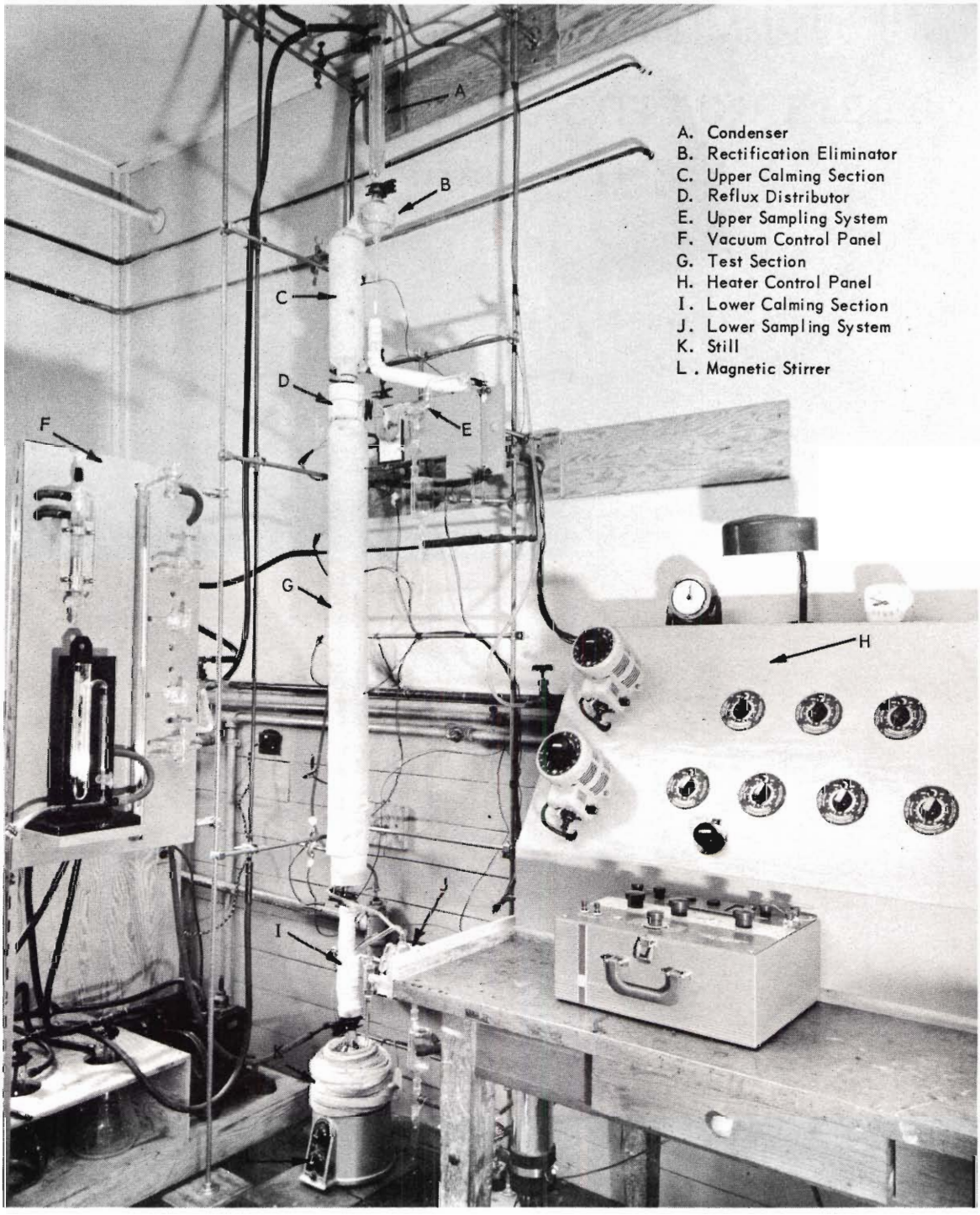

Figure 1. Photograph of Column and Auxiliary Equipment.

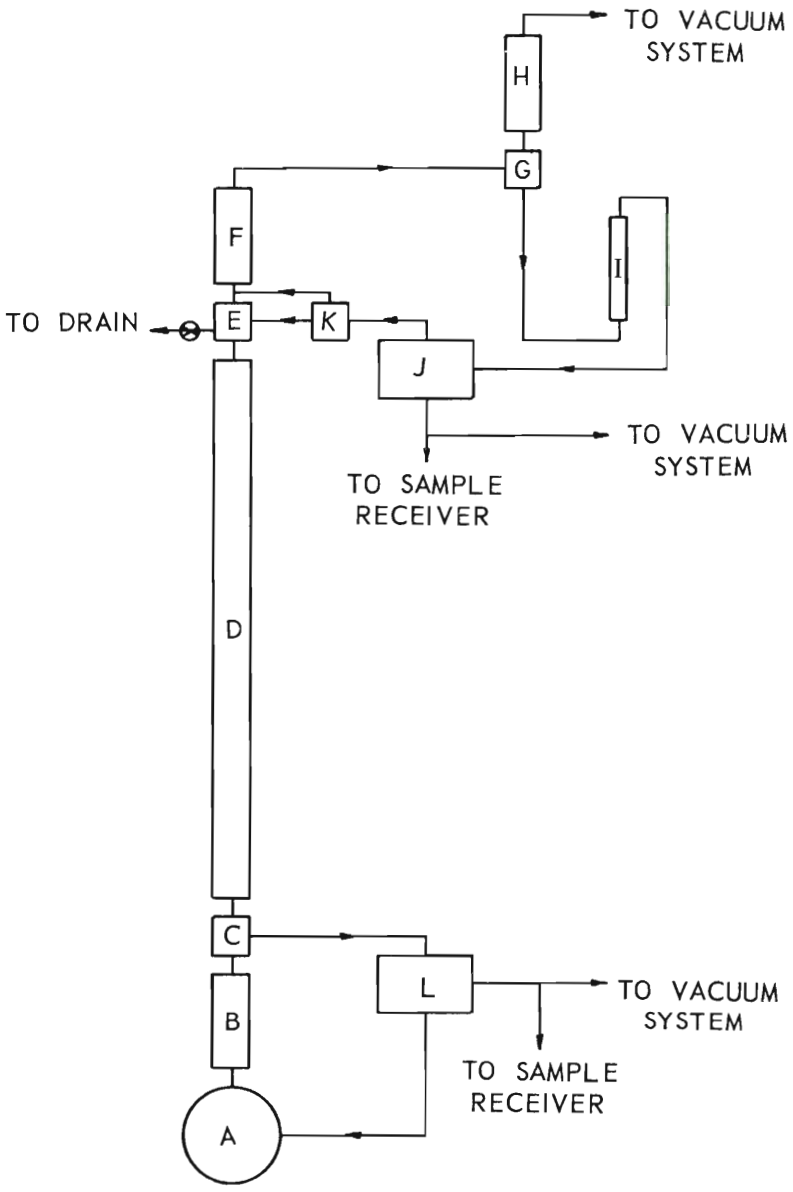

A. Still
B. Lower Calming Section
C. Reflux Removal Device
D. Test Section
E. Reflux Distributor
F. Upper Calming Section
G. Rectification Eliminator
H. Condenser
I. Rotometer
J. Upper Sampling System
K. Reflux Heater
L. Lower Sampling System

Figure 2. Schematic Drawing of Column.

during vacuum operation. Stirring was accomplished by placing a small glass encased magnet inside the still and then mounting the still on a "Gyratherm" magnetic stirrer. The still and stirrer are shown in Figure 3.

The still was attached to the lower calming section by a standard spherical, ground glass joint. This section was constructed from a length of 22 millimeter I. D. glass tubing and included a 45 degree offset to eliminate liquid entrainment. The overall length of the lower calming section was approximately 32 centimeters. The lower calming section was joined to the bottom of the test section by a standard spherical ground glass joint.

The test section was constructed from 19 millimeter I. D., standard wall glass tubing and provided a mass transfer length of 125.1 centimeters. Even distribution of the reflux liquid on the test section wall was attained by means of a baffled, weir-type reflux distributor sealed to the top of the test section. The details of the reflux distribution device are shown in Figure 4. Reflux was removed from the wall at the bottom of the test section by flaring out the tube to 32 millimeters I. D. and collecting the reflux below the level of vapor entry. The reflux was led from the bottom of the test section to the lower sampling system by a short length of glass tubing. The reflux removal provisions are shown in Figure 5. A plumb bob was used to insure vertical alignment during the installation of the test section.

The upper calming section was attached to the top of the reflux distributor by a standard spherical, ground glass joint. This section

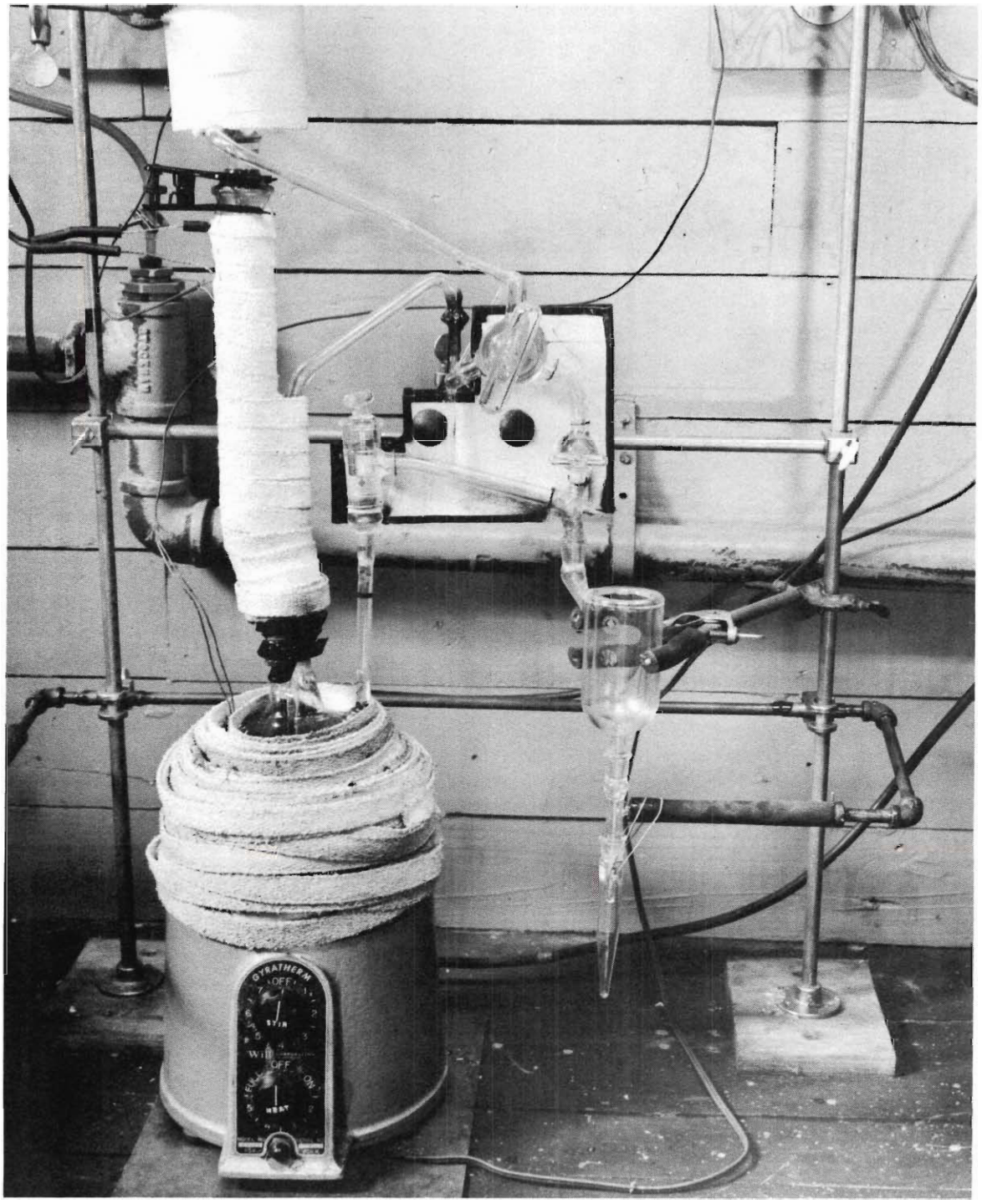

Figure 3. Photograph of Still, Magnetic Stirrer, Lower Calming Section, Reflux Return Line, and Lower Sampling Section.

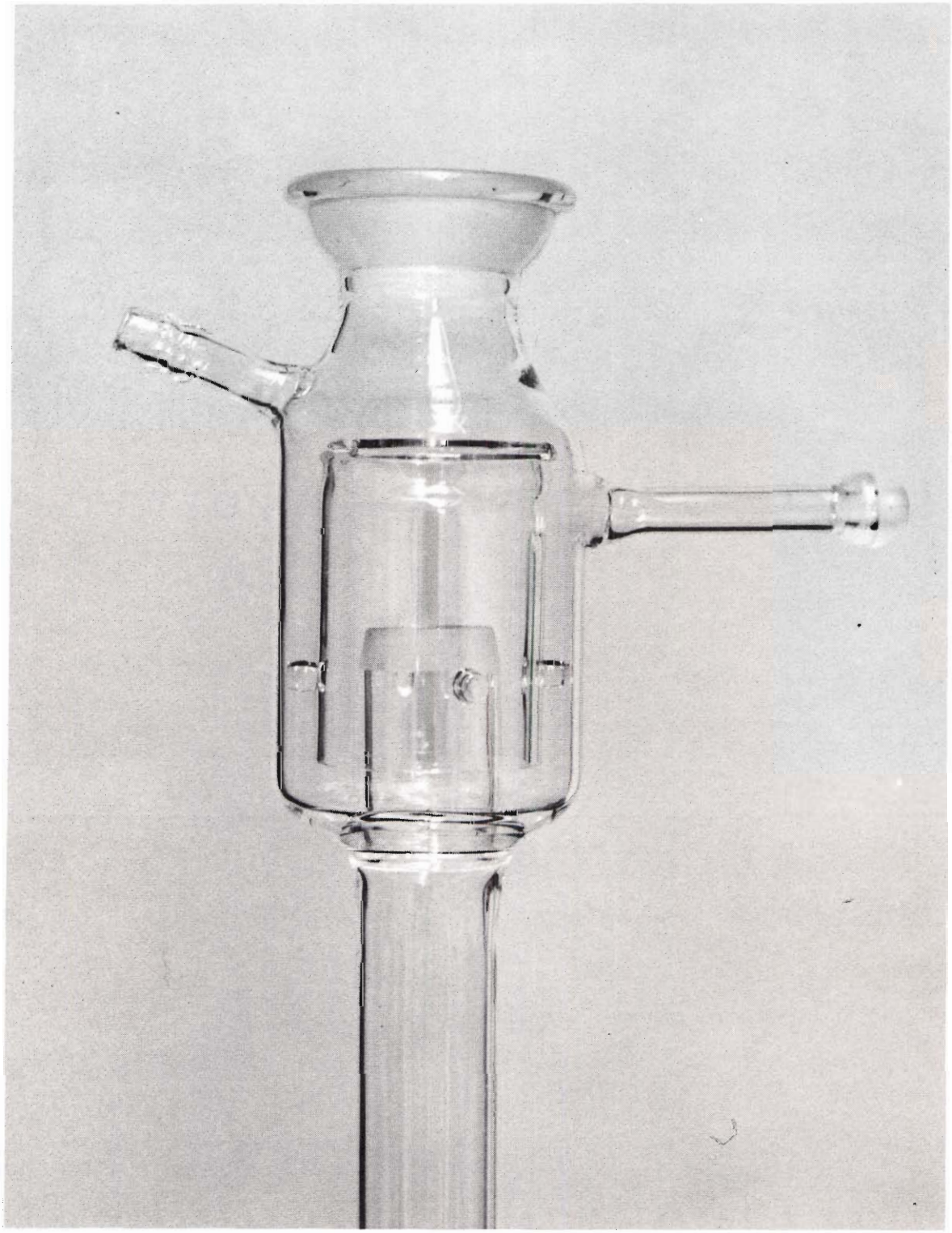

Figure 4. Photograph of Reflux Distributor.

Figure 5. Photograph of Reflux Removal Device.

was constructed from 22 millimeter I. D., glass tubing and was approximately 45 centimeters in overall length. The upper calming section served to conduct the vapor from the top of the test section to the condenser and was made long enough to provide sufficient head for gravity flow of the condensate back to the top of the test section.

Vapor from the upper calming section passed through a rectification elimination device before entering the condenser. This device prevented mass transfer between the entering vapor and the condensate leaving the condenser by keeping the vapor on the wall while the condensate dropped rapidly through the center. This device is shown in Figure 6.

The condenser was of the cold-finger type and had a 40 centimeter jacket length. It was attached to the rectification elimination device by a standard spherical, ground glass joint. Tap water was used as the condensing medium. The condenser is also shown in Figure 6.

Liquid from the condenser dropped into a 30 centimeter length of 19 millimeter I. D., glass tubing which was inclined about 30 degrees from the horizontal. This inclined tube provided a large area to volume ratio and thus smoothed out variations in head which would have caused fluctuations in the flow measuring rotometer.

Rotometer

The reflux rate was measured by a small glass rotometer (Ace Glass Incorporated, Vineland, New Jersey, Catalog No. 3575C) which included both a Pyrex and a stainless steel float and hence covered a wide

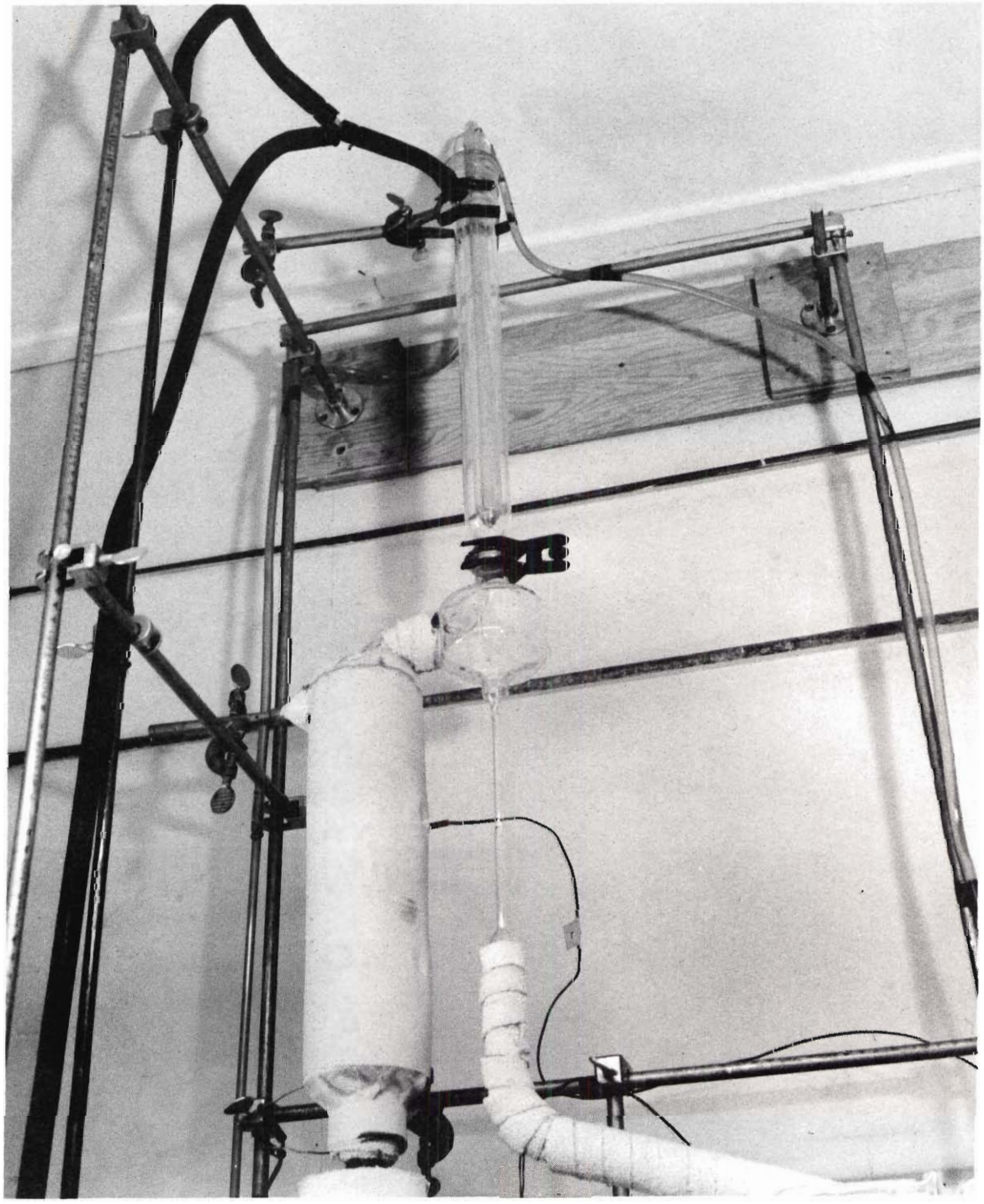

Figure 6. Photograph of Upper Calming Section, Rectification Eliminator, and Column Condenser.

range of flow rates. The scale was 15.0 centimeters long and was graduated in millimeters. The instrument is shown mounted in position in Figure 7.

Since the rotometer was quite small and employed spherical floats an elaborate calibration scheme was necessary to allow for the effects of density and viscosity on the float height corresponding to a given flow rate. A constant head apparatus constructed by the author was used to obtain calibration data for chlorobenzene at 23 degrees centigrade, ethylbenzene at 24 degrees centigrade, and water at 21 degrees centigrade. In addition, four points for ethylbenzene at 31 degrees centigrade were obtained. These data are summarized in Tables 1 through 4 in Appendix II.

The calibration data were correlated by a scheme based on dimensional analysis (87) which consisted of plotting the flow coefficient, K, versus the viscous influence number, N, with float neight, h_f, as a parameter. The quantities N and K are defined by the following equations:

$$N = \frac{\mu_L}{\sqrt{W_f\left(\frac{\rho_f - \rho_L}{\rho_f}\right)\rho_L}} \tag{96}$$

$$K = \frac{Q}{D_f\sqrt{W_f\left(\frac{\rho_f - \rho_L}{\rho_f}\right)\rho_L}\left(\frac{453.6}{\rho_L}\right)} = \frac{Q}{I.C.} \tag{97}$$

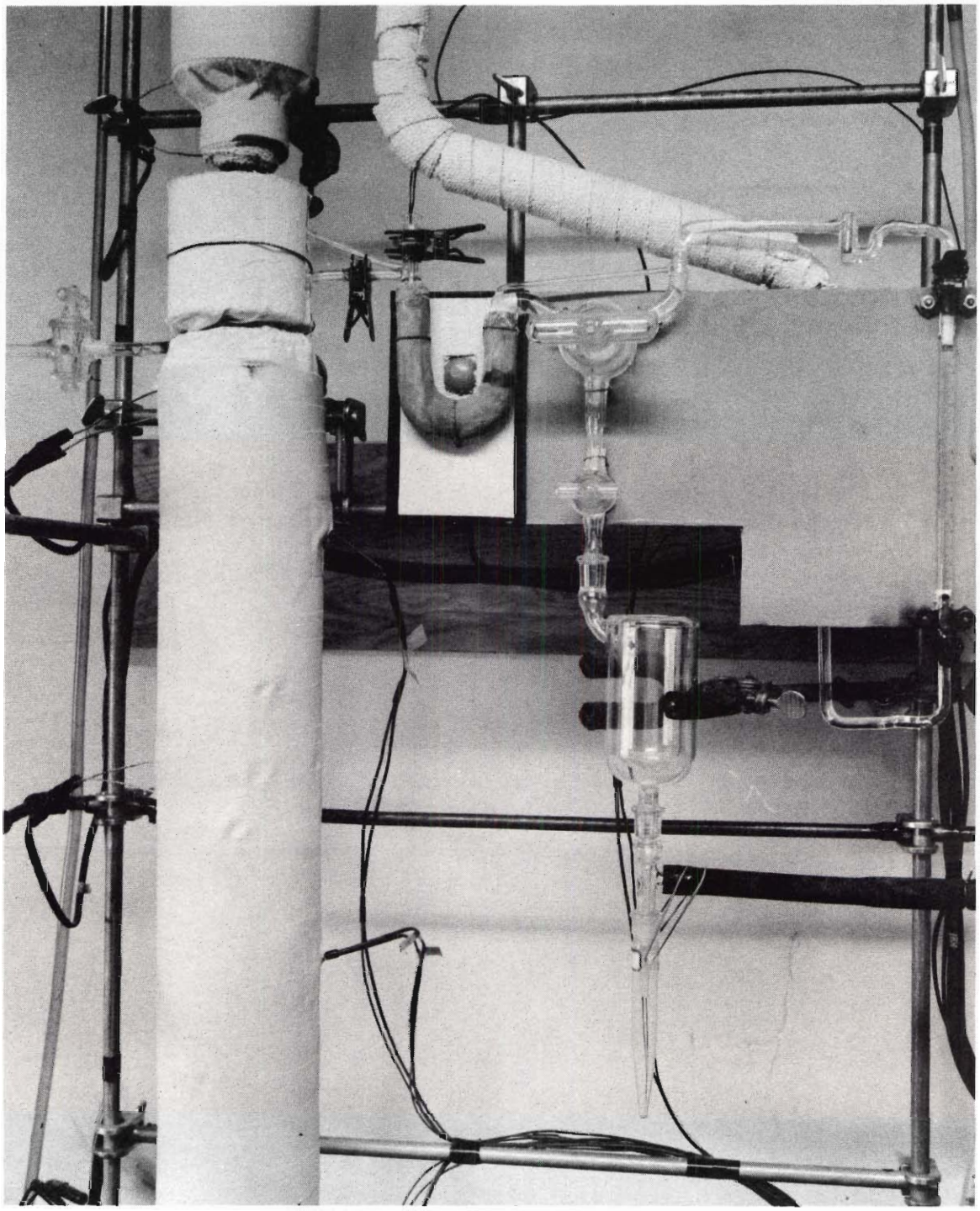

Figure 7. Photograph of Upper Sampling Section, Rotometer, and Reflux Heater.

The calibration data were plotted as Q versus h_f and graphically smoothed. The resulting curves, in conjunction with equations (96) and (97), were used to calculate values of N and K for unit increments of float height from 1.0 through 15.0 centimeters. These values were then used to prepare a calibration chart of K versus N, with float height as a parameter. The float data required for the computation of N and K are given in Table 5 in Appendix II. The calibration chart reproduced the calibration data within ± 5.0 per cent over the entire range of float heights.

The procedure used for determining the flow rate for a given float height was as follows:

(1) Values of ρ_L and μ_L were calculated for the temperature and composition of the reflux.

(2) Values of N and I. C. were then calculated from ρ_L, μ_L, and the float properties given in Table 5.

(3) Using N and h_f, K was read from the calibration chart.

(4) Then the flow rate was calculated from equation (97).

Sampling System

Liquid samples could be withdrawn at the top and bottom of the test section. The upper sampling system, as shown in Figure 7, was located between the rotometer and the reflux heater and was designed to eliminate the possibility of obtaining a sample from a stagnant area not representative of the liquid being fed to the top of the test section. The heart of the sampling system was a 120 degree angle bore,

high vacuum, precision grade stopcock. In the normal position (non-sampling) the reflux flowed through the stopcock to the reflux heater. When the stopcock was rotated to the sampling position the material trapped in the bore of the plug flowed out, thus giving a true instantaneous sample of the liquid being fed to the test section. A small diameter glass tube provided a by-pass around the stopcock, thereby preventing complete interruption of flow to the test section while a sample was being taken.

An ice filled Dewar-type condenser cooled the liquid sample and prevented flashing. The cooled sample was collected in a small centrifuge tube joined to the bottom of the sample condenser by a standard taper, ground glass joint. The sample receiver could be evacuated or vented by manipulation of a stopcock in the vacuum system.

The lower sampling system was located between the bottom of the test section and the still, and except for minor variations in arrangement was exactly like the upper sampling system. In normal operation reflux from the bottom of the column passed directly through the lower sampling system into a small diameter glass tube which entered the lower calming section at the 45 degree offset and extended a few centimeters below the liquid level in the still. The lower sampling system is shown in Figure 3.

Heating System

Before being returned to the test section, the reflux was heated to approximately its bubble point by a small heater which, as is shown

in Figure 7, was placed between the upper sampling system and the reflux distributor. The reflux heater consisted of a 20 centimeter length of one-half inch O. D., medium wall, glass tubing bent in a U-shape. The heating element was constructed by applying to the tubing in successive layers:

(1) Two wraps of 1/16 inch thick asbestos cloth tape.

(2) A winding of 10 feet of Nichrome wire of 11 ohms per foot resistance.

(3) Two wraps of 1/16 inch thick asbestos cloth tape.

(4) A 1/8 inch thick layer of asbestos furnace cement.

The still was heated by an 850 watt element incorporated in the "Gyratherm" magnetic stirrer and an auxiliary element consisting of 15 ohms of flexible heating tape wound around the upper part of the still. The still heating elements were separately controlled by two "Powerstat," variable transformers manufactured by the Superior Electric Company of Bristol, Connecticut, each of which had a maximum output of 1000 watts.

The upper calming section was insulated and heated to prevent premature condensation of the vapor leaving the top of the test section. This was accomplished by applying to the glass tube, in successive layers:

(1) One wrap of 1/16 inch thick asbestos cloth tape.

(2) A winding of 20 feet of Nichrome wire of 11 ohms per foot resistance.

(3) Three wraps of 1/16 inch thick asbestos cloth tape.

(4) A 13 inch length of 1-3/4 inch, 85 per cent magnesia, standard pipe insulation.

(5) Two wraps of moisture resistant cloth tape.

Heat losses in the lower calming section were prevented by heating and insulation provisions similar to those used on the upper calming section except that the standard pipe insulation and the moisture resistant cloth tape were omitted.

Provision was made for eliminating heat losses from the test section by encasing it in four separately controlled compensating heaters, each approximately one foot long. Each of these heaters was constructed by applying to the glass tube, in successive layers:

(1) Five wraps of 1/16 inch thick asbestos cloth tape.

(2) A winding of 20 feet of Nichrome wire of 11 ohms per foot resistance.

(3) Two wraps of 1/16 inch thick asbestos cloth tape.

(4) A one foot length of two inch, 85 per cent magnesia, standard pipe insulation.

(5) Two wraps of moisture resistant cloth tape.

The upper and lower calming section heaters, the reflux heater, and the four test section heaters were individually controlled by 132 watt, "Powerstat" variable transformers manufactured by the Superior Electric Company of Bristol, Connecticut. These seven transformers and the two larger transformers which controlled the still heaters were mounted on the heater control panel shown in Figure 8. Constant output from the transformers was assured by connecting the primary windings to a 115 volt, 3000 watt, voltage stabilizer.

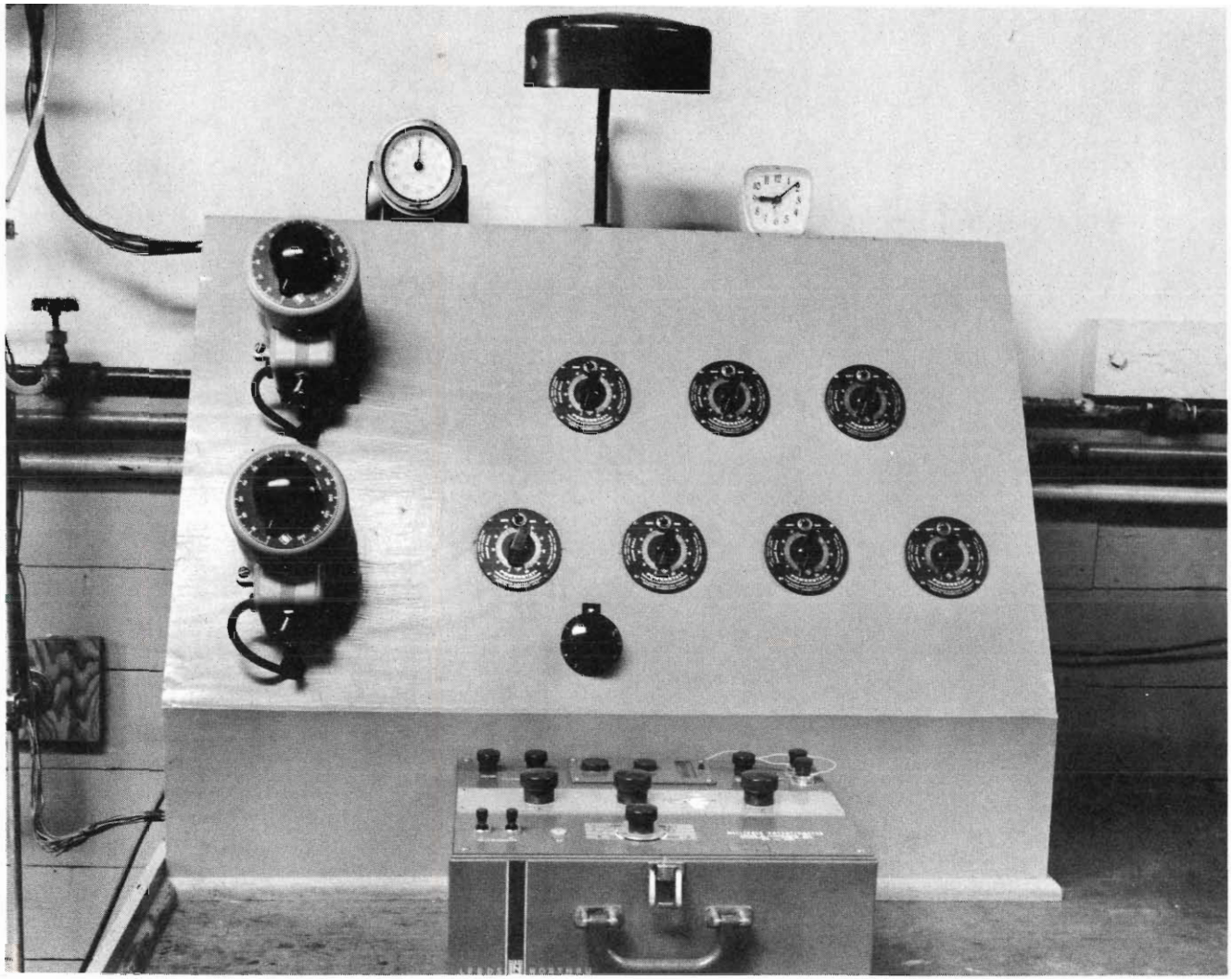

Figure 8. Photograph of Heater Control Panel, Thermocouple Switch, and Potentiometer.

Temperature Measurement

Iron-constantan thermocouples were used to measure the temperature at 13 points in the apparatus. The thermocouples were fabricated from duplex wire containing both the iron and constantan in a single strand. The wire, as supplied, was insulated with a combination of asbestos and glass fiber which provided resistance to both heat and moisture. All of the thermocouples were made from a single lot of wire purchased from the Leeds and Northrup Company of Philadelphia, Pennsylvania.

A pair of thermocouples was located at the middle of each of the four compensating heaters, one at the test section wall and one between the third and fourth wraps of asbestos cloth tape. Adiabatic operation was achieved by adjusting the transformers controlling the heaters so that each thermocouple pair indicated the same e.m.f.

One thermocouple, which could be moved, was used to measure the temperature of the liquid leaving the reflux heater. The same thermocouple was used to measure the temperature of the liquid leaving the rotometer by moving it, as required, to a thermocouple well located in the rotometer exit line. Single thermocouples were located at the walls of the upper and lower calming sections, and in a thermocouple well in the still.

The voltage, in millivolts, generated in each thermocouple circuit was measured with a Portable Millivolt Potentiometer (Leeds and Northrup Catalog No. 8686) having a range of -10.1 to +101.1 millivolts and a limit of error of ± (0.05 per cent of the scale reading + 0.003 millivolts). The potentiometer is shown in Figure 8.

The thermocouple circuits were connected to the potentiometer through a 24 Point Rotary Selector Switch (Leeds and Northrup Type 31-3). Using this switch made it possible to use only one ice bath cold junction and only one connection to the potentiometer for all 12 thermocouple circuits. In addition, the switch permitted a complete set of voltage determinations to be made in rapid succession. The switch was conveniently located on the heater control panel shown in Figure 8.

Complete calibration data were obtained for two of the thermocouples by determining the e.m.f. at 10 temperatures between 25 degrees centigrade and 140 degrees centigrade. The temperatures were measured by a National Bureau of Standards Certified thermometer placed in a thermostated container of mercury with the thermocouple junctions. The calibration data are given in Table 6 in Appendix II.

A fourth degree polynomial was fitted to the data which reproduced the calibration data within the limit of error of the potentiometer. A calibration table was prepared by using the polynomial to compute the e.m.f. at temperatures between 25 and 140 degrees centigrade in increments of 0.05 degrees centigrade. A small portion of this table is reproduced in Table 7 in Appendix II. The temperature corresponding to a given e.m.f. could be read from the calibration table to 0.05 degrees centigrade without interpolation.

The 10 remaining thermocouples were checked against the two calibrated thermocouples at 46.60 and 72.35 degrees centigrade and, as is shown in Table 8 in Appendix II, within the limit of error of the potentiometer all generated the same e.m.f. Therefore, only one

calibration table was required for all 12 thermocouples. Taking into account the calibration data and the limits of error of the potentiometer it is estimated that in this investigation the temperature could be determined to within ± 0.50 degrees centigrade.

Analysis

Liquid samples from the top and bottom of the test section were analyzed by refractive index using a Bausch and Lomb Optical Company, Rochester, New York, modified Abbe type, precision refractometer. A constant temperature bath manufactured by the Precision Scientific Company of Chicago, Illinois, maintained the temperature of analysis at a constant 25.0 degrees centigrade.

Calibration data were obtained by determining the refractive index at 16 compositions ranging from pure chlorobenzene to pure ethylbenzene. These data are given in Table 9 in Appendix II. A calibration table was prepared by fitting a fifth degree polynomial to the calibration data and then using the polynomial to compute compositions at 0.005 increments of the refractometer scale reading. Since 0.005 was the smallest scale increment which could be read (one-half of the smallest scale division, 0.01) compositions could be determined from the calibration table without interpolation. A portion of the calibration table is given in Table 10 in Appendix II. The refractive index spread and the accuracy of the refractometer were such that sample compositions could be determined to within ± 0.001 mole fraction.

Vacuum System

The vacuum system consisted of one pump, two cold traps, four surge tanks, one needle valve, two manometers and four stopcocks. A schematic of the system is shown in Figure 9.

A "Duo-Seal Vacuum Pump" manufactured by the Welch Manufacturing Company of Chicago, Illinois, was used to produce and maintain the desired vacuum in the apparatus. The pump was capable of producing a vacuum of less than one millimeter of mercury throughout the entire system in less than five minutes. The pump was protected from condensable vapors by two cold traps maintained at the ice point.

The system pressure was regulated by a Cartesian diver (88) manostat. The device used in this investigation was manufactured by the Manostat Corporation of New York, New York, and had an advertised sensitivity of ± 0.2 per cent or ± 0.2 millimeters of mercury, whichever is the greater. In practice the manostat was able to control the pressure to within ± 1.0 millimeters of mercury. A small needle valve was used in conjunction with the manostat for coarse pressure control. The manostat was protected from condensable vapors by a cold trap immersed in an ice bath. Pressure fluctuations were smoothed out by including two, 2-liter surge tanks between the pump and the manostat and one, 2-liter surge tank between the manostat and the top of the column condenser.

The system pressure was measured at the top of the column condenser by two mercury manometers connected in series. The manometers were protected from condensable vapors and sudden pressure fluctuations

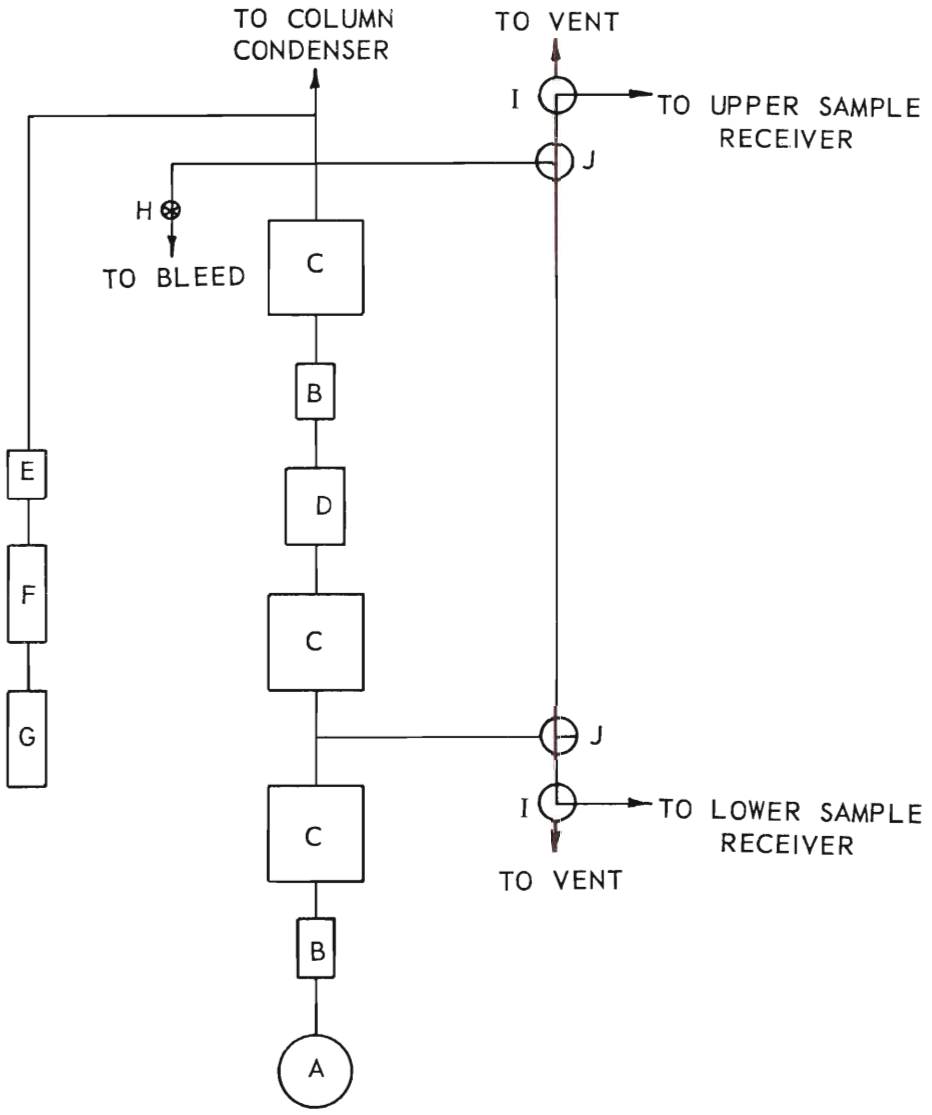

A. Pump
B. Cold Trap
C. Surge Tank
D. Manostat
E. Surge Flask
F. U-tube Manometer
G. Bennert Manometer
H. Needle Valve
I. Two-way Stopcock
J. Three-way Stopcock

Figure 9. Schematic Drawing of Vacuum System.

by a surge tank of 250 cubic centimeter capacity. For pressures below 240 millimeters of mercury, the pressure was read from a Bennert type manometer (Fisher Scientific Company, New York, New York, Catalog No. 11-292). This manometer had a movable 240 millimeter scale, graduated in millimeters, which was mirrored to eliminate parallax errors in reading. For pressures from 240 millimeters to atmospheric, a U-tube manometer constructed by the author was used. Both manometers were frequently checked for accuracy at low pressures with a McLeod gauge (Ace Glass, Incorporated, Vineland, New Jersey, Catalog No. 8726) having a range of 0.050 to 15.0 millimeters of mercury.

Two T-bore and two diagonal bore, high vacuum, precision grade stopcocks were included in the vacuum system to permit operation of the system in various modes. By appropriate manipulation of these stopcocks it was possible to operate with the sample receivers at the manostated pressure, the pump inlet pressure, or atmospheric pressure without disturbing other parts of the system. The required settings for various modes of operation may be deduced from the schematic given in Figure 9. The four stopcocks, the manostat, and the two manometers were conveniently mounted on the vacuum control panel shown in Figure 10.

The various elements of the vacuum system were joined together by a combination of rubber tubing and 1/8 inch brass pipe. Connections were made with wire clamps or standard pipe fittings, as appropriate. The tightness of all connections was assured by an application of sealing varnish.

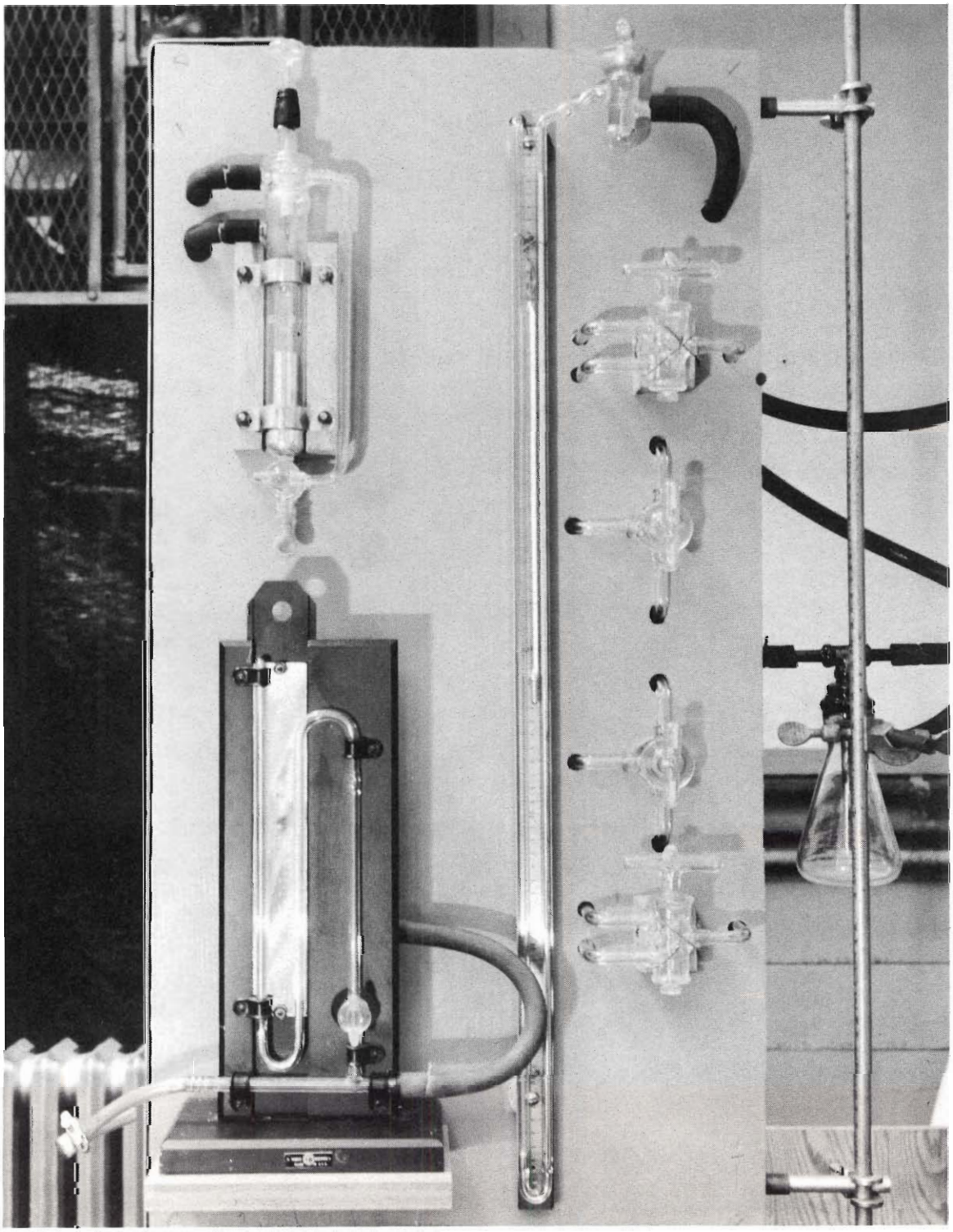

Figure 10. Photograph of Vacuum Control Panel

Sealing and Lubrication

Finding suitable sealing and lubricating materials for use in those parts of the apparatus which were in contact with the test mixture was a formidable task. The chlorobenzene-ethylbenzene mixture used in this investigation proved to be an excellent solvent for the conventional vacuum sealing and lubricating compounds.

After trying many different sealing materials it was found that the application of an alkyd resin (89) to the outside of the ground glass joints furnished a satisfactory vacuum seal. The resin was prepared by reacting glycerol and phthalic anhydride at approximately 130 degrees centigrade. Polymerization was allowed to proceed until a fusible resin which softened at about 100 degrees centigrade was obtained. The hot fluid resin was applied to the outside of the ground glass joints and allowed to cool with the system under vacuum. The resin was insoluble in the chlorobenzene-ethylbenzene mixture but slightly soluble in water. A thin coating of insulating varnish was used to protect the seal from moisture.

The stopcocks which were in contact with the test mixture were lubricated by a light application of glycerol. To maintain a satisfactory seal, it was necessary to renew the glycerol coating after about each twenty hours of operation.

CHAPTER IV

EXPERIMENTAL PROCEDURES AND LIMITATIONS

General Procedure

Before beginning an experimental run the apparatus was carefully inspected to locate and correct potential sources of difficulty which might cause the equipment to malfunction. Particular care was taken to insure that the stopcocks in the sampling systems were properly lubricated and sealed.

The still charge for all runs was about 1200 cubic centimeters of the chlorobenzene-ethylbenzene test mixture of approximately 0.500 mole fraction chlorobenzene composition. These values were maintained by replenishing the still as necessary.

After the vacuum system cold traps were supplied with ice and the condenser cooling water was turned on, the start-up procedure was begun. An experimental run was started by energizing the compensating heaters, starting the vacuum pump, and turning on the magnetic still stirrer.

The apparatus was slowly pumped down to the approximate operating pressure by gradually closing the needle valve in the vacuum system. After the column had been inspected for leaks the desired operating pressure was precisely set by the manostat and the still heaters were energized.

When vapor reached the condenser periodic temperature measurements were begun. The transformers controlling the test section heaters were

adjusted until the thermocouples indicated that the test section wall and insulation were at the same temperature. The wall of the lower calming section was maintained at approximately the temperature of the boiling mixture in the still. To prevent premature condensation, the upper calming section wall was maintained at a temperature 10 to 15 degrees centigrade higher than the boiling point of the test mixture. About two hours were required, from the time the test mixture began to boil, to reach thermal equilibrium. After thermal equilibrium had been attained the column compensating heaters required very little further adjustment.

During the approach to thermal equilibrium a high rate of boiling was maintained to assist in heating up the column and to insure complete wetting of the test section wall. When thermal equilibrium was reached the boil-up rate was slowly reduced until the rotometer float indicated approximately the desired flow rate. Simultaneously, the reflux heater was energized and adjusted to bring the reflux up to the bubble point temperature. The reflux heater was considered to be properly adjusted when small bubbles became visible in the exit line of the heater.

No attempt was made to obtain an exact predetermined flow rate. When the rotometer indicated the approximate boil-up rate desired the still heaters were left unchanged and the boil-up rate was allowed to freely seek an equilibrium value.

Mass transfer equilibrium was reached from two to four hours after thermal equilibrium had been attained. The length of time

required varied with pressure and boil-up rate but with experience could be predicted within one hour.

When it was estimated that mass transfer equilibrium had been attained liquid samples were withdrawn from the top and bottom of the test section. This was accomplished by evacuating the sample receivers and then rotating the sampling stopcocks to the proper position. The sample from the bottom of the test section was taken first since sampling at the top slightly disturbed the column whereas sampling at the bottom did not. Both samples were collected within twenty seconds and the column recovered from the disturbance in less than two minutes. Each sample was of about five cubic centimeters volume. Just prior to sampling a complete set of temperature, pressure, and flow rate readings was recorded.

Sampling was continued at 30 minute intervals until refractive index measurements indicated no further change in composition at the top and bottom of the test section. The last pair of compositions were taken as the equilibrium values and were recorded with a final set of temperature, pressure, and flow rate readings.

Another run was often begun at this point by changing the boil-up rate and making the necessary adjustments in the column heater controls. When this was done the second boil-up rate was always made significantly different from the first. A large change in the boil-up rate caused a large change in the compositions at the top and bottom of the test section and consequently made the detection of equilibrium in the succeeding run more certain.

Column operation was stopped by turning off the still and column heaters and allowing the column to cool down under vacuum. When boiling ceased the column was slowly vented to the atmosphere. This procedure prevented sudden temperature and pressure changes which could have damaged the vacuum seals.

Limitations

The lowest boil-up rate at which data could be obtained was set by the limitations of the compensating heating system. At sufficiently low boil-up rates no vapor reached the top of the test section even though there was reflux at the bottom and thermocouple readings indicated that the test section was operating adiabatically. The effect of this limitation is discussed in Chapter VI, RESULTS AND DISCUSSION.

The limitations of the still heaters determined the maximum boil-up rate at which data could be obtained. At high impressed voltages the still heater elements tended to overheat due to poor heat transfer between the elements and the glass still.

In spite of these limitations the apparatus used in this investigation provided data over as wide a range of boil-up rates as any previously obtained.

The temperature of the tap water used in the column condenser determined the lowest pressure at which data could be obtained. It was found that below 20 millimeters of mercury pressure the condenser cooling water was not cold enough to condense all of the vapor which entered the condenser.

CHAPTER V

PHYSICAL PROPERTIES OF THE TEST MIXTURE

General

The test mixture used in this work was composed of chlorobenzene and ethylbenzene. This mixture possessed many of the preferred characteristics (90) of a binary mixture for determining efficiencies in distillation columns.

The chlorobenzene was manufactured by the J. T. Baker Company of Phillipsburg, New Jersey, and had a boiling range of one degree centigrade. The ethylbenzene was manufactured by the Eastman Kodak Company of Rochester, New York, and had a boiling range of three degrees centigrade.

The components were purified before use by distillation in a column constructed by the author having a four foot section packed with a one-eighth inch pertruded Nickel packing. The center cut of a single distillation of chlorobenzene and the center cut of a double distillation of ethylbenzene were used to prepare the test mixture. After purification both the chlorobenzene and the ethylbenzene had a boiling range of less than 0.2 degree centigrade. The refractive indices of the purified components are compared with the literature values below:

Refractive Index at 25° C.	Chlorobenzene	Ethylbenzene
This work	1.52186	1.49328
Hawkins and Brent (12)	1.5215	1.4933

The general properties of the test mixture components are listed in Table 11 in Appendix III.

To evaluate distillation data the properties of the mixture being distilled must be known. There are few systems for which all of the required physical properties have been determined experimentally. Therefore, it is frequently necessary to estimate values of those properties for which experimental data are not available.

The determination of the physical properties of the chlorobenzene-ethylbenzene test mixture required to evaluate the data of this investigation is discussed in succeeding sections of this chapter. Where experimental data were not available the necessary physical properties were estimated by conventional methods.

The pressure drop in wetted wall columns is so small (33)(68) that the operating temperature and pressure need only be determined at one point in the column. In this investigation, all of the physical properties of the mixture in the test section were evaluated at the temperature measured in the still and at the pressure measured at the top of the column condenser.

Density

Vapor

The density of the vapor mixture was calculated by assuming the ideal gas law using a mole fraction weighted, average molecular weight. The composition used for the calculation was the arithmetic average of the compositions at the top and bottom of the test section. The calculation was made for the measured operating pressure and the temperature

in the column still. The vapor density for each run is given in Table 12 in Appendix III.

Liquid

The density of liquid ethylbenzene is available in the literature (91). The density of liquid chlorobenzene was estimated by the methods of Lydersen (92). Liquid mixture densities were calculated by assuming that the molal volumes of the pure components were additive on a mole fraction basis and that the change in volume on mixing was zero.

The density of the liquid reflux film was based on the arithmetic average of the compositions at the top and bottom of the test section and the temperature in the column still. Densities used for the calculation of the boil-up rate were based on the composition at the top of the test section and the temperature in the exit line of the rotometer. The average liquid density for each run is given in Table 13 in Appendix III.

Viscosity

Vapor

Viscosities of the pure vapors were estimated by the method of Licht and Stechert given by Reid and Sherwood (93). Vapor mixture viscosities were taken as the arithmetic average of the viscosities of the pure components at the temperature in the column still. The vapor viscosity for each run is given in Table 12 in Appendix III.

Liquid

The viscosity of liquid ethylbenzene was taken from the literature (91). The viscosity of liquid chlorobenzene was obtained

by fitting the Andrade equation to a limited amount of experimental viscosity data (94). Liquid mixture viscosities were taken as the mole fraction weighted, average of the viscosities of the pure components.

The viscosity of the liquid reflux film was based on the arithmetic average of the compositions at the top and bottom of the test section and the temperature in the column still. Viscosities used for the calculation of the boil-up rate were based on the composition at the top of the test section and the temperature in the exit line of the rotometer. The average liquid viscosity for each run is given in Table 13 in Appendix III.

Diffusivity

The volumetric diffusion coefficient of the vapor was estimated by an empirical equation due to Slattery and given by Reid and Sherwood (95). The calculation was based on the column operating pressure and the temperature in the column still. The volumetric diffusion coefficient for each run is given in Table 12 in Appendix III.

Vapor Pressure

Vapor pressure data for both ethylbenzene (91) and chlorobenzene (96) are available in the literature. These data are given in Tables 14 and 15 in Appendix III. Interpolation between reported values was accomplished by fitting three-constant Antoine equations to the data for each component.

Vapor-Liquid Equilibrium Data

Hawkins and Brent (12) determined vapor-liquid equilibrium data for the chlorobenzene-ethylbenzene system. Extensive data for 760 and 20 millimeters of mercury pressure are reported. In addition, a limited amount of data is reported at a pressure of 300 millimeters of mercury. These data are presented in Table 16 in Appendix III.

The equilibrium data show that the relative volatility of the mixture is independent of the composition between the limits of 0.10 and 0.90 mole fraction chlorobenzene. At 760 millimeters of mercury the relative volatility is 1.10 and at 20 millimeters of mercury the relative volatility is 1.12. The Raoult's Law values at these two pressures are 1.11 and 1.19, respectively. Logarithmic interpolation was used to obtain values of the relative volatility at intermediate pressures.

CHAPTER VI

RESULTS AND DISCUSSION

General

The results of this investigation of the effect of reduced pressure on a wetted wall distillation column operating at total reflux are reported in terms of H_G, the gas film height of a transfer unit, and B, the effective gas film thickness.

Various runs were conducted at each of the following four pressures: 736, 300, 100, and 20 millimeters of mercury. The flow rates studied covered a vapor Reynolds number range of from 520 to 18,600 and thus provided data in the laminar, transitional, and turbulent regions of vapor flow. Only one other investigation (33), which is entirely in the region of turbulent vapor flow, has covered as wide a range of flow rates.

At 20 millimeters of mercury pressure the column flooded before the turbulent region of vapor flow was entered. Hence, at this pressure the data cover only the laminar and transitional regions.

Figures 11 and 12, plots of H_G/d versus $\overline{Re}_V$ and d/B versus $\overline{Re}_V$, respectively, show the general character of the data obtained and the relationship among the three regions of vapor flow. The experimental data upon which these figures are based are summarized in Tables 17 and 18 in Appendix IV. In succeeding sections of this chapter the data obtained in each region of vapor flow are discussed

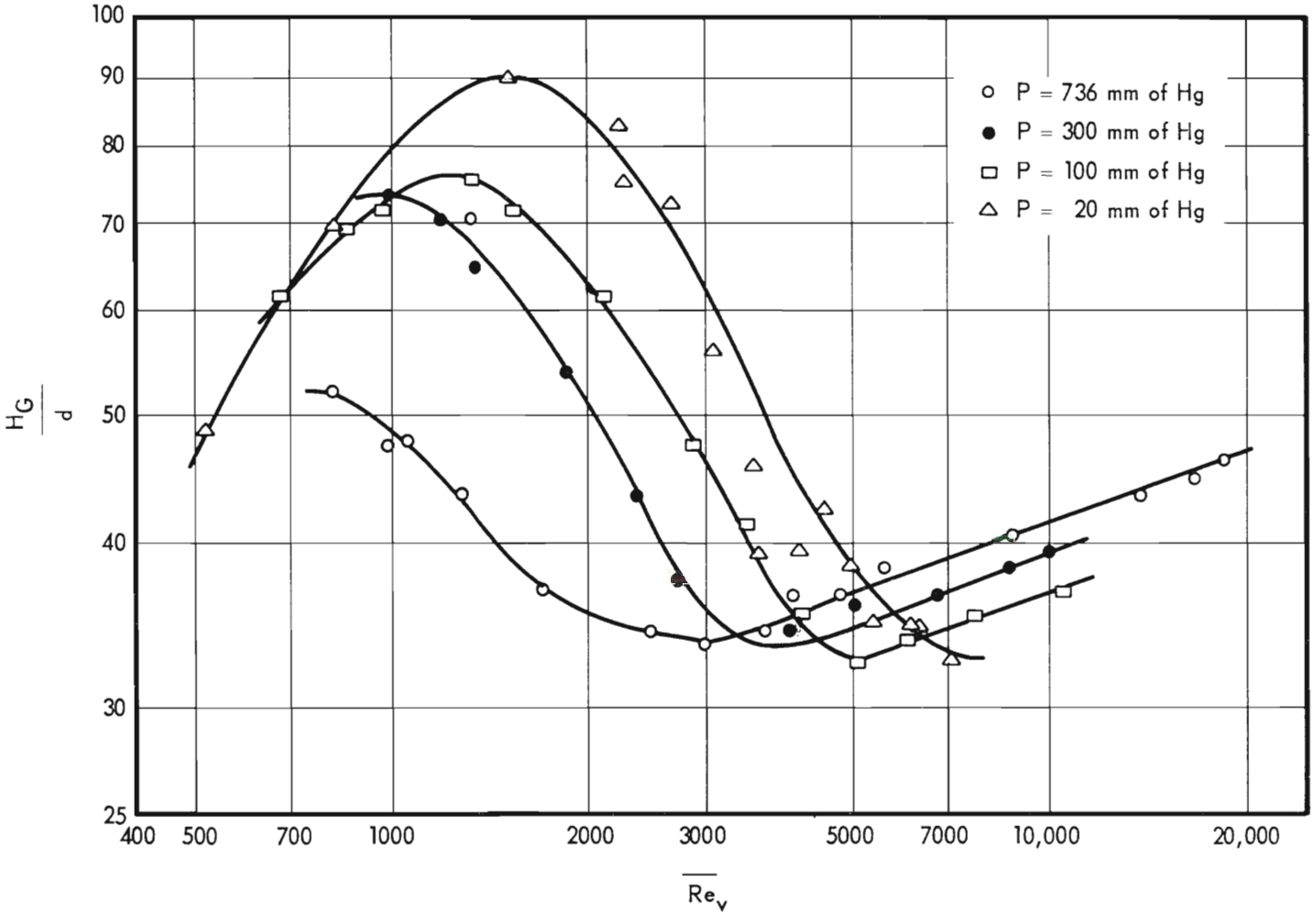

Figure 11. Effect of Pressure on H_G/d: Laminar, Transition, and Turbulent Regions.

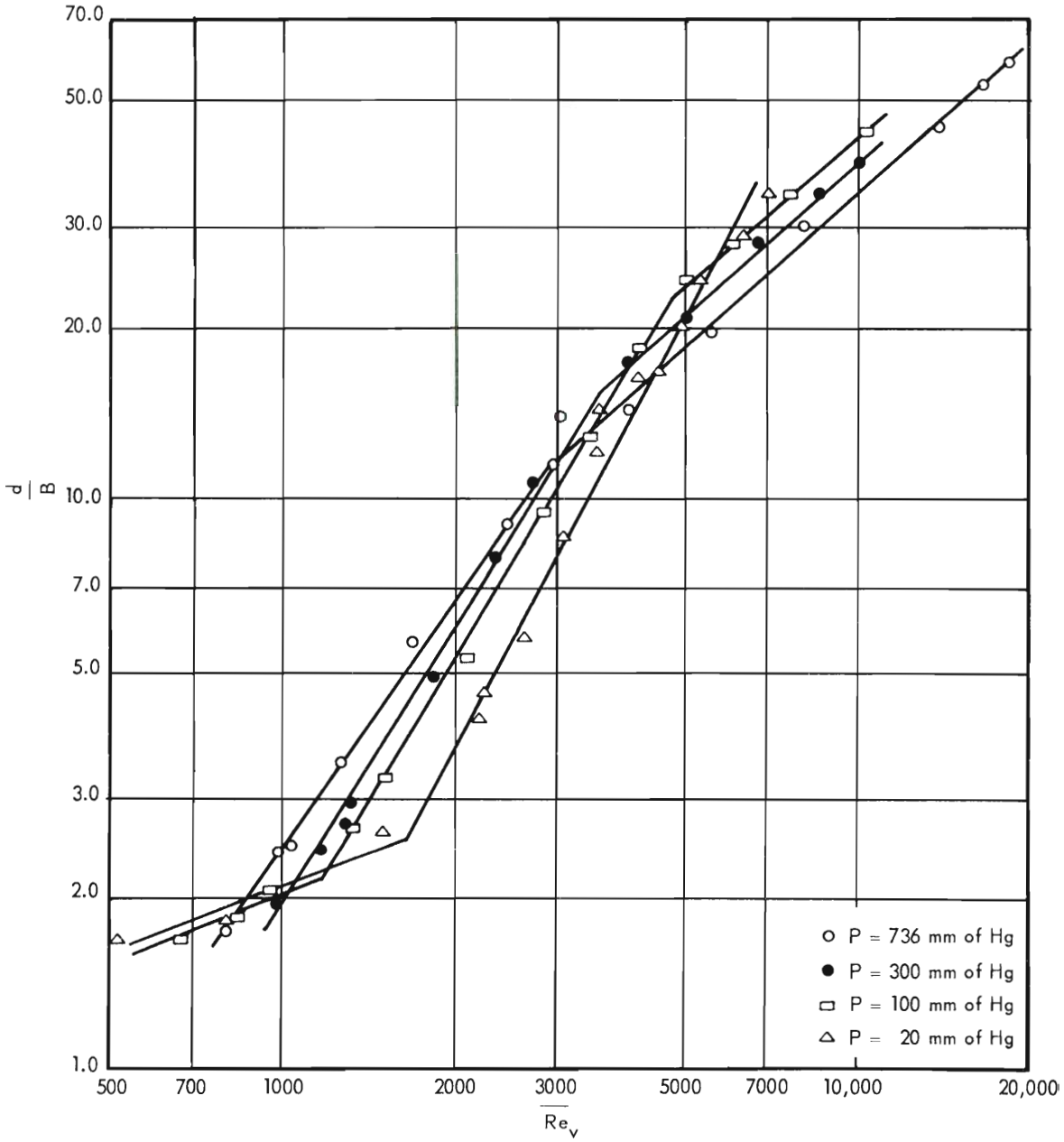

Figure 12. Effect of Pressure on d/B: Laminar, Transition, and Turbulent Regions.

and compared with the predictions presented in CHAPTER II, DISTILLATION THEORY.

Laminar Region

The results of this investigation show that in the region of laminar vapor flow a decrease in pressure at constant vapor velocity causes an increase in column efficiency as is predicted by the theory. The data in the laminar region are compared with Westhaver's (63) relation, equation (87), in Figure 13 by plotting H_G versus $\overline{U}_V$, which is the customary method of presenting data in the laminar region.

The quantitative agreement between the data and the theory is not good. It is evident from Figure 13 that the observed values of H_G are about 2.5 times greater than are predicted by equation (87); however, the discrepancy does not seem unduly great when compared with the discrepancies which have been observed (63)(68) in the data of previous investigations at low vapor flow rates.

As Rose (25) has pointed out, the practical difficulties encountered in the operation of wetted wall distillation columns at low flow rates are great and are caused by small departures of the column from adiabatic performance. The sensitivity to departures from adiabatic operation is easily explained. A given rate of heat loss (or heat input) from the test section must necessarily produce a greater response at low flow rates since the total mass content (on a unit time basis) of the material within the test section is smaller at low flow rates than it is at high flow rates.

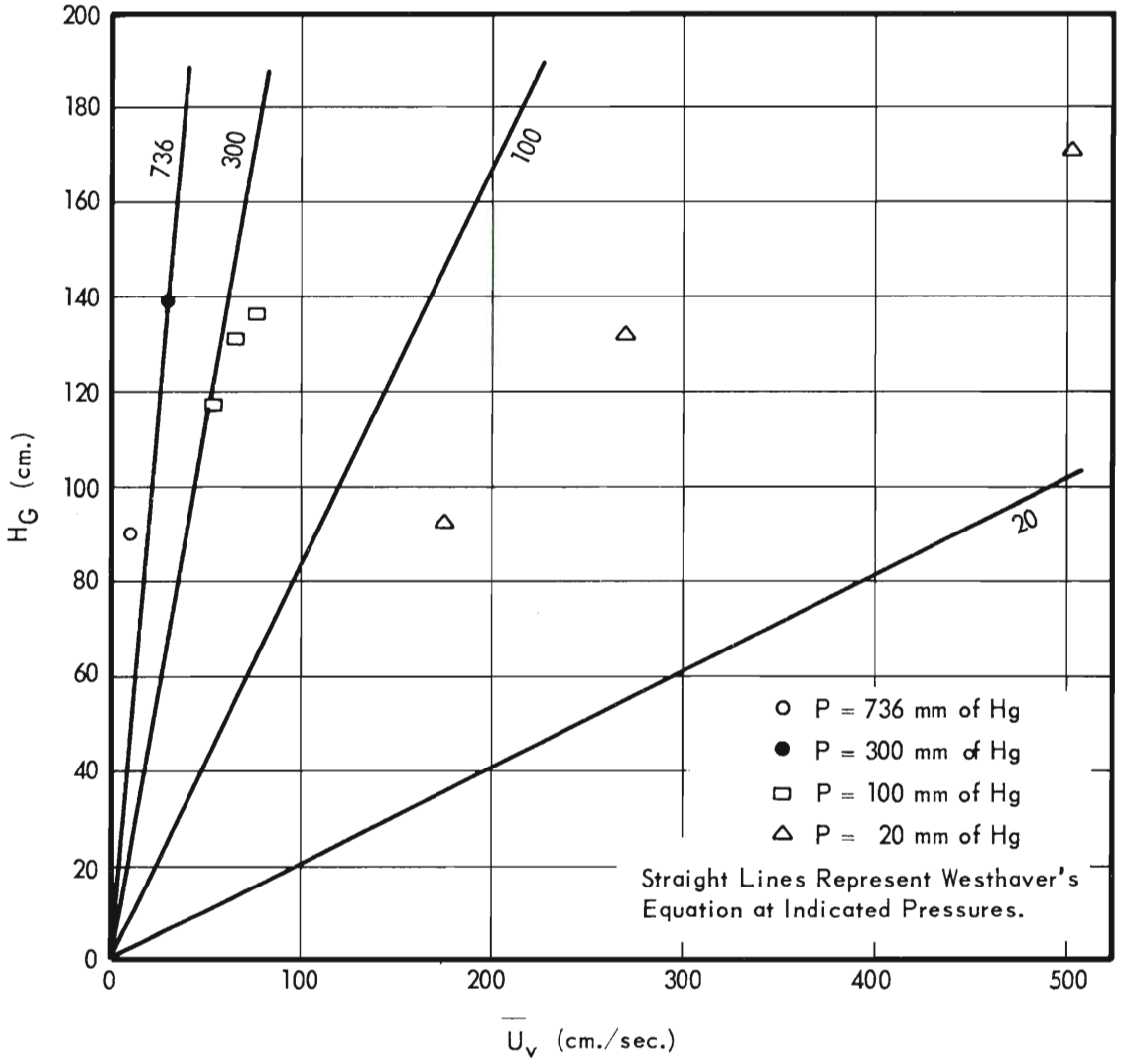

Figure 13. Comparison of Laminar Flow Data with Westhaver (63) Relation.

The fact that the theoretical lines lie to the right of the observed data in Figure 13 indicates that the column compensating heating system (See CHAPTER III) failed to supply enough heat to make the column adiabatic; i.e., a small heat loss existed during all runs. Since a heat loss from the test section would cause extra condensation within the column the flow rate which was measured at the top of the column was less than the flow rate at the bottom of the column and consequently the true average flow rate was larger than that measured at the top. Then, the true average flow rates corresponding to each point in Figure 13 were higher than the measured values used in plotting the points. Therefore, the theoretical lines should lie to the right of the data as is shown in Figure 13.

It is estimated that a heat compensation system capable of keeping temperature differences in the test section wall to less than 0.1 degree centigrade would be required to obtain data in close agreement with Westhaver's equation. For example, at 20 millimeters of mercury pressure, a heat loss corresponding to a 0.5 degree centigrade temperature drop through the test section wall would cause the flow rate at the bottom of the column to be 9.6 grams per minute when the flow rate measured at the top of the test section was only 5.0 grams per minute.

Qualitatively, equation (87) states that

$$\frac{H_G}{\bar{U}_V} \propto \frac{1}{D_V} \tag{98}$$

which suggests that the effect of pressure should be correlated by plotting $H_G / \bar{U}_V$ versus $1/D_V$. The applicability of this relation to the correlation of the observed data in the laminar region is shown in Figure 14. All of the data are well correlated except the single point obtained at 736 millimeters of mercury. Since it fails to correlate, this point is probably not in the region of laminar flow.

Although the amount of data obtained in the laminar region is not large and close agreement between theory and experiment was not obtained, the theoretical prediction of the effect of reduced pressure on column efficiency is qualitatively in excellent agreement with the data. Therefore, it is concluded that Westhaver's equation, equation (87), will satisfactorily predict the effect of reduced pressure on distillation efficiency in the region of laminar vapor flow.

Transition Region

The results of this investigation show that in the region of transitional vapor flow a decrease in pressure at constant vapor Reynolds number causes a decrease in column efficiency. This effect of pressure is illustrated in Figure 15 where the data in the transition region are plotted as d/B versus $\overline{\overline{Re}}_V$.

Although no distillation theory applicable to this region was found in the literature, the results observed may be explained by a consideration of the hydrodynamic state of the vapor and the liquid film on the walls of the column. Those parts of the available literature concerning the transition from laminar to turbulent flow in pipes

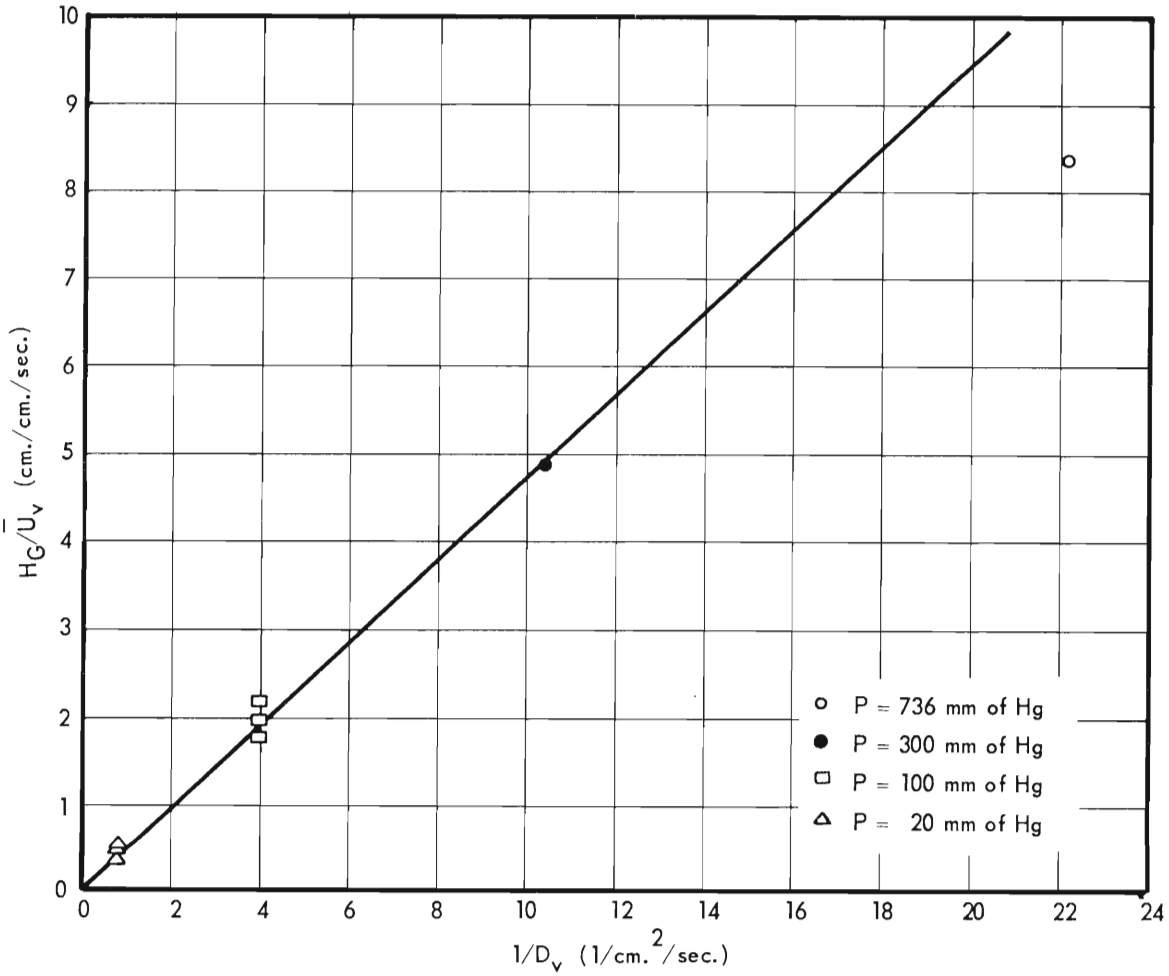

Figure 14. Correlation of Pressure Effect: Laminar Region.

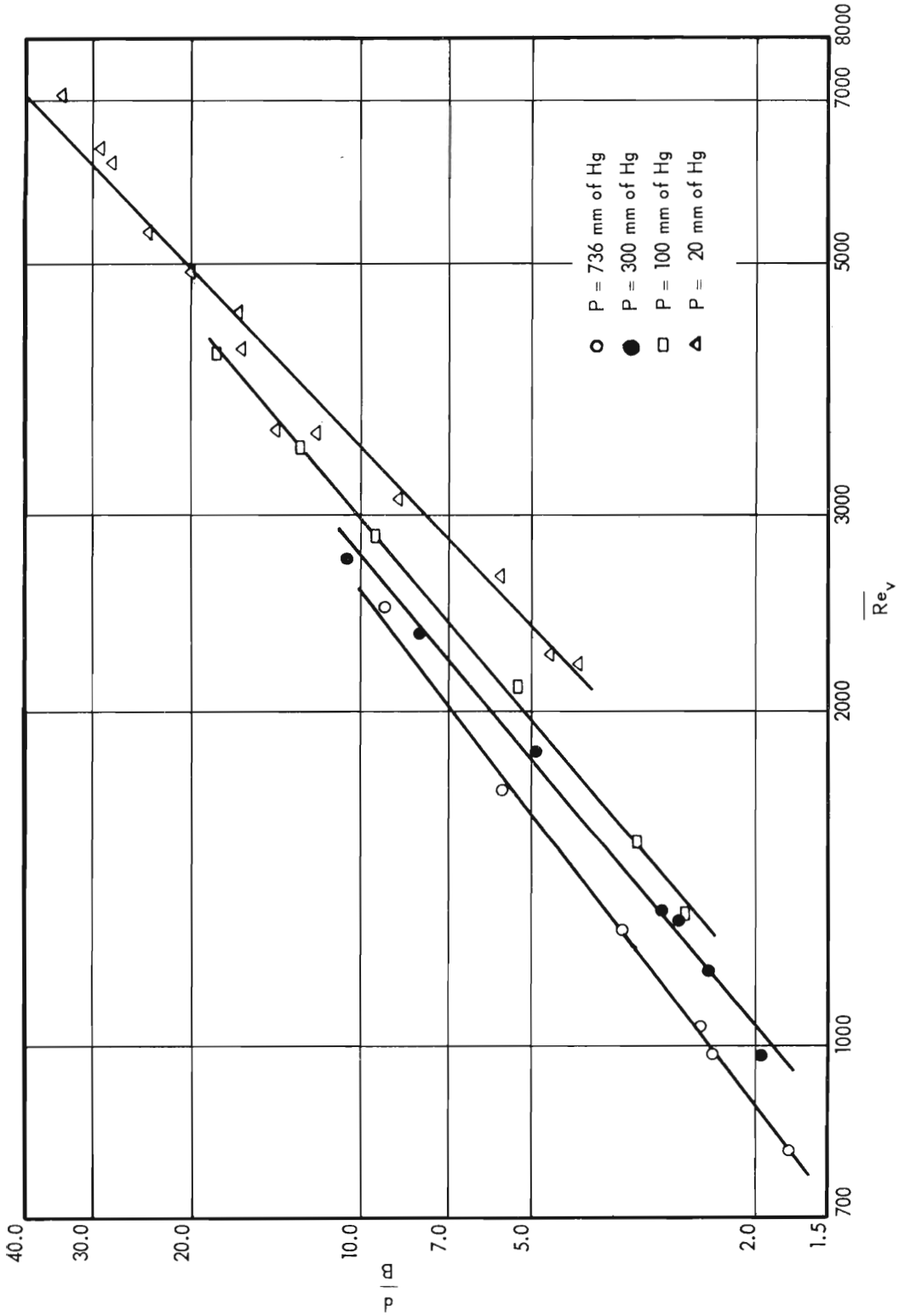

Figure 15. Effect of Pressure on d/B: Transition Region.

and the phenomena of liquid film rippling which are necessary to explain the data are reviewed and summarized in CHAPTER I, INTRODUCTION.

The design of the column used in this investigation (See CHAPTER III, APPARATUS) afforded considerably smoother vapor entry conditions than those normally encountered in flow through pipes. Since the still pot was stirred, vapor evolution from the boiling liquid was smooth and steady. The offset in the calming section between the still pot and the test section further contributed to even vapor flow and the entry to the test section was smooth and well rounded. Thus, the entry conditions created very little disturbance in the entering vapor stream. Therefore, rippling of the reflux film within the test section would be expected to strongly influence the degree of turbulence in the vapor stream and consequently, exert a strong influence on the values of the vapor Reynolds number which define the transition region.

The expected influence of liquid rippling on turbulence in the vapor phase is confirmed by the data. Figure 16, a plot of d/B versus Re_L, shows that the transition from laminar to turbulent flow in the vapor phase begins at a liquid Reynolds number of about 20, that the flow becomes fully turbulent at a liquid Reynolds number of about 80, and that the system pressure has no influence on the range of transition. Thus, the first departure from laminar vapor flow is almost exactly coincident with the inception of the surface waves noted by investigators of liquid film flow and the end of the transition region closely coincides with the attainment of a stable liquid surface configuration which is unaffected by further increase in the liquid Reynolds number.

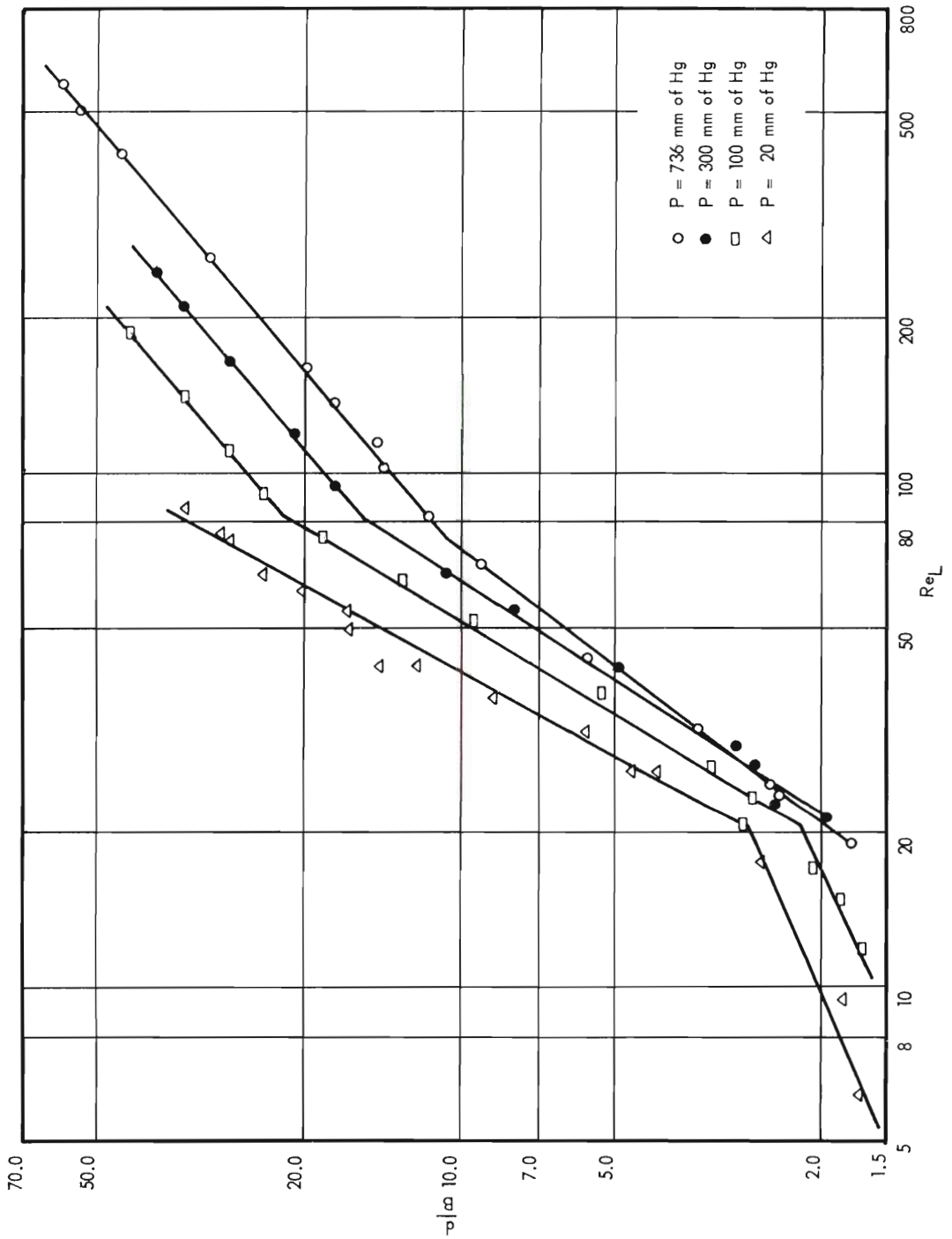

Figure 16. Influence of Liquid Reynolds Number.

The fact that the transition range, when considered in terms of the liquid Reynolds number, is independent of the operating pressure indicates that the degree of vapor turbulence is controlled by the liquid Reynolds number, i.e., by the degree of rippling of the liquid surface. It was concluded in CHAPTER II that in fully developed turbulent flow a reduction in pressure at constant turbulence conditions (constant vapor Reynolds number) should cause an increase in column efficiency. It would be expected that in the transition region a decrease in pressure at constant turbulence conditions should also cause an increase in column efficiency. Since the turbulence conditions in transitional flow are determined by the liquid Reynolds number, a reduction in pressure at constant liquid Reynolds number should therefore cause an increase in column efficiency. This effect of pressure is exhibited by the data shown in Figure 16.

The explanation of the effect of pressure at constant vapor Reynolds number requires an examination of the relationship between the vapor and liquid Reynolds numbers. This investigation was conducted under conditions of total reflux and hence the liquid and vapor Reynolds numbers are closely related. Figure 17 presents the actual relationship derived from the data by plotting $\overline{\overline{Re}}_V$ versus Re_L for each run with operating pressure as a parameter. The data points are omitted from Figure 17 for the sake of clarity.

Since the decrease in operating temperature accompanying a decrease in pressure causes an increase in the liquid viscosity and a decrease in the vapor viscosity, Figure 17 shows that the magnitude

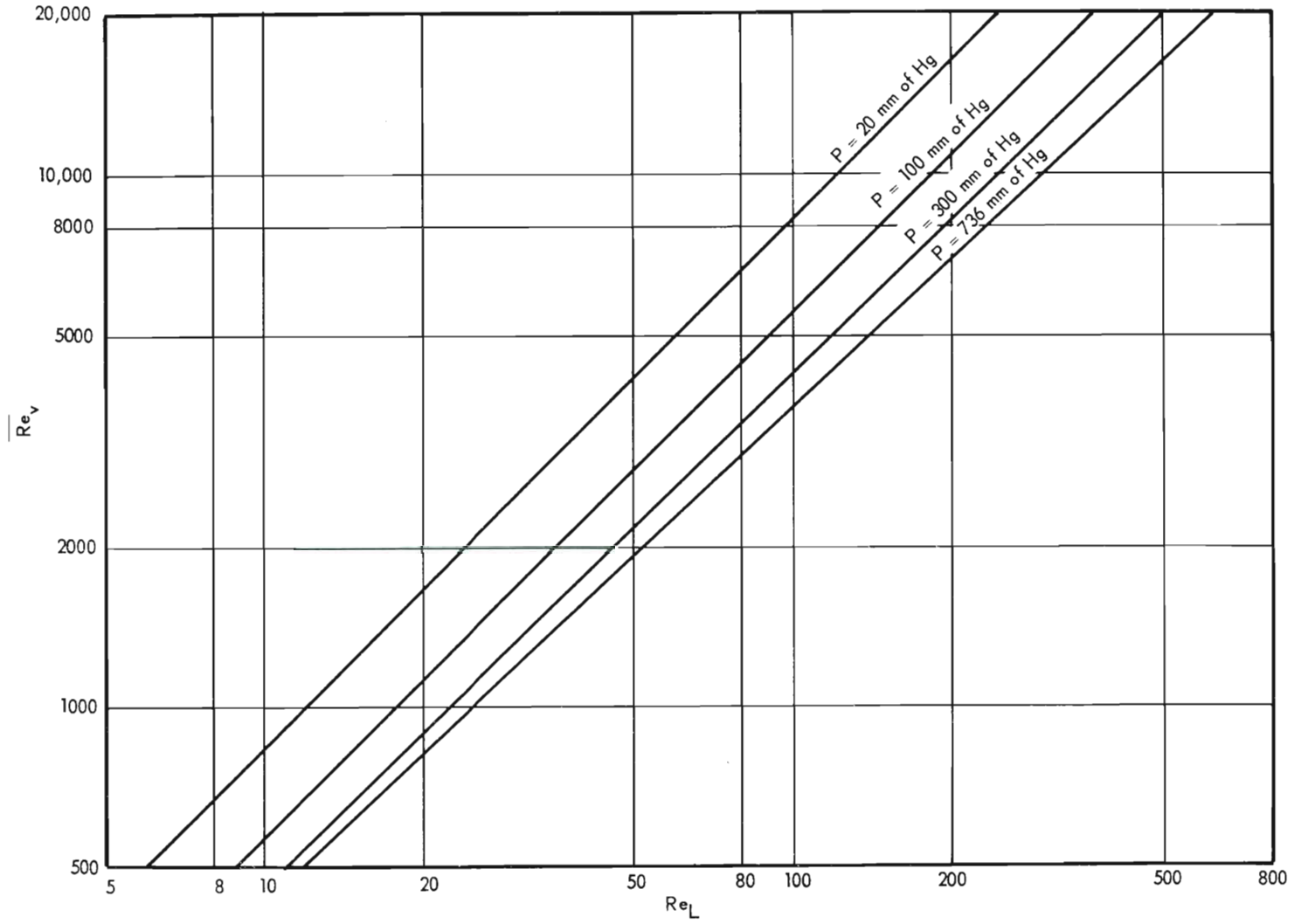

Figure 17. Relation Between Liquid and Vapor Reynolds Numbers at Total Reflux.

of the liquid Reynolds number corresponding to a given vapor Reynolds number decreases as the pressure decreases. Therefore, the degree of rippling decreases and the degree of vapor turbulence decreases as the pressure is decreased at constant vapor Reynolds number. This causes an increase in the thickness of the true laminar layer and an increase in the resistance of the turbulent core which results in an increase in the overall resistance to mass transfer and consequently, a decrease in the column efficiency.

The only data in the transition region available for comparison are that of Nikolaev (36). In Figure 18 the atmospheric pressure data are compared with a line representing Nikolaev's data by plotting d/B versus $\overline{\overline{Re}}_V$. The data of this investigation lie about 15 per cent below the data of Nikolaev. This is probably due to the fact that Nikolaev's column had no calming section before the test section and therefore the entering vapor turbulence conditions were higher than they would have been if a calming section similar to that used in this investigation had been employed.

Turbulent Region

In the region of turbulent vapor flow a decrease in pressure at constant vapor Reynolds number causes an increase in column efficiency as predicted by the turbulent core-laminar layer concept. This pressure effect is shown in Figures 19 and 20 where H_G/d and d/B, respectively, are plotted versus $\overline{\overline{Re}}_V$. No data are shown for the tests at 20 millimeters of mercury because at this pressure the column flooded before a flow rate in the turbulent region could be reached.

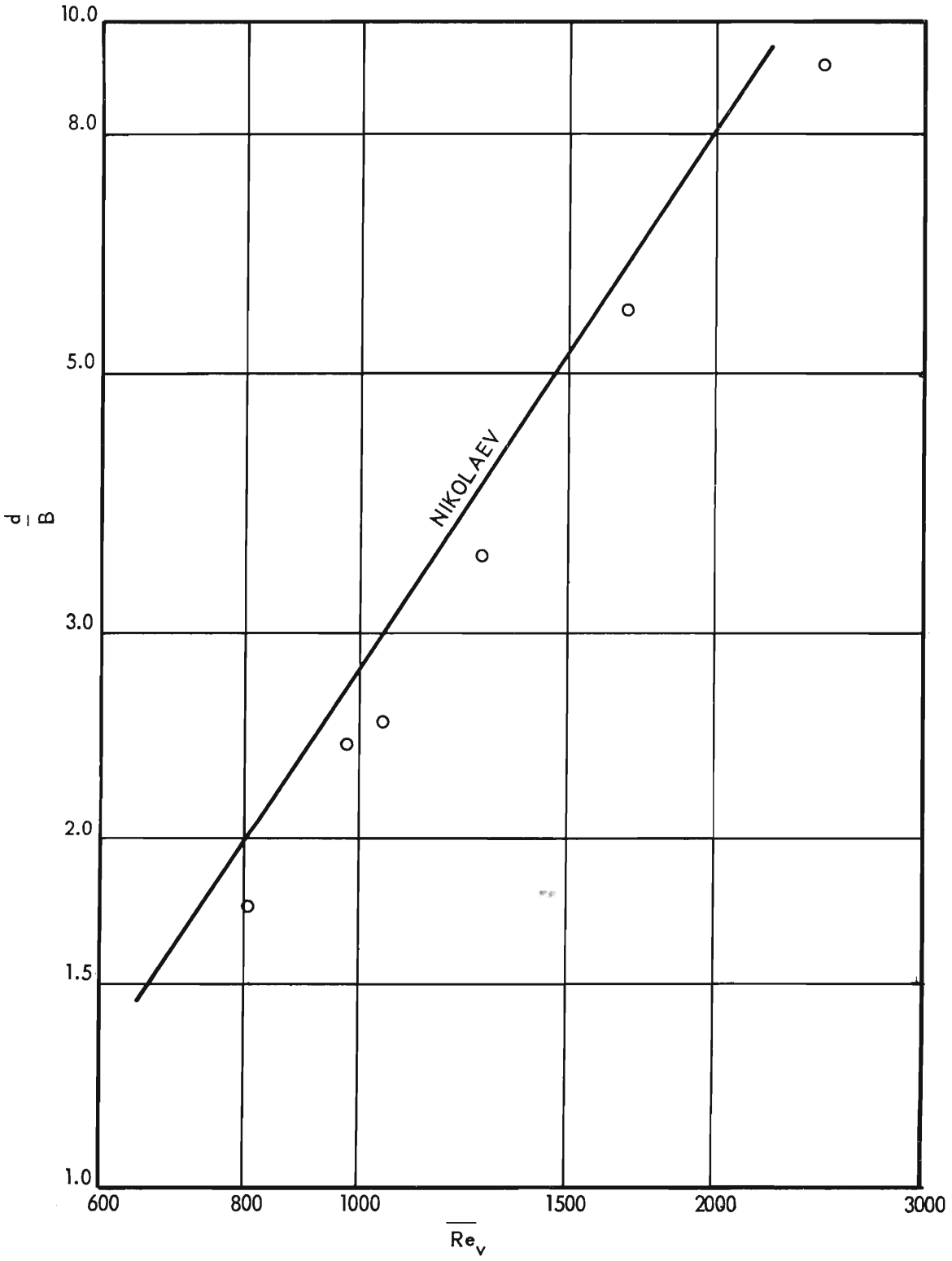

Figure 18. Comparison of Atmospheric Data with Data of Nikolaev (36): Transition Region.

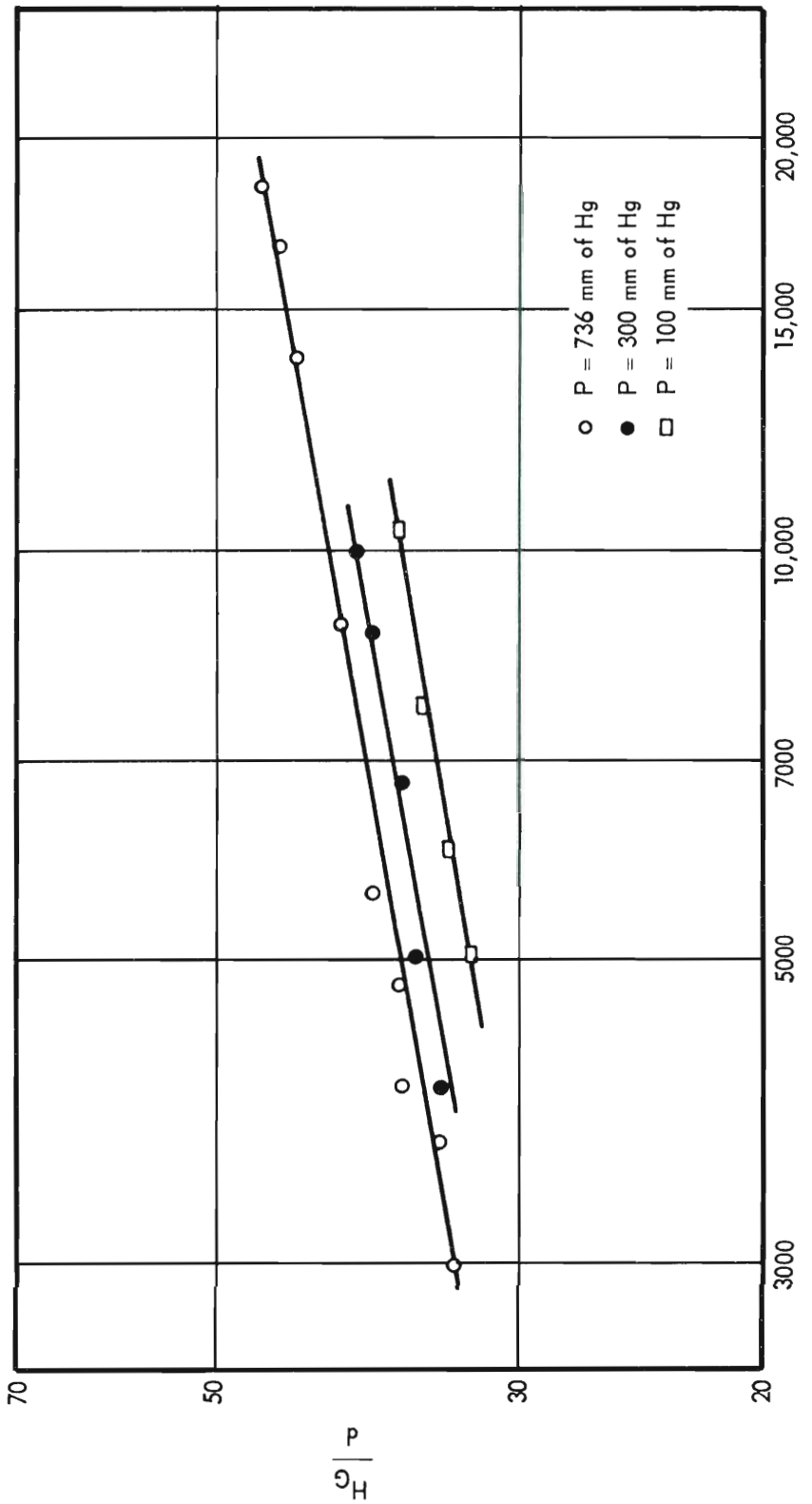

Figure 19. Effect of Pressure on H_G/d: Turbulent Region.

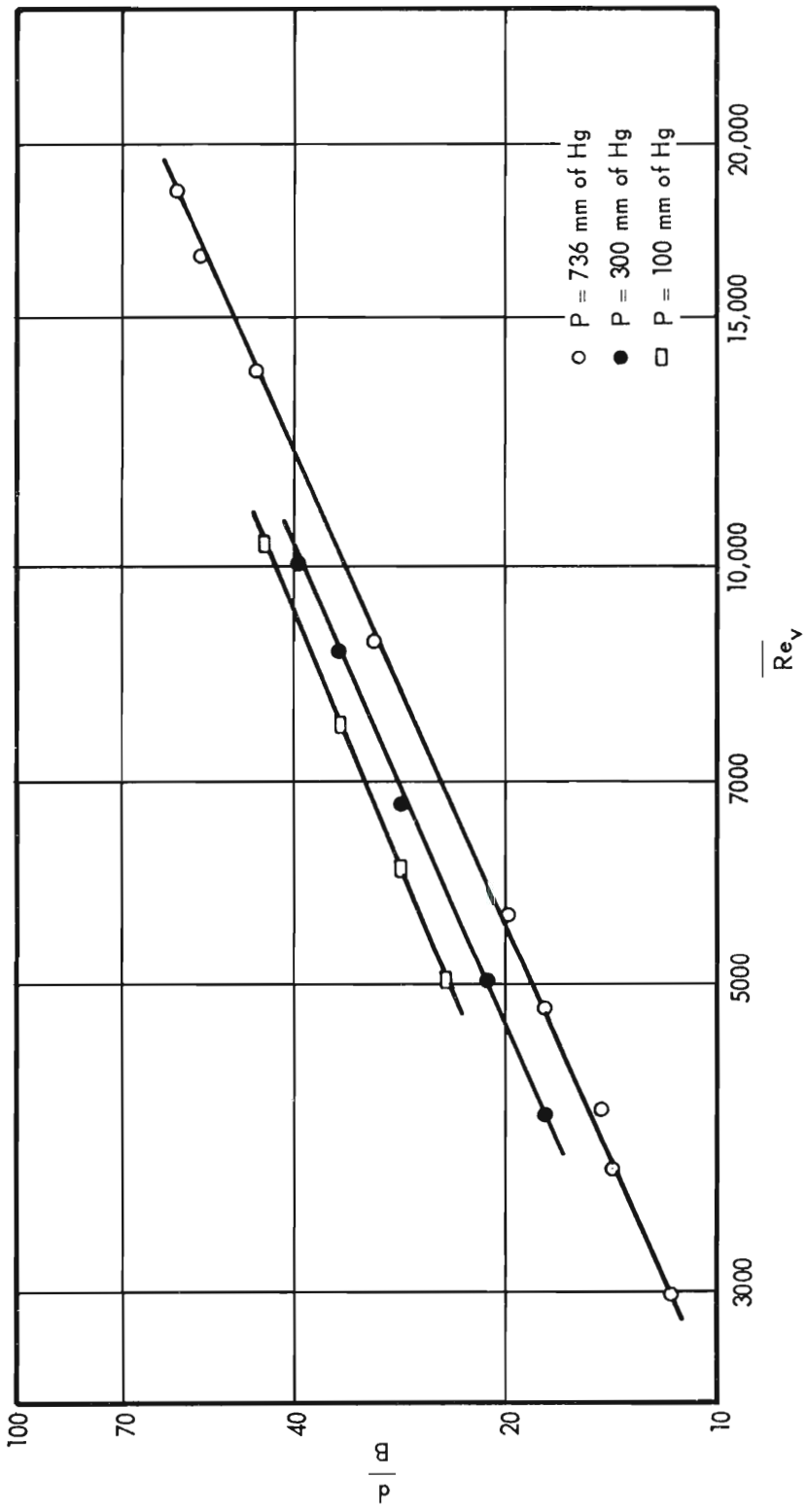

Figure 20. Effect of Pressure on d/B: Turbulent Region.

It was pointed out in CHAPTER II, DISTILLATION THEORY, that the effect of pressure predicted by the conventional correlations depends on whether the correlation is expressed in terms of d/B or H_G/d. This inconsistency was assumed to be symptomatic of a fundamental fault in the form of the correlations. The data of this investigation support this view. Figure 19 shows that a decrease in pressure at constant vapor Reynolds number causes a decrease in H_G/d and hence an increase in column efficiency. Figure 20 shows that a decrease in pressure at constant vapor Reynolds number causes an increase in d/B and hence an increase in column efficiency. Thus, the data and the interpretation of the quantities H_G/d and d/B are consistent regardless of the method by which the data are expressed.

The turbulent core-laminar layer concept explicitly assumes that the vapor phase turbulence conditions are defined by the vapor Reynolds number. The fact that the observed effect of pressure is predicted by the turbulent core-laminar layer concept implies that in the region of turbulent vapor flow the vapor Reynolds number adequately defines the turbulence conditions as contrasted with the transition region where the degree of turbulence is determined by the liquid Reynolds number.

The relationship between the vapor and liquid Reynolds numbers shown in Figure 17 applies in the turbulent region as well as in the transition region. Therefore, a decrease in pressure at constant vapor Reynolds number causes a decrease in the liquid Reynolds number. In the transition region a decrease in liquid Reynolds number causes a decrease in liquid rippling and hence a decrease in vapor turbulence but

in the turbulent region the data indicate that a decrease in liquid Reynolds number has no effect on the vapor turbulence.

Investigations of liquid film flow show that in the liquid Reynolds number range between 20 and 80 the degree of rippling increases as the liquid Reynolds number is increased but at a liquid Reynolds number of approximately 80 a stable surface configuration is attained which remains relatively unchanged up to a liquid Reynolds number of about 2000. As Figure 16 shows, the transition region is confined to a liquid Reynolds number range of 20 to 80 and turbulent vapor flow prevails at all pressures for liquid Reynolds numbers greater than 80. Hence, in the turbulent region, a change in pressure at constant vapor Reynolds number causes no change in the liquid surface. Therefore, the degree of vapor turbulence must be determined by the vapor Reynolds number.

In Figure 21 the data obtained at atmospheric pressure are compared with the correlations of previous investigators by plotting d/B versus $\overline{\overline{Re}}_V$. The atmospheric pressure data are in excellent agreement with Gilliland and Sherwood's (18) correlation of vaporization data, equation (61), and with Johnstone and Pigford's (28) correlation of distillation data, equation (60). The line representing the Chilton-Colburn analogy (80)(81), equation (85), is about 20 per cent below the data.

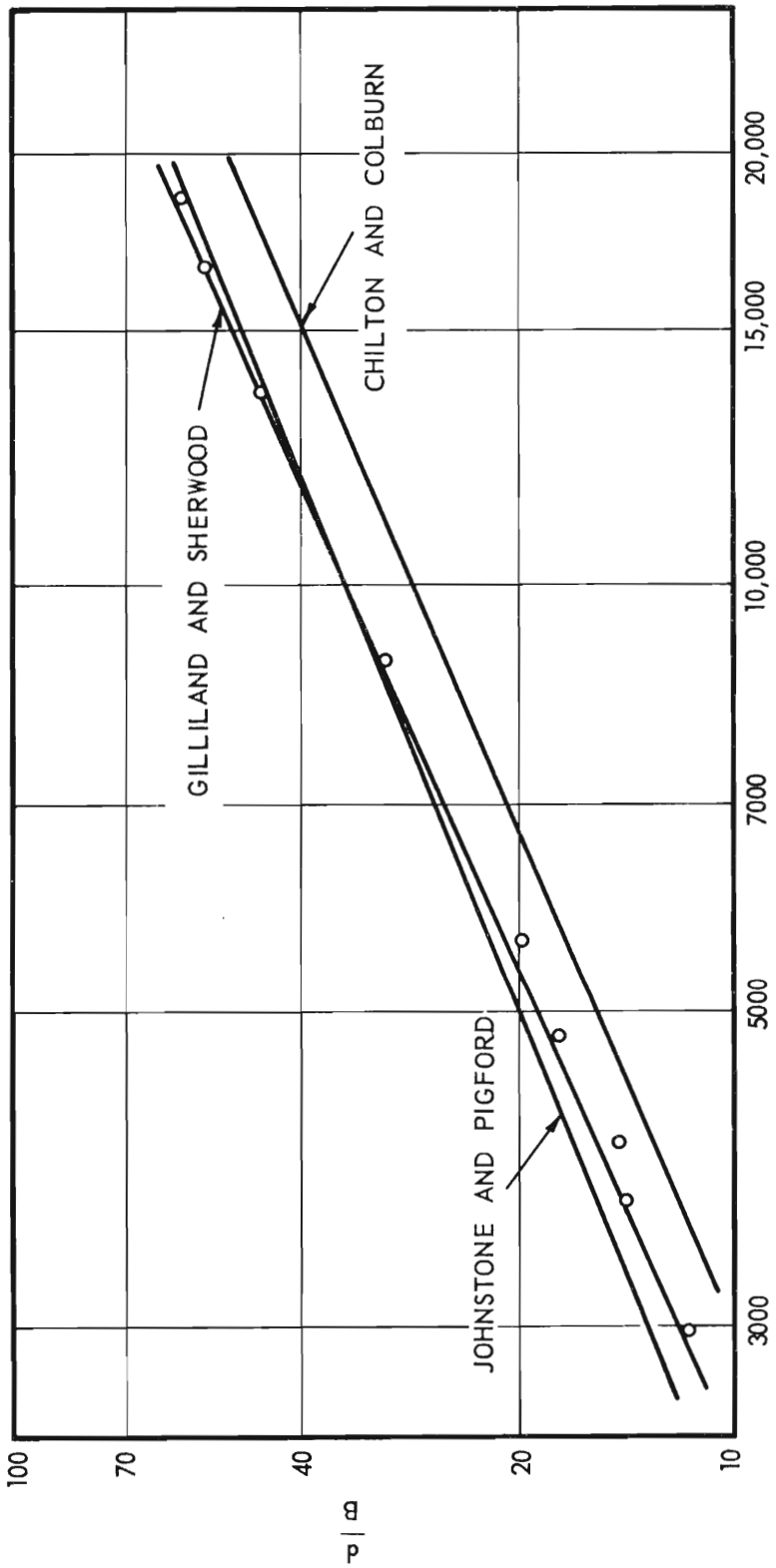

Figure 21. Comparison of Atmospheric Data with Correlations of Johnstone and Pigford (28), Gilliland and Sherwood (18), and Chilton and Colburn (80) (81).

CHAPTER VII

CONCLUSIONS

The following conclusions were drawn from the results of this investigation:

1. In all regions of vapor flow, laminar, transitional, and turbulent, a decrease in operating pressure at constant vapor turbulence conditions causes an increase in column efficiency.

2. In the region of laminar vapor flow there is no turbulence; therefore, vapor turbulence conditions are constant and a decrease in pressure at constant vapor velocity causes an increase in column efficiency.

3. The effect of reduced pressure in the region of laminar vapor flow is correlated by the Westhaver (63) equation,

$$\frac{H_G}{\bar{U}_V} \propto \frac{1}{D_V} \tag{98}$$

4. In the region of transitional vapor flow the degree of turbulence of the vapor is determined by the degree of rippling of the liquid reflux film which, in turn, is determined by the liquid Reynolds number; hence, in this region a decrease in operating pressure at constant liquid Reynolds number causes an increase in column efficiency.

5. In the region of transitional vapor flow the relation between the vapor Reynolds number and the liquid Reynolds number is such that a

decrease in operating pressure at constant vapor Reynolds number causes a decrease in column efficiency.

6. In the region of turbulent vapor flow the degree of turbulence of the vapor is determined by the vapor Reynolds number; consequently, in this region a decrease in operating pressure at constant vapor Reynolds number causes an increase in column efficiency.

7. The effect of reduced pressure in the region of turbulent vapor flow is qualitatively predicted by the turbulent core-laminar layer concept introduced by Yoshida (34) and Gilliland (35).

8. Empirical relations which include the Schmidt number to a fractional power, such as those of Gilliland and Sherwood (18), Johnstone and Pigford (28), and Chilton and Colburn (80)(81), cannot correlate the effect of reduced pressure on distillation efficiency.

9. The vapor Reynolds number at which turbulent flow begins in the vapor is a function of the degree of rippling of the liquid reflux film and varies with the operating pressure.

APPENDICES

APPENDIX I

SAMPLE CALCULATIONS

SAMPLE CALCULATIONS

General

The determination of the physical properties of the test mixture required to evaluate the data of this investigation was discussed in CHAPTER V, PHYSICAL PROPERTIES OF THE TEST MIXTURE. The physical properties of the column mixture for each run are presented in Tables 12 and 13.

The sample calculations are based on the experimental data for Run 32 given in Table 17. The experimental data and the physical properties of the column mixture for this run are summarized below:

Run 32

P, Operating Pressure	100 mm. of Hg.
T, Operating Temperature	72.9°C.
$\bar{W}$, Mass Flow Rate	54.9 gm./min.
Y_T, Mole Fraction Chlorobenzene at Top	0.5918
Y_B, Mole Fraction Chlorobenzene at Bottom .	0.5470
μ_V, Vapor Viscosity	0.8194×10^{-4} poise
ρ_V, Vapor Density	5.090×10^{-4} gm./cm.^{3}
D_V, Vapor Diffusivity	0.2473 cm.^{2}/sec.
μ_L, Liquid Film Viscosity	4.347×10^{-3} poise
ρ_L, Liquid Film Density	0.9363 gm./cm.^{3}

Liquid Reynolds Number

The Reynolds number for the flow of a viscous, isothermal, falling film (43) is

$$Re_L = \frac{4\Gamma}{\mu_L}$$

The mass rate of flow per unit width of wall is given by

$$\Gamma = \frac{(\text{Mass Flow Rate})}{(\text{Circumference})} \times (\text{Conversion Factor})$$

$$= \frac{(54.9 \text{ gm./min.})}{(5.969 \text{ cm.})} \times \frac{1}{(60 \text{ sec./min.})}$$

$$= 0.1533 \text{ gm./sec.-cm.}$$

Thus,

$$Re_L = \frac{(4)(0.1533 \text{ gm./sec.-cm.})}{(4.347 \times 10^{-3} \text{ gm.}_c/\text{sec.-cm.})}$$

$$= 141$$

Vapor Reynolds Number Relative to the Liquid Surface

The vapor Reynolds number relative to the liquid surface is

$$\overline{Re}_V = \frac{\rho_V \, \overline{U}'_V \, d}{\mu_V}$$

The average vapor velocity relative to the liquid surface is

$$\overline{U}'_V = \overline{U}_V + U_S$$

The average vapor velocity relative to the tube wall is

$$\bar{U}_V = \frac{\text{(Mass Flow Rate)}}{\text{(Vapor Density)(Cross-Section Area)}} \times \text{(Conversion Factor)}$$

$$= \frac{(54.9 \text{ gm./min.})}{(5.090 \times 10^{-4} \text{ gm./cm.}^3)(2.835 \text{ cm.}^2)} \times \frac{1}{(60 \text{ sec./min.})}$$

$$= 634 \text{ cm./sec.}$$

The liquid surface velocity was calculated from the average liquid film thickness given by equation (1) as follows:

$$m = \left(\frac{3 \mu_L \Gamma}{\rho_L^2 g_c}\right)^{1/3}$$

$$= \left(\frac{(3)(4.347 \times 10^{-3} \text{ gm./sec.-cm.})(0.1533 \text{ gm./sec.-cm.})}{(0.9363 \text{ gm./cm.}^3)^2 (980.6 \text{ cm./sec.}^2)}\right)^{1/3}$$

$$= 1.325 \times 10^{-2} \text{ cm.}$$

The average liquid velocity is given by

$$\bar{U}_L = \frac{\text{(Mass Flow Rate Per Unit Wall Width)}}{\text{(Liquid Film Density)(Liquid Film Thickness)}}$$

$$= \frac{(0.1533 \text{ gm./sec.-cm.})}{(0.9363 \text{ gm./cm.}^3)(1.325 \times 10^{-2} \text{ cm.})}$$

$$= 12.35 \text{ cm./sec.}$$

The liquid surface velocity is given by equation (2) as

$$U_S = 1.5\ \bar{U}_L$$

$$= (1.5)(12.35\ \text{cm./sec.})$$

$$= 18.5\ \text{cm./sec.}$$

Thus,

$$\bar{U}'_V = \bar{U}_V + U_S$$

$$= 634\ \text{cm./sec.} + 18.5\ \text{cm./sec.}$$

$$= 652.5\ \text{cm./sec.}$$

Finally,

$$\overline{Re}_V = \frac{\rho_V\ \bar{U}'_V\ d}{\mu_V}$$

$$= \frac{(5.090 \times 10^{-4}\ \text{gm./cm.}^3)(652.5\ \text{cm./sec.})(1.9\ \text{cm.})}{(0.8194 \times 10^{-4}\ \text{gm./sec.-cm.})}$$

$$= 7700$$

Height of a Transfer Unit

The height of a transfer unit is given by equation (53) as

$$H_G = Z/N_{tG}$$

For constant relative volatility and total reflux, equation (55) gives the number of transfer units required to effect a given separation. Thus,

$$N_{tG} = \frac{2.303}{\alpha_R - 1}\left[\text{Log}\ \frac{Y_T}{Y_B} - \alpha_R\ \text{Log}\ \frac{1 - Y_T}{1 - Y_B}\right]$$

Since vapor-liquid equilibrium data were not available at 100 millimeters of mercury pressure it was necessary to estimate the relative volatility at this pressure. This was accomplished by logarithmic interpolation between the reported values at 760 and 20 millimeters given in Table 16.

The interpolation equation used was

$$\text{Log } \alpha_R = 0.04118 + \frac{0.16083}{P}$$

For 100 millimeters of mercury pressure, this equation gives

$$\alpha_R = 1.104$$

Thus,

$$N_{tG} = \frac{2.303}{\alpha_R - 1}\left[\text{Log } \frac{Y_T}{Y_B} - \alpha_R \text{ Log } \frac{1 - Y_T}{1 - Y_B}\right]$$

$$= \frac{2.203}{1.104 - 1}\left[\text{Log } \frac{0.5918}{0.5470} - 1.104 \text{ Log } \frac{1 - 0.5918}{1 - 0.5470}\right]$$

$$= 1.864$$

Then,

$$\frac{H_G}{d} = \frac{Z}{N_{tG}\, d}$$

$$= \frac{(125.1 \text{ cm.})}{(1.864)(1.9 \text{ cm.})}$$

$$= 35.3$$

Effective Film Thickness

The effective film thickness is given by equation (57) as

$$B = \frac{4 D_m M_m Z}{G N_{tG} d} = \frac{4 D_V \rho_V Z}{G N_{tG} d}$$

The mass flow rate per unit area is

$$G = \frac{(\text{Mass Flow Rate})}{(\text{Cross-Section Area})} \times (\text{Conversion Factor})$$

$$= \frac{(54.9 \text{ gm./min.})}{(2.835 \text{ cm.}^2)} \times \frac{1}{(60 \text{ sec./min.})}$$

$$= 0.3228 \text{ gm./sec. - cm.}^2$$

Thus,

$$B = \frac{4 D_V \rho_V Z}{G N_{tG} d}$$

$$= \frac{(4)(0.2473 \text{ cm.}^2/\text{sec.})(5.090 \times 10^{-4} \text{ gm./cm.}^3)(125.1 \text{ cm.})}{(0.3228 \text{ gm./sec. - cm.}^2)(1.864)(1.9 \text{ cm.})}$$

$$= 0.05510 \text{ cm.}$$

Then,

$$\frac{d}{B} = \frac{(1.9 \text{ cm.})}{(0.05510 \text{ cm.})}$$

$$= 34.5$$

APPENDIX II

CALIBRATION DATA

Table 1. Rotometer Calibration Data: Chlorobenzene at 23° C.

Float Height (cm.)		
Pyrex	Steel	Flow Rate ($cm.^3/min.$)
14.60	6.90	73.6
14.45	7.00	75.0
13.75	6.45	69.1
13.20	6.15	64.7
12.90	6.10	64.5
12.10	5.50	58.7
11.45	5.20	53.2
11.35	5.20	53.1
10.90	4.90	51.8
10.75	4.85	48.2
10.40	4.60	47.7
9.90	4.35	47.0
9.80	4.30	41.6
9.25	4.00	43.2
9.15	4.00	39.5
9.00	3.80	40.2
8.85	3.70	40.0
8.55	3.50	38.1
8.25	3.20	36.2
8.05	3.10	33.1
7.55	2.75	31.1

Table 1 (Continued)

Float Height (cm.) Pyrex	Steel	Flow Rate ($cm.^3/min.$)
7.40	3.20	32.6
6.80	2.45	28.5
6.45	2.25	25.1
6.25	2.15	23.0
6.25	2.10	25.4
5.05	1.65	19.1
4.60	1.55	16.7
4.60	1.40	15.7
3.95	1.20	12.5
3.90	1.20	12.1
3.50	1.00	11.8
3.15	1.05	9.45
2.90	0.85	7.35
1.90	0.30	4.57
1.70	0.15	3.60
1.00	----	2.52

Table 2. Rotometer Calibration Data: Ethylbenzene at 24° C.

Float Height (cm.) Pyrex	Steel	Flow Rate ($cm.^3/min.$)
13.10	6.50	81.0
11.85	5.80	71.4
10.35	4.95	61.2
9.55	4.45	53.0
8.85	4.05	48.2
8.30	3.65	45.2
8.05	3.45	43.0
6.40	2.60	32.2
6.20	2.30	31.9
5.40	1.80	24.8
4.15	1.35	18.7
3.10	0.95	13.6
2.95	0.90	12.2
1.00	----	2.95

Table 3. Rotometer Calibration Data: Water at 21° C.

Float Height (cm.)		
Pyrex	Steel	Flow Rate ($cm.^3/min.$)
14.60	7.25	78.2
14.10	6.90	71.6
12.90	6.20	61.9
12.75	6.20	64.2
10.80	5.15	50.0
10.35	4.95	48.8
9.10	4.00	38.7
8.95	4.00	39.3
8.10	3.40	33.1
7.45	2.80	28.2
5.05	1.85	14.0
3.70	1.30	8.41
3.65	1.20	8.04
1.90	0.45	3.80

Table 4. Rotometer Calibration Data: Ethylbenzene at 31° C.

Float Height (cm.)		
Pyrex	Steel	Flow Rate ($cm.^3/min.$)
9.60	4.50	57.1
7.70	3.20	43.8
4.85	1.60	25.2
2.90	0.80	13.6

Table 5. Rotometer Float Data

	Pyrex	Steel
D_f, Float Diameter (inches)	0.1562	0.1562
W_f, Float Weight (grams)	0.0926	0.2619
ρ_f, Float Density (gm./cm.^{3})	2.833	8.012

Table 6. Thermocouple Calibration Data: Numbers O and 11

Temperature (°C.)	e.m.f. (millivolts) Number O	Number 11
26.70	1.345	1.345
26.70	1.344	1.344
26.71	1.344	1.344
39.05	2.979	1.980
39.05	1.979	1.980
39.05	1.979	1.980
51.08	2.606	2.607
51.08	2.606	2.607
51.08	2.605	2.606
51.10	2.605	2.606
51.10	2.605	2.605
63.18	3.244	3.245
63.18	3.244	3.245
63.18	3.244	3.245
75.00	3.870	3.871
75.00	3.870	3.871
75.00	3.870	3.871

Table 6 (Continued)

Temperature (°C.)	e.m.f. (millivolts) Number 0	Number 11
87.00	4.506	4.508
87.00	4.506	4.508
87.00	4.508	4.509
87.00	4.507	4.509
99.40	5.175	5.175
99.40	5.175	5.176
99.40	5.175	5.176
113.00	5.902	5.905
113.00	5.902	5.904
113.00	5.902	5.905
113.00	5.902	5.904
113.00	5.904	5.905
126.40	6.627	6.631
126.40	6.626	6.631
126.40	6.626	6.629
126.40	6.628	6.630
126.40	6.628	6.630
138.00	7.270	7.272

Table 6 (Continued)

Temperature (°C.)	e.m.f. (millivolts) Number 0	Number 11
138.00	7.270	7.272
138.00	7.270	7.275
138.00	7.271	7.275
138.00	7.269	7.275
138.00	7.271	7.275

Table 7. Thermocouple Calibration Table: 72.00 to 73.00 °C.

e.m.f. (millivolts)	Temperature (°C.)
3.712	72.00
3.714	72.05
3.717	72.10
3.720	72.15
3.722	72.20
3.725	72.25
3.728	72.30
3.730	72.35
3.733	72.40
3.735	72.45
3.738	72.50
3.741	72.55
3.743	72.60
3.746	72.65
3.749	72.70
3.751	72.75
3.754	72.80
3.757	72.85
3.759	72.90
3.762	72.95
3.765	73.00

Table 8. Comparison of Thermocouples Numbers 1 to 5 with Number 11

Temp. (°C.)	e.m.f. (millivolts) Number: 1	2	3	4	5	11
46.60	2.361	2.361	2.361	2.361	2.361	2.355
46.60	2.361	2.356	2.356	2.360	2.361	2.355
46.60	2.359	2.359	2.359	2.360	2.360	2.355
72.35	3.730	3.730	3.730	3.732	3.732	3.724
72.35	3.730	3.731	3.731	3.734	3.734	3.724
72.35	3.734	3.730	3.730	3.733	3.733	3.725
72.35	3.731	3.731	3.731	3.734	3.734	3.724

Comparison of Thermocouples Numbers 6 to 10 with Number 11

Temp. (°C.)	e.m.f (millivolts) Number: 6	7	8	9	10	11
46.60	2.361	2.361	2.361	2.360	2.356	2.355
46.60	2.361	2.361	2.360	2.360	2.356	2.355
46.60	2.360	2.360	2.360	2.360	2.356	2.355
72.35	3.735	3.735	3.735	3.735	3.726	3.725
72.35	3.734	3.734	3.734	3.734	3.726	3.724
72.35	3.733	3.733	3.733	3.733	3.726	3.725
72.35	3.735	3.735	3.735	3.735	3.726	3.724

Table 9. Refractive Index - Composition Calibration Data: T = 25°C.

Mole Fraction Chlorobenzene	Refractometer Scale Reading
0.0000	15.755
0.1068	16.260
0.1943	16.670
0.2780	17.075
0.3471	17.415
0.4191	17.770
0.4795	18.075
0.5488	18.435
0.6004	18.705
0.6484	18.960
0.6932	19.200
0.7565	19.550
0.8110	19.850
0.8604	20.125
0.8974	20.335
1.0000	20.925

Table 10. Refractive Index - Compsition Calibration: T = 25°C.: 0.4997 to 0.5181 Mole Fraction Chlorobenzene

Refractometer Scale Reading	Mole Fraction Chlorobenzene
18.180	0.4997
18.185	0.5006
18.190	0.5016
18.195	0.5026
18.200	0.5035
18.205	0.5045
18.210	0.5055
18.215	0.5065
18.220	0.5074
18.225	0.5084
18.230	0.5094
18.235	0.5103
18.240	0.5113
18.245	0.5123
18.250	0.5133
18.255	0.5142
18.260	0.5152
18.265	0.5162
18.270	0.5171
18.275	0.5181

APPENDIX III

PHYSICAL PROPERTIES

Table 11. General Properties of the Test Mixture Components

Property	Chlorobenzene	Ethylbenzene
Molecular Weight (gm./gm.-mole)	112.56	106.16
Specific Gravity (20/4)	1.107	0.867
Normal Boiling Point (°C.)	132.1	136.2
Refractive Index	1.52479 at 25°C.	1.49828 at 14.5°C.
Critical Temperature (°C.)	359	346.6
Critical Pressure (atm.)	44.6	38

References: (96) (97)

Table 12. Physical Properties of the Column Vapor Mixture
P = 736 Millimeters of Mercury

Run	T(°C.)	$\mu_V \times 10^4$ (poise)	$\rho_V \times 10^3$ (gm./cm.^{3})	$D_V \times 10^2$ (cm.^{2}/sec.)	Sc_V
1	132	0.9695	3.178	4.496	0.6785
2	132	0.9695	3.189	4.477	0.6790
3	132	0.9695	3.189	4.477	0.6790
4	133	0.9720	3.218	4.449	0.6789
5	134	0.9745	3.189	4.499	0.6792
6	133	0.9720	3.191	4.486	0.6790
7	133	0.9720	3.179	4.504	0.6788
8	133	0.9720	3.144	4.554	0.6788
9	133	0.9720	3.182	4.498	0.6792
10	133	0.9720	3.158	4.529	0.6797
11	133	0.9720	3.179	4.504	0.6787
12	133	0.9720	3.179	4.504	0.6787
13	134	0.9745	3.189	4.499	0.6790
14	133	0.9720	3.191	4.486	0.6792
15	133	0.9720	3.191	4.486	0.6792

Table 12 (Continued)

P = 20 Millimeters of Mercury

Run	T(°C.)	$\mu_V \times 10^4$ (poise)	$\rho_V \times 10^4$ (gm./cm.^{3})	D_V (cm.^{2}/sec.)	Sc_V
16	38.1	0.7280	1.134	1.018	0.6306
17	38.6	0.7305	1.121	1.024	0.6364
18	37.9	0.7280	1.124	1.018	0.6362
19	37.1	0.7255	1.128	1.012	0.6355
20	39.6	0.7330	1.126	1.030	0.6320
21	38.6	0.7305	1.129	1.024	0.6319
22	40.0	0.7330	1.127	1.030	0.6314
23	38.0	0.7280	1.133	1.018	0.6311
24	37.0	0.7255	1.136	1.012	0.6310
25	37.8	0.7280	1.133	1.018	0.6311
26	38.6	0.7305	1.129	1.024	0.6318
27	39.6	0.7330	1.125	1.030	0.6326
28	38.9	0.7305	1.128	1.024	0.6324
29	38.1	0.7280	1.132	1.018	0.6317
30	38.0	0.7280	1.132	1.018	0.6317
31	38.2	0.7280	1.132	1.018	0.6317

Table 12 (Continued)

P = 100 Millimeters of Mercury

Run	T(°C.)	$\mu_V \times 10^4$ (poise)	$\rho_V \times 10^4$ (gm./cm.^{3})	D_V (cm.^{2}/sec.)	Sc_V
32	72.9	0.8194	5.090	0.2473	0.6510
33	72.8	0.8194	5.090	0.2473	0.6510
34	72.1	0.8170	5.104	0.2460	0.6507
35	71.9	0.8170	5.104	0.2460	0.6507
36	72.6	0.8194	5.090	0.2473	0.6510
37	72.6	0.8194	5.090	0.2473	0.6510
38	71.9	0.8170	5.107	0.2460	0.6503
39	71.5	0.8170	5.104	0.2460	0.6507
40	72.9	0.8194	5.092	0.2473	0.6506
41	72.4	0.8194	5.092	0.2473	0.6506
42	73.2	0.8194	5.090	0.2473	0.6510
43	72.9	0.8194	5.092	0.2473	0.6506
44	72.0	0.8170	5.104	0.2460	0.6507
45	72.8	0.8194	5.090	0.2473	0.6510

Table 12 (Continued

P = 300 Millimeters of Mercury

Run	T(°C.)	$\mu_V \times 10^4$ (poise)	$\rho_V \times 10^3$ (gm./cm.^{3})	$D_V \times 10^2$ (cm.^{2}/sec.)	Sc_V
46	103	0.8947	1.405	9.592	0.6639
47	103	0.8947	1.406	9.592	0.6634
48	103	0.8947	1.406	9.592	0.6634
49	102	0.8920	1.409	9.546	0.6632
50	103	0.8947	1.406	9.592	0.6634
51	104	0.8974	1.401	9.640	0.6644
52	103	0.8947	1.405	9.592	0.6639
53	102	0.8920	1.409	9.546	0.6632
54	104	0.8974	1.402	9.640	0.6640
55	103	0.8947	1.405	9.592	0.6639
56	103	0.8947	1.405	9.592	0.6639
57	104	0.8974	1.402	9.640	0.6640

Table 13. Physical Properties of the Column Liquid Mixture

P = 736 Millimeters of Mercury

	Reflux Film			Rotometer Exit		
Run	T(°C.)	$\mu_L \times 10^3$ (poise)	ρ_L (gm./cm.^{3})	T(°C.)	$\mu_L \times 10^3$ (poise)	ρ_L (gm./cm.^{3})
1	132	2.737	0.8625	100	3.449	0.9006
2	132	2.737	0.8627	93	3.641	0.9097
3	132	2.737	0.8625	84	3.929	0.9182
4	133	2.719	0.8615	75	4.247	0.9276
5	134	2.705	0.8616	76	4.212	0.9277
6	133	2.722	0.8623	58	4.956	0.9445
7	133	2.717	0.8606	37	6.154	0.9625
8	133	2.718	0.8610	24	7.152	0.9764
9	133	2.720	0.8619	25	7.073	0.9765
10	133	2.717	0.8605	105	3.320	0.8939
11	133	2.719	0.8611	87	3.827	0.9156
12	133	2.718	0.8610	78	4.133	0.9238
13	134	2.705	0.8616	65	4.645	0.9386
14	133	2.720	0.8615	27	6.904	0.9741
15	133	2.718	0.8609	25	7.065	0.9752

Table 13 (Continued)

P = 20 Millimeters of Mercury

	Reflux Film			Rotometer Exit		
Run	T(°C.)	$\mu_L \times 10^3$ (poise)	ρ_L (gm./cm.^{3})	T(°C.)	$\mu_L \times 10^3$ (poise)	ρ_L (gm./cm.^{3})
16	38.1	6.143	0.9757	29	6.833	0.9906
17	38.6	5.957	0.9443	30	6.609	0.9599
18	37.9	6.004	0.9447	28	7.744	0.9608
19	37.1	6.052	0.9440	27	6.889	0.9585
20	39.6	6.029	0.9725	29	6.849	0.9908
21	38.6	6.097	0.9727	29	6.816	0.9888
22	40.0	6.008	0.9734	29	6.875	0.9912
23	38.0	6.142	0.9738	26	7.043	0.9898
24	37.0	6.212	0.9746	25	7.184	0.9914
25	37.8	6.155	0.9737	24	7.256	0.9930
26	38.6	6.098	0.9727	24	7.263	0.9943
27	39.6	6.008	0.9681	31	6.647	0.9837
28	38.9	6.055	0.9683	31	6.621	0.9828
29	38.1	6.115	0.9700	27	6.952	0.9847
30	38.0	6.125	0.9705	28	6.902	0.9857
31	38.2	6.110	0.9701	29	6.834	0.9863

Table 13 (Continued)

P = 100 Millimeters of Mercury

	Reflux Film			Rotometer Exit		
Run	(T°C.)	$\mu_L \times 10^3$ (poise)	ρ_L (gm./cm.^{3})	T(°C.)	$\mu_L \times 10^3$ (poise)	ρ_L (gm./cm.^{3})
32	72.9	4.347	0.9363	54	5.226	0.9603
33	72.8	4.351	0.9366	51	5.340	0.9633
34	72.1	4.375	0.9367	48	5.516	0.9658
35	71.9	4.378	0.9364	44	5.766	0.9683
36	72.6	4.361	0.9378k	34	6.410	0.9774
37	72.6	4.356	0.9364	56	5.116	0.9573
38	71.9	4.394	0.9405	41	5.986	0.9746
39	71.5	4.403	0.9392	26	7.026	0.9866
40	72.9	4.359	0.9396	27	6.968	0.9877
41	72.4	4.368	0.9390	37	6.235	0.9764
42	73.2	4.341	0.9376	26	7.042	0.9866
43	72.9	4.357	0.9392	24	7.204	0.9905
44	72.0	4.384	0.9383	24	7.262	0.9896
45	72.8	4.355	0.9374	24	7.256	0.9898

Table 13 (Continued)

P = 300 Millimeters of Mercury

	Reflux Film			Rotometer Exit		
Run	T(°C.)	$\mu_L \times 10^3$ (poise)	ρ_L (gm./cm.^{3})	T(°C.)	$\mu_L \times 10^3$ (poise)	ρ_L (gm./cm.^{3})
46	103	3.399	0.9050	73	4.369	0.9414
47	103	3.402	0.9061	46	5.647	0.9686
48	103	3.401	0.9060	32	6.544	0.9807
49	102	3.423	0.9060	70	4.472	0.9445
50	103	3.402	0.9062	37	6.198	0.9759
51	104	3.375	0.9046	26	7.043	0.9867
52	103	3.400	0.9055	64	4.715	0.9502
53	102	3.426	0.9069	57	5.062	0.9574
54	104	3.377	0.9046	24	7.268	0.9907
55	103	3.401	0.9061	55	5.173	0.9598
56	103	3.400	0.9060	23	7.337	0.9917
57	104	3.375	0.9044	23	7.307	0.9906

Table 14. Vapor Pressure of Chlorobenzene

Vapor Pressure (mm. of Hg)	Temperature (°C.)
5	10.6
10	22.2
20	35.3
40	49.7
60	58.3
100	70.7
200	89.4
400	110.0
760	132.2

Antoine Equation: $\log P = 7.05312 - \frac{1472.076}{T + 220.620}$

Reference| (96)

Table 15. Vapor Pressure of Ethylbenzene

Vapor Pressure (mm. of Hg)	Temperature (°C.)
20	38.60
40	52.75
60	61.798
80	68.596
100	74.105
200	92.680
300	104.703
400	113.823
500	121.266
600	127.603
700	133.152
710	133.672
720	134.185
730	134.693
740	135.196
750	135.694
760	136.186

Antoine Equation: $\log P = 6.95719 - \frac{1424.255}{T + 213.206}$

Reference: (91)

Table 16. Vapor-Liquid Equilibrium Data

P = 760 Millimeters of Mercury

Mole Fraction Chlorobenzene		
Liquid	Vapor	Relative Volatility
0.000	0.000	-----
0.060	0.067	1.125
0.106	0.115	1.096
0.176	0.191	1.106
0.221	0.240	1.115
0.273	0.291	1.094
0.326	0.348	1.104
0.378	0.399	1.094
0.432	0.457	1.108
0.461	0.486	1.104
0.515	0.539	1.102
0.550	0.574	1.101
0.594	0.618	1.108
0.658	0.678	1.096
0.696	0.716	1.100
0.736	0.756	1.111
0.777	0.793	1.099

Reference: (12)

Table 16 (Continued)

P = 760 Millimeters of Mercury

Mole Fraction Chlorobenzene		
Liquid	Vapor	Relative Volatility
0.820	0.833	1.096
0.864	0.874	1.093
0.895	0.904	1.105
0.921	0.927	1.088
1.000	1.000	-----
		1.10 = Average

Reference: (12)

Table 16 (Continued)

P = 20 Millimeters of Mercury

Mole Fraction Chlorobenzene		
Liquid	Vapor	Relative Volatility
0.000	0.000	-----
0.107	0.118	1.117
0.150	0.165	1.121
0.210	0.226	1.100
0.285	0.311	1.132
0.359	0.388	1.130
0.439	0.468	1.124
0.514	0.543	1.118
0.546	0.574	1.118
0.584	0.611	1.119
0.659	0.685	1.126
0.726	0.749	1.125
0.817	0.833	1.118
0.877	0.888	1.102
0.921	0.930	1.135
1.000	1.000	-----
		1.12 = Average

Reference: (12)

Table 16 (Continued)

P = 300 Millimeters of Mercury

Mole Fraction Chlorobenzene		
Liquid	Vapor	Relative Volatility
0.333	0.359	1.12
0.497	0.525	1.11
0.824	0.840	1.12
		1.12 = Average

Reference: (12)

APPENDIX IV

EXPERIMENTAL AND CALCULATED DATA

Table 17. Summary of Experimental Data

P = 736 Millimeters of Mercury

Run	Flow Rate (gm./min.)	Mole Fraction Chlorobenzene	
		Top	Bottom
1	139.4	0.5355	0.5016
2	101.6	0.5374	0.5016
3	63.5	0.5384	0.4997
4	33.3	0.5393	0.4967
5	25.0	0.5460	0.5006
6	16.2	0.5441	0.4987
7	10.8	0.5335	0.4928
8	6.16	0.5326	0.4997
9	5.85	0.5364	0.5035
10	124.3	0.5307	0.4958
11	39.2	0.5374	0.4967
12	27.5	0.5374	0.4948
13	19.9	0.5451	0.4987
14	7.79	0.5364	0.5006
15	4.67	0.5307	0.5006

Table 17 (Continued)

P = 20 Millimeters of Mercury

Run	Flow Rate (gm./min.)	Mole Fraction Chlorobenzene	
		Top	Bottom
16	29.5	0.6173	0.5757
17	34.8	0.4880	0.4348
18	23.1	0.4821	0.4348
19	17.0	0.4645	0.4388
20	40.1	0.6155	0.5642
21	32.0	0.6098	0.5633
22	23.0	0.6164	0.5776
23	14.5	0.6004	0.5766
24	9.66	0.5975	0.5776
25	5.19	0.6004	0.5747
26	3.36	0.6060	0.5690
27	46.3	0.5985	0.5432
28	41.4	0.5947	0.5422
29	14.2	0.5823	0.5604
30	20.0	0.5899	0.5576
31	27.1	0.5966	0.5508

Table 17 (Continued)

P = 100 Millimeters of Mercury

Run	Flow Rate (gm./min.)	Mole Fraction Chlorobenzene	
		Top	Bottom
32	54.9	0.5918	0.5470
33	43.1	0.5937	0.5470
34	35.7	0.5918	0.5432
35	29.5	0.5871	0.5422
36	14.7	0.5861	0.5604
37	73.3	0.5890	0.5460
38	24.2	0.6032	0.5652
39	8.14	0.5871	0.5623
40	10.6	0.5947	0.5728
41	20.2	0.5947	0.5614
42	9.15	0.5861	0.5652
43	6.68	0.5928	0.5709
44	5.76	0.5852	0.5623
45	4.63	0.5871	0.5614

Table 17 (Continued)

P = 300 Millimeters of Mercury

Run	Flow Rate (gm./min.)	Mole Fraction Chlorobenzene	
		Top	Bottom
46	74.3	0.5918	0.5528
47	19.4	0.5975	0.5566
48	12.9	0.5899	0.5614
49	64.1	0.5909	0.5508
50	16.6	0.5937	0.5585
51	9.11	0.5871	0.5633
52	49.9	0.5956	0.5537
53	36.4	0.5966	0.5537
54	9.19	0.5899	0.5681
55	29.0	0.5956	0.5508
56	6.84	0.5909	0.5700
57	8.28	0.5871	0.5652

Table 18. Summary of Calculated Data

P = 736 Millimeters of Mercury

Run	Re_L	$\overline{Re}_V$	H_G/d	d/B
1	572	18,600	46.3	58.6
2	417	13,800	43.7	45.3
3	261	8,840	40.6	30.5
4	137	4,810	36.8	17.6
5	102	3,680	34.5	14.4
6	66.5	2,480	34.4	9.20
7	44.1	1,700	37.0	5.68
8	25.3	1,030	47.8	2.51
9	24.0	984	47.5	2.41
10	510	16,700	44.8	54.1
11	161	5,620	38.4	19.9
12	113	4,040	36.7	14.6
13	81.8	2,990	33.6	11.6
14	32.0	1,270	43.6	3.48
15	19.2	804	52.0	1.75

Table 18 (Continued)

P = 20 Millimeters of Mercury

Run	Re_L	$\overline{Re}_V$	H_G/d	d/B
16	54.3	4,560	42.6	16.8
17	63.9	5,360	34.9	24.1
18	42.5	3,580	39.3	14.3
19	31.2	2,640	72.2	5.71
20	73.6	6,140	34.8	27.9
21	58.8	4,930	38.5	20.2
22	42.3	3,540	45.7	12.2
23	26.6	2,240	75.0	4.67
24	17.7	1,500	89.8	2.61
25	9.53	806	69.6	1.81
26	6.17	521	48.3	1.68
27	85.1	7,110	32.7	34.3
28	76.1	6,380	34.5	29.1
29	26.2	2,210	82.7	4.17
30	36.7	3.090	55.9	8.65
31	49.7	4,180	39.4	16.6

Table 18 (Continued)

P = 100 Millimeters of Mercury

Run	Re_L	$\overline{Re}_V$	H_G / d	d/B
32	141	7,700	35.3	34.5
33	110	6,060	33.9	28.2
34	91.2	5,040	32.6	24.3
35	75.4	4,180	35.4	18.5
36	37.7	7,100	61.5	5.32
37	187	10,300	36.9	44.1
38	61.8	3,430	41.3	13.0
39	20.8	1,170	63.6	2.84
40	27.1	1,520	71.6	3.28
41	51.7	2,870	47.3	9.49
42	23.4	1,310	75.4	2.69
43	17.1	964	71.6	2.07
44	14.7	836	69.0	1.85
45	11.8	673	61.5	1.67

Table 18 (Continued)

P = 300 Millimeters of Mercury

Run	Re_L	$\overline{Re}_V$	H_G/d	d/B
46	244	10,000	39.5	39.0
47	63.8	2,730	37.5	10.8
48	42.3	1,840	53.8	4.96
49	210	8,710	38.4	34.6
50	54.4	2,340	43.6	7.87
51	29.9	1,320	64.5	2.93
52	164	6,790	36.6	28.2
53	119	5,020	35.8	21.1
54	27.2	1,300	70.2	2.71
55	95.3	4,020	34.3	17.5
56	22.5	980	73.2	1.94
57	27.4	1,170	70.1	2.45

LITERATURE CITED

LITERATURE CITED

1. Docksey, P., and May, C. J., "Relative Efficiencies of Packed Fractionating Columns," Journal of the Institution of Petroleum Technologists, 21, 176 (1935).

2. Skoble, A. I., and Driatskaya, Z. V., Neftyanoye Khozyaystvo, 24, No. 5, 39 (1946); Reviewed by Daniel, L. R., The Effect of Pressures Below One Atmosphere on the Performance of a Packed Column, Ph. D. Thesis, Georgia Institute of Technology (1952).

3. Nandi, S. K., and Jalota, P. L., Transactions of the Indian Institute of Chemical Engineers, 1, 57 (1947-48); Reviewed by Daniel, L. R., The Effect of Pressures Below One Atmosphere on the Performance of a Packed Column, Ph. D. Thesis, Georgia Institute of Technology (1952).

4. Smoker, E. H., "A High Efficiency Multi-Tubular Packed Column," Transactions of the American Institute of Chemical Engineers, 40, 105 (1944).

5. Schofield, R. C., "Industrial Fractionating Tower Packing," Chemical Engineering Progress, 46, 405 (1950).

6. Feldman, J., Myles, M., Wender, I., and Orchin, M., "Evaluation of Vacuum Rectification Columns," Industrial and Engineering Chemistry, 41, 1032 (1949).

7. Berg, L., and Popovac, D. P., "Effect of Reduced Pressure on Efficiency of a Packed Rectification Column," Chemical Engineering Progress, 45, 683 (1949).

8. Struck, R. T., and Kenney, C. R., "Efficiency of Packed Fractionating Columns: Effect of Vacuum Operation," Industrial and Engineering Chemistry, 42, 77 (1950).

9. Myles, M., Feldman, J., Wender, I., and Orchin, M., "Fractionating Efficiency of Various Packings in Distillation Column Operating at Reduced Pressure," Industrial and Engineering Chemistry, 43, 1452 (1951).

10. Daniel, L. R., The Effect of Pressures Below One Atmosphere on the Performance of a Packed Column, Ph. D. Thesis, Georgia Institute of Technology (1952).

11. Morton, F., "The Operation of Commercial and Semi-Commercial Stedman Packed Fractionating Columns," Transactions of the Institution of Chemical Engineers (London),29, 240 (1951).

12. Hawkins, J. E., and Brent, J. A., Jr., "Performance of Packed Columns During Batch Fractionation," Industrial and Engineering Chemistry, 43, 2611 (1951).

13. Bliss, H., Eshaya, A. M., and Frisch, N. W., "Rectification at Reduced Pressures," Chemical Engineering Progress, 48, 627 (1952).

14. Peters, M. S., and Cannon, M. R., "Vacuum Distillation: Variables in Packed Column Distillation at Subatmospheric Pressures," Industrial and Engineering Chemistry, 44, 1452 (1952).

15. Kirschbaum, E., and David, A., "Untersuchungen über die Rektifikation verschiedener Gemische in Füllkörpersäulen bei Atmosphärendruck and Unterdrucken," Chemie Ingenieur Technik, 25, 592 (1953).

16. Walsh, T. J., Sugimura, G. H., and Reynolds, T. W., "Evaluation of Packed Distillation Columns," Industrial and Engineering Chemistry, 45, 2629 (1953).

17. Ergle, J. L., A Study of Low Pressure Distillation in a Packed Column, M. S. Thesis, Georgia Institute of Technology (1956).

18. Gilliland, E. R., and Sherwood, T. K., "Diffusion of Vapors into Air Streams," Industrial and Engineering Chemistry, 26, 516 (1934).

19. Craig, L. C., "A Fractional-Distillation Microapparatus," Industrial and Engineering Chemistry, Analytical Edition, 9, 441 (1937).

20. Bragg, L. B., "Laboratory Columns for Close Fractionation," Industrial and Engineering Chemistry, Analytical Edition, 11, 283 (1939).

21. Bragg, L. B., "Semicommercial Columns for Close Fractionation," Industrial and Engineering Chemistry, 33, 279 (1941).

22. Bragg, L. B., "Packed Columns for Close Fractionation - Stedman Packing," Transactions of the American Institute of Chemical Engineers, 37, 19 (1941).

23. Fenske, M. R., Lawroski, S., and Tongberg, C. O., "Packing Materials: Study in a 5.1-cm. Fractionating Column," Industrial and Engineering Chemistry, 30, 297 (1938).

24. Selker, M. L., Burk, R. E., and Lankelma, H. P., "An Efficient Low-Holdup Laboratory Column," Industrial and Engineering Chemistry, Analytical Edition, 12, 352 (1940).

25. Rose, A., "Distillation Efficiency in 3 and 6 MM Fractionating Columns," Industrial and Engineering Chemistry, 28, 1210 (1936).

26. Surowiec, A. J., and Furnas, C. C., "Distillation in a Wetted-Wall Tower," Transactions of the American Institute of Chemical Engineers, 38, 53 (1942).

27. Furnas, C. C., and Taylor, M. L., "Distillation in Packed Columns," Transactions of the American Institute of Chemical Engineers, 36, 135 (1940).

28. Johnstone, H. F., and Pigford, R. L., "Distillation in a Wetted-Wall Column," Transactions of the American Institute of Chemical Engineers, 38, 25 (1942).

29. Kuhn, W., and Ryffel, K., "Einiges über Trenngüte und Mengenleistung bei der Destillation," Helvetica Chimica Acta, 26, 1693 (1943).

30. Peck, R. E., and Wagner, E. F., "Film Resistances in Rectification," Transactions of the American Institute of Chemical Engineers, 41, 737 (1945).

31. Storrow, J. A., "The Effect of Vapour Composition on the Assessment of Fractionating Columns in Terms of Heights of a Transfer Unit. Part 1," Journal of the Society of Chemical Industry, 66, 41 (1947).

32. Chari, K. S., and Storrow, J. A., "Film Resistances in Rectification," Journal of Applied Chemistry, 1, 45 (1951).

33. Jackson, M. L., and Ceaglske, N. H., "Distillation, Vaporization, and Gas Absorption in a Wetted-Wall Column," Industrial and Engineering Chemistry, 42, 1188 (1950).

34. Yoshida, F., "Rectification in a Wetted-Wall Column," Japan Science Review, Serial 1, Engineering Science 1, 43 (1950).

35. Gilliland, E. R., "Fundamentals of Drying," Industrial and Engineering Chemistry, 30, 506 (1938).

36. Nikolaev, A. P., "Mass Transfer in Distillation in Wetted-Wall Columns," Journal of Applied Chemistry of the USSR, 31, 704 (1958).

37. Reynolds, O., Scientific Papers of Osborne Reynolds, Cambridge University Press, New York (1901), Volume II, 51.

38. Knudsen, J. G., and Katz, D. L., Fluid Dynamics and Heat Transfer, McGraw-Hill Book Company, Inc., New York (1958), 107.

39. Goldstein, S., Modern Developments in Fluid Dynamics, Clarendon Press, Oxford (1938), Volume I, 319.

40. Schlichting, H., Boundary Layer Theory, Translated by Kestin, J., McGraw-Hill Book Company, Inc., New York (1955), 308.

41. Prengle, R. S., and Rothfus, R. R., "Transition Phenomena in Pipes and Annular Cross Sections," Industrial and Engineering Chemistry, 47, 379 (1955).

42. Rothfus, R. R., and Prengle, R. S., "Laminar-Turbulent Transition in Smooth Tubes," Industrial and Engineering Chemistry, 44, 1683 (1952).

43. Bird, R. B., Stewart, W. E., and Lightfoot, E. N., Transport Phenomena, John Wiley and Sons, Inc., New York (1960), 40.

44. Cooper, C. M., Drew, T. B., and McAdams, W. H., "Isothermal Flow of Liquid Layers," Industrial and Engineering Chemistry, 26, 428 (1934).

45. Kirkbride, C. G., "Heat Transfer by Condensing Vapor on Vertical Tubes," Transactions of the American Institute of Chemical Engineers, 30, 170 (1933-34)

46. Fallah, R., Hunter, T. G., and Nash, A. W., "The Application of Physico-Chemical Principles to the Design of Liquid Contact Equipment. Part III. Isothermal Flow in Liquid Wetted-Wall Systems," Journal of the Society of Chemical Industry, 53, 369 (1934).

47. Friedman, S. J., and Miller, C. O., "Liquid Films in the Viscous Flow Region," Industrial and Engineering Chemistry, 33, 885 (1941).

48. Grimley, S. S., "Liquid Flow Conditions in Packed Towers," Transactions of the Institution of Chemical Engineers (London) 23, 228 (1948).

49. Jackson, M. L, Johnson, R. T., and Ceaglske, N. H., "Surface Velocities of Liquid Films in the Streamline Flow Region," Proceedings of the Midwestern Conference on Fluid Dynamics, 226 (1950).

50. Dukler, A. E., and Bergelin, O. P., "Characteristics of Flow in Falling Liquid Films," Chemical Engineering Progress, 48, 557 (1952).

51. Jackson, M. L., "Liquid Films in Viscous Flow," American Institute of Chemical Engineers Journal, 1, 231 (1955).

52. Emmert, R. E., and Pigford, R. L., "A Study of Gas Absorption in Falling Liquid Films," Chemical Engineering Progress, 50, 87 (1954).

53. Rouse, H., Fluid Mechanics for Hydraulic Engineers, McGraw-Hill Book Company, Inc., New York (1938), 369.

54. Thomas, W. J., and Portalski, S., "Hydrodynamics of Countercurrent Flow in Wetted-Wall Columns," Industrial and Engineering Chemistry, 50, 1081 (1958).

55. Zuiderweg, F. J., and Harmens, A., "The Influence of Surface Phenomena on the Performance of Distillation Columns," Chemical Engineering Science, 9, 89 (1958).

56. Qureshi, A. K., and Smith, W., "The Distillation of Binary and Ternary Mixtures," The Journal of the Institute of Petroleum, 44, 137 (1958).

57. Fenske, M. R., "Fractionation of Straight-Run Pennsylvania Gasoline," Industrial and Engineering Chemistry, 24, 482 (1932).

58. Treybal, R. E., Mass-Transfer Operations, McGraw-Hill Book Company, Inc., New York (1955), 257.

59. Robinson, C. S., and Gilliland, E. R., Elements of Fractional Distillation, Fourth Edition, McGraw-Hill Book Company, Inc., New York (1950).

60. Maxwell, J. C., Scientific Papers, Cambridge University Press, Cambridge (1890), Volume II, 57.

61. Lewis, W. K, and Chang, K. C., "The Mechanism of Rectification," Transactions of the American Institute of Chemical Engineers, 21, 127 (1928).

62. Sherwood, T. K., and Pigford, R. L., Absorption and Extraction, Second Edition, McGraw-Hill Book Company, Inc., New York (1952), 81.

63. Westhaver, J. W., "Theory of Open-Tube Distillation Columns," Industrial and Engineering Chemistry, 34, 126 (1942).

64. Bird, Stewart, and Lightfoot, Op. cit., 46.

65. Peters, W. A., "The Efficiency and Capacity of Fractionating Columns," Journal of Industrial and Engineering Chemistry, 14, 476 (1922).

66. Kuhn, W., "Die Destillation," Helvetica Chimica Acta, 25, 252 (1942).

67. Aris, R., "On the Dispersion of a Solute by Diffusion, Convection and Exchange Between Phases," Proceedings of the Royal Society (London), 252A, 538 (1959).

68. Glasebrook, A. L., and Williams, F. E., "Ordinary Fractional Distillation," Technique of Organic Chemistry, Ed. Weissberger, A., Interscience Publishers, Inc., New York (1951), Volume IV, 179.

69. Sherwood, T. K., and Woertz, B. B., "Mass Transfer Between Phases: Role of Eddy Diffusion," Industrial and Engineering Chemistry, 31, 1034 (1939).

70. Whitman, W. G., and Keats, J. L., "Rates of Absorption and Heat Transfer Between Gases and Liquids," Journal of Industrial and Engineering Chemistry, 14, 186 (1922).

71. Sherwood, T. K., Absorption and Extraction, First Edition, McGraw-Hill Book Company, Inc., New York (1937), 22.

72. Lewis, W. K., and Whitman, W. G., "Principles of Gas Absorption," Industrial and Engineering Chemistry, 16, 1215 (1924).

73. Treybal, Op. cit., 85.

74. Chilton, T. H., and Colburn, A. P., "Distillation and Absorption in Packed Columns: A Convenient Design and Correlation Method," Industrial and Engineering Chemistry, 27, 255 (1935).

75. Treybal, Op. cit., 40.

76. Sherwood and Pigford, Op. cit., 77.

77. Treybal, Op. cit., 48.

78. Bird, Stewart, and Lightfoot, Op. cit., 642.

79. Sherwood, T. K., "Mass, Heat and Momentum Transfer Between Phases," Chemical Engineering Progress, Symposium Series, 25, 71 (1959).

80. Chilton, T. H., and Colburn, A. P., "Mass Transfer (Absorption) Coefficients: Prediction from Data on Heat Transfer and Fluid Friction," Industrial and Engineering Chemistry, 26, 1183 (1934).

81. Colburn, A. P., "A Method of Correlating Forced Convection Heat Transfer Data and a Comparison with Fluid Friction," Transactions of the American Institute of Chemical Engineers, 29, 174 (1933).

82. Treybal, Op. cit., 52.

83. Reid, R. C., and Sherwood, T. K., The Properties of Gases and Liquids, McGraw-Hill Book Company, Inc., New York (1958), 267.

84. Dodge, B. F., Chemical Engineering Thermodynamics, McGraw-Hill Book Company, Inc., New York (1944), 138.

85. Reid and Sherwood, Op. cit., 299.

86. Ibid., 185.

87. McCabe, W. L., and Smith, J. C., Unit Operations of Chemical Engineering, McGraw-Hill Book Company, Inc., New York (1956), 121.

88. Glasebrook and Williams, Op, cit., 283.

89. Noller, C. R., Chemistry of Organic Compounds, W. B. Saunders Company, Philadelphia (1951), 532.

90. Fenske, M. R., Myers, H. S., and Quiggle, D., "Binary Mixture for Determining Efficiencies of Fractionating Columns Operating at Reduced Pressures," Industrial and Engineering Chemistry, 42, 649 (1950).

91. Rossini, F. D., et. al., Selected Values of Physical and Thermodynamic Properties of Hydrocarbons and Related Compounds, Carnegie Press, Pittsburgh (1953).

92. Lydersen, A. L., Greenkorn, R. A., and Hougen, O. A., Generalized Thermodynamic Properties of Pure Fluids, University of Wisconsin Engineering Experiment Station Report No. 4 (1955).

93. Reid and Sherwood, Op. cit., 189.

94. Ibid., 210.

95. Ibid., 271.

96. Perry, J. H., Chemical Engineers' Handbook, Ed. Perry, J. H., McGraw-Hill Book Company, Inc., New York (1950).

97. Hodgman, C. D., Handbook of Chemistry and Physics, Ed. Hodgman, C. D., Thirty-First Edition, Chemical Rubber Publishing Company, Cleveland (1949).

VITA

Sydney Vaughn Stern was born in New York City on August 10, 1932. He graduated from the Munich Dependents High School, Munich, Germany, in June of 1950.

He entered the Georgia Institute of Technology in September, 1950, on a U. S. Navy Holloway Plan Scholarship. He was awarded the degree of Bachelor of Chemical Engineering in June of 1954.

Immediately after graduation he was commissioned Ensign, USN, and ordered to active duty. During his tour of naval duty he completed courses of instruction at the Destroyer Engineer Officers School, San Diego, California, and the Explosive Ordnance Disposal School, Indian Head, Maryland. He was released from active duty in March of 1958.

He entered the Graduate Division of the Georgia Institute of Technology in March of 1958 and completed the requirements for the degree Master of Science in Chemical Engineering in December of 1960.

He was awarded the Phillips Petroleum Company Fellowship for the academic year 1959-1960 and the Ethyl Corporation Fellowship for the academic year 1960-1961.

He is a member of Sigma Xi, honorary research society.

In 1954 he married the former Marion Shelton Jones of Miami, Florida.